Dilatometric investigation on the phase transformations during thermal treatment of a low silicon TRIP-aided multiphase steel

UCL

Université catholique de Louvain

TU Delft

Delft University of Technology

This work is submitted as part fulfilment for the Degree of Materials Science Engineer.

Valéry ROLIN

Academic Year '99 – '00

Supervisors :
Prof. F. Delannay
Prof. S. van der Zwaag

Acknowledgements

In the chronological order of the elaboration of this thesis work,

I would like to thank Professor Francis Delannay for having helped me to go and study at the TUDelft.

I thank especially Dr Lie Zhao for his interest in my work and the time he spent with me.

I also thank Professor Sybrand van der Zwaag, Dr Jilt Sietsma, Theo Kop, Yvonne van Leeuwen and Pieter van der Wolk for their help, their judicious advices and their sympathy.

I still would like to thank Pascal Jacques for his 'internet' pieces of advice.

And I owe a special acknowledgement to Anne Mertens for all the time she has given to me, and for her conscientious help.

Abstract

TRIP-aided multiphase steels owe their high strength and high formability mostly to the austenite that they contain at room temperature. This is what makes of them the challenging material for automotive industry. In the low-alloyed steels, the retention of the austenite is obtained by a specific thermal treatment, which includes a bainitic transformation. In order to prevent the precipitation of cementite in the enriched austenite, a graphitising element such as silicon is usually added to the composition. But the presence of silicon creates several problems within the finished products, this is why researches are carried out on low-silicon TRIP-aided multiphase steels.

The main experimental technique that was used is dilatometry. (1) In a first time the allotropic transformation $\alpha \rightarrow \gamma$ upon heating was studied. A Matlab program was designed for the calculation (on the basis of the experimental data) of the amount of austenite that appears in a sample during an intercritical annealing. (2) In a second time, several thermal treatments have been designed in order to get information for the drawing of TTT diagrams. Therefore, samples were quenched from the austenitic region to several temperatures where an isothermal holding was applied for 15 minutes. Once again, the measured data was used by a Matlab program for the calculation of the fraction transformed, which finally lead to the TTT diagram.

Scanning electron microscopy as well as optical microscopy were used on the samples in order to verify the results found by dilatometry and calculation. (1) Image analysis allowed to measure the distribution of phases determined by the regulation of the intercritical annealings. (2) And, by comparing the samples having undergone the different isothermal holding, it was possible to determine the influence of the heat treatments on the microstructures.

Table of contents

1. Introduction

1.1 Objectives

As suggested in its title, this work is an investigation on the thermal treatments for the production of a low silicon TRIP-aided multiphase steel. This material belongs to the family of high-strength formable steels. The exceptional mechanical properties of the TRIP-aided multiphase steels have been studied for several years by now, and they will be detailed in this introduction. What is more recent is the interest born to the low silicon family, which should be more appropriated on a technological point of view for industrial production.

Practically, a low carbon - low silicon steel was chosen to be studied in a first time by means of dilatometry, and eventually by other characterisation techniques : optical microscopy, scanning electron microscopy and X-ray diffraction.

Besides the experimentation, the second main part of the work has been the development of a calculation method for the interpretation of the dilatometric data. Two kinds of transformations were analysed by this method: (1) the allotropic transformation $\alpha \rightarrow \gamma$ upon heating, i.e. the calculation of the fraction of austenite that appears during an intercritical annealing, (2) the isothermal transformation in the bainitic region following a quench from the austenitic region.

The idea of these calculation was to get data on the fraction transformed for the drawing of TTT diagrams corresponding to three annealing temperatures : two intercritical, and one over Ac3.

In the whole set of dilatometric experiments, some have served for an additional investigation on intercritical annealings. The obtained microstructure still constitutes a mystery since it cannot be explained from the thermal treatments undergone by the samples.

1.2 TRIP-aided multiphase steels

Steel is still the first choice material for the construction of car bodies in the automotive industry. In the current conjuncture, the big challenge is the fuel consumption, which demands a reduction of the weight. If the iron and steel industries want their material to keep its place, they must improve its strength. This can be achieved with the TRIP effect [1]. Although they are low alloyed material, the TRIP-aided multiphase steels show an excellent combination of strength and ductility. These performances can be attributed to the **TR**ansformation **I**nduced **P**lasticity, i.e. the continuous transformation of retained austenite into martensite during straining [2-3].

1.2.1 TRIP effect

The schematical free energy curves on Figure 1 help to understand how the mechanically induced transformation of the austenite works. For a fixed composition, T_0 is the equilibrium temperature between austenite and martensite, and Ms is the temperature at which the undercooling is sufficient to provoke transformation. If T_1 is an intermediate temperature between Ms and T_0, the austenite that exists at T_1 is said to be metastable since its free energy curve is above the curve of the martensite. The fact is that the difference between the free energy curves at T_1 ($\Delta G_{T_1}^{\gamma\rightarrow\alpha'}$) has not yet reached the critical driving force ($\Delta G_{Ms}^{\gamma\rightarrow\alpha'}$). However, it is possible for the austenite at T_1 to transform into martensite if a sufficient mechanical energy is provided (U'). This mechanically induced transformation bears the name of TRIP effect.

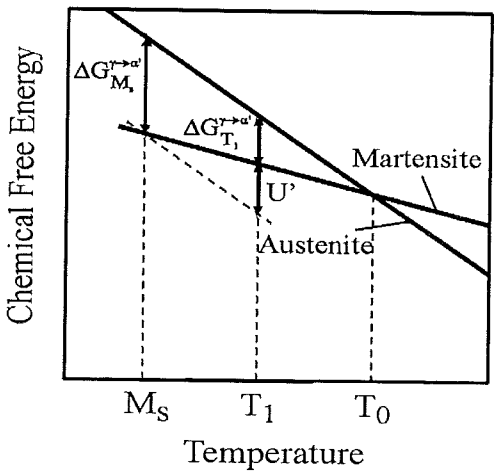

Figure 1: Free energy curves of the austenite and the martensite [4].

1.2.2 Usual processes for the production of TRIP steels

TRIP-aided multiphase steels can be produced in two ways : (i) heat treatment after cold rolling [5] and, (ii) a continuous thermomechanical treatment including a hot rolling [6] .

(i) Figure 2 shows the heat treatment used for cold-rolled TRIP-assisted multiphase steels. The aim of this process is to stabilise some austenite at room temperature thanks to a two steps carbon enrichment. In a first time, the austenite is formed during the intercritical annealing and it is enriched in carbon coming from the neighbouring ferrite [7] . Secondly, a bainitic holding provokes a partial transformation of the intercritical austenite into bainite, and the carbon enrichment of the remaining austenite, which is therefore not transformed into martensite during the final quench to room temperature [8] . Those low alloyed steels usually contain up to 1.5 - 2.0 wt. % silicon in order to prevent the precipitation of cementite in the carbon-enriched austenite. During the further processing of the material, the metastable austenite can transform into martensite when there is a strong plastic deformation.

(ii) The processing of TRIP steels via thermomechanical treatment is quite similar, except that the material is hot-rolled, then directly cooled to the intercritical region, where the annealing is carried out in a continuous way. The continuation of the process is identical to the one for cold-rolled steels (i).

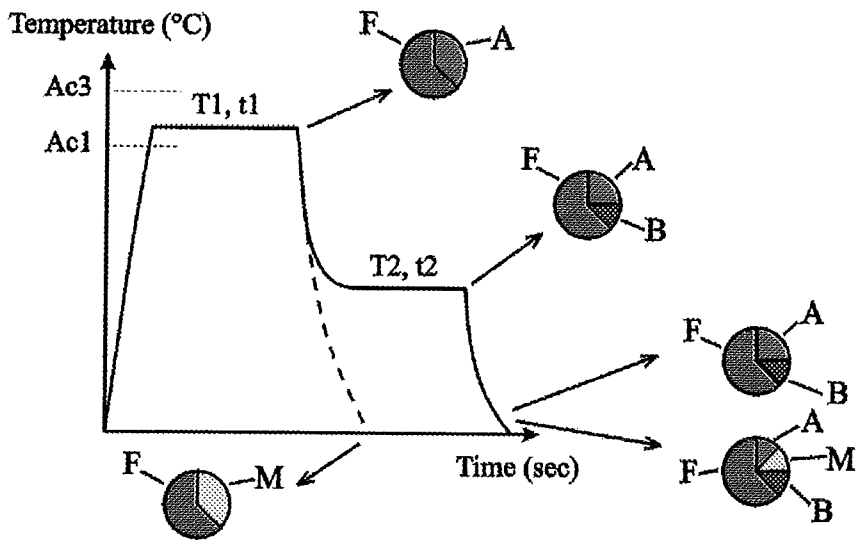

Figure 2: Typical heat treatment scheme for the production of TRIP-aided multiphase steel [4]

1.2.3 Stabilisation of austenite during the bainitic transformation

1.2.3.1 Bainitic transformation

Before entering into the specificities of the multiphase TRIP-aided steels, it is necessary to examine the bainitic transformation. It is worth remembering that the bainite is the microstructure that forms when a steel is quenched from the austenitic region to a range of temperatures below the ferritic region and above the martensitic region. While the formation of ferrite is a diffusive transformation, the formation of martensite is displacive. What about bainite ? It has been accepted now that its formation is displacive, even though there is some diffusion in the nucleation process [9].

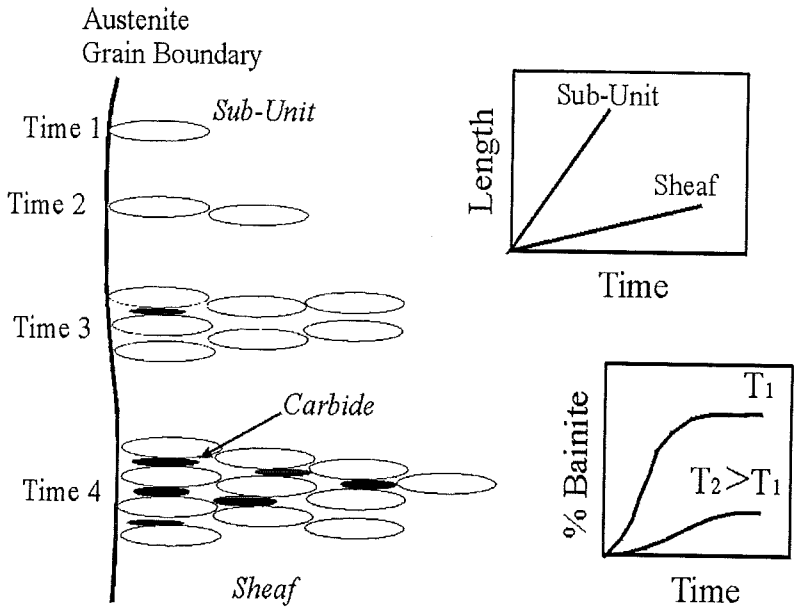

Figure 3: Schematic representation of the development of a sheaf of bainite [4].

The growth of the bainite is sketched in Figure 3. The sub-units have the cristallographic lattice of the ferrite, and are sometimes called "bainitic ferrite". They nucleate at the grain boundaries of the austenite and grow very fast as a plate until the dislocation pile-up at the austenite/ferrite interface stops them. Then new nucleation occurs at the tip of the laths, leading to a sheaf structure.

As their formation is displacive, the ferrite laths are supersaturated with carbon during a short instant, after their formation, carbon then diffuses into the surrounding austenite. This becomes the place for carbide precipitation, unless silicon or aluminium has been added. These elements, which are substitutional, do not diffuse during bainitic transformation. Two diffusion processes exist that lead to two kinds of bainite, as sketched in Figure 4.

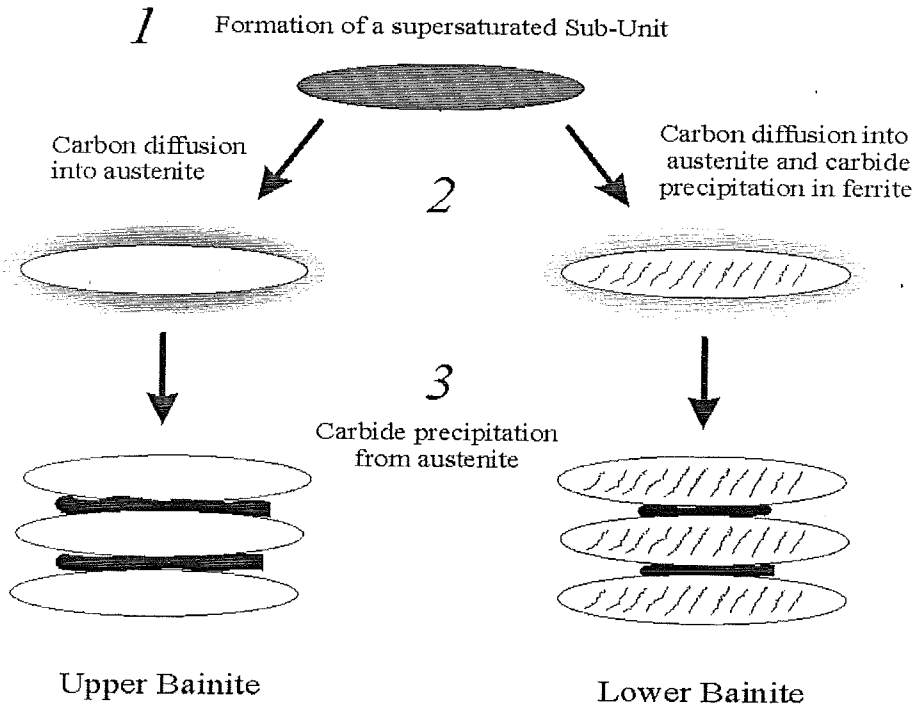

Figure 4: Schematic illustration of the formation of either upper bainite or lower bainite [4].

The difference between upper bainite and lower bainite comes from kinetic effects [4]. Upper bainite appears when the transformation is performed at such a high temperature that the carbon diffusion out of the ferritic laths can take place very quickly. On the other hand, at lower temperatures, a part of the carbon cannot diffuse out of the lath and thus, carbides precipitate inside. This is the case of the lower bainite.

1.2.3.2 The incomplete reaction phenomenon

The fact that some austenite can be stabilised during the formation of bainite is called an incomplete reaction [9]. It will be showed hereafter that this incomplete reaction is possible because the bainitic transformation is displacive.

Figure 5 presents the free energy curves of ferrite and bainite at the temperature T_1 represented as a function of the carbon content. The crossing of these curves defines the carbon concentration above which the austenite cannot transform into ferrite in a displacive way. The line that represents this maximum carbon content as a function of the temperature of transformation is called the T_0 curve. The result is that, for an isothermal transformation at T_1, and if there is no carbide precipitation in the austenite, the bainitic transformation will stop when the carbon concentration in the austenite reaches the value defined by the T_0 curve.

On the other hand, if the austenite had transformed by a reconstructive process, the carbon concentration in the ferrite and in the austenite would have been respectively defined by the Ae_1 and the Ae_3 lines, according to the tangent rule.

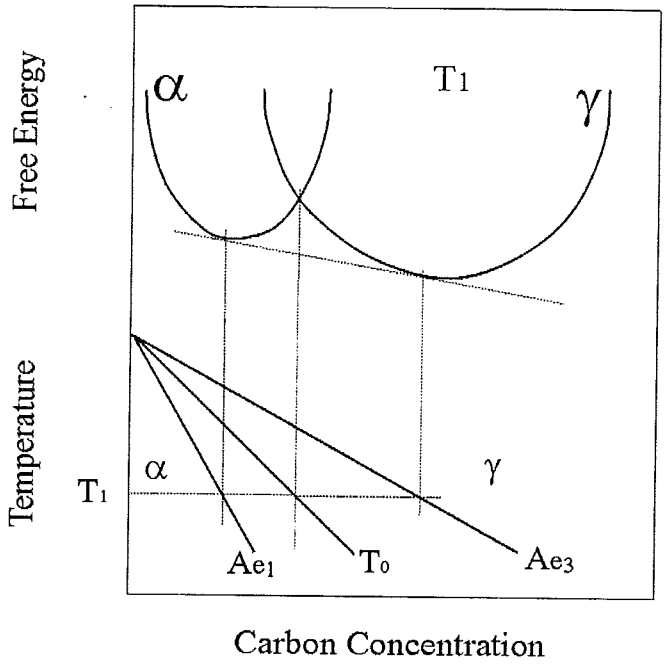

Figure 5: Schematic illustration of the origin of the T_0 curve on a phase diagram as resulting at each temperature of specific points of the free energy curves of ferrite and austenite [4].

Besides the fact that the bainitic transformation must be displacive, a second condition for the retention of austenite is that there must not be any carbide precipitation. It is possible to get rid of that precipitation by adding silicon to the steel. Indeed, the solubility of the silicon in the cementite is very small and therefore carbon cannot precipitate [4]. If this requirement is met, the high carbon content of the austenite has the effect to drop Ms below room temperature, and the austenite can therefore be retained.

1.2.4 Low silicon TRIP-aided multiphase steels

Significant amount of austenite can be retained in bainitically transformed steels highly alloyed with a silicon concentration around 2 % [7] and it is accepted that a conventional TRIP-aided multiphase steel must contain at least 1 wt. % of silicon [10]. But the problem is that besides its good effect on the hindering of the cementite precipitation, silicon, when it is added to more than 0.5 wt. % in steel, creates problems on the finished product. Firstly, a silicon oxide layer appears on the material after the hot-rolling. Secondly, at the galvanisation, too much silicon provoke the formation of intermetallics Fe-Zn that renders the protection

layer fragile [11]. This is why a real interest exists for low silicon TRIP-aided multiphase steels. The steel that is going to be studied in this work has the following composition : 0.16 wt. % C, 1.5 wt. % Mn, and 0.4 wt. % Si, which is similar to the composition of typical cold-rolled dual-phase steels [12]. As a matter of fact, the silicon content is much lower than in conventional TRIP-aided multiphase steels, and it should be difficult to get retained austenite. However, the dilatometric investigation is interesting since it can bring many information on that grade of steel.

2. Material and methods

2.1 Material

The one and only material studied in this work is a low silicon steel that was provided by the research and development department of Hoogovens [13]. As it was to be studied by dilatometry, we have received the samples of industrially produced hot-rolled FeCMnSi steel in the shape of solid cylinders of 10 mm long and 4 mm in diameter.

	Mn	Si	C
Wt. %	1.5	0.4	0.16

Table 1: Composition given by Hoogovens.

This steel was said to have a composition with lean chemistries, and that means a maximum of 0.16 wt. % C, 1.5 wt. % Mn and 0.4 wt. % Si. Those values were retained for the calculations based on the lattice parameters. Meanwhile, in order to have a second source for the composition, we confided three samples, as they were received from Hoogovens, to the department of Chemical Technology of Delft.

The samples were digested in a mixture of 20 ml aqua regia and 5 ml HF in a closed Teflon vessel using a microwave furnace. The ICP-OES technique was used to analyse the sample solutions. The concentrations found are :

Weight [mg]		Mn	Si	C
975.5 ± 0.8	**Wt. %**	1.47 ± 0.015	0.27 ± 0.015	0.14 ± 0

Table 2: Composition measured at the TUDelft.

The silicon concentration is much lower than the previous value of 0.4 wt. %. That would mean that this is a "very low silicon steel". Anyway, we will see that it will not be a problem for the calculations as the silicon concentration does not play any role. An explanation that was proposed for this lower measured value was that a precipitate including a part of the silicon forms in the batch, so that this part is not blown in the plasma torch.

On the other hand, the measured concentration for the carbon was also lower than the value given by Hoogovens (0.14 < 0.16). This has more critic consequences as it influences the results of the calculation. Nevertheless, we made the choice to work with the first numbers.

We asked our contacts in Hoogovens to repeat the same composition measurements with more details (Table 3). The results follow in weight percent :

	Mn	Si	C	Al	Ni	Cr	Cu	P	S	Mo, Sn
Wt. %	1.48	0.414	0.154	0.046	0.022	0.019	0.015	0.012	0.011	<0.001

Table 3: Composition measured by Hoogovens.

These measurements confirm the choice to take into account the three first alloying elements (Mn, Si, C), and to assume that their concentrations are 1.5, 0.4 and 0.16 wt. % respectively. Internet provides some information on steels: the web site of the university of Cambridge, department of H.K.D.H.Bhadeshia, can release TTT and CCT diagrams [14].

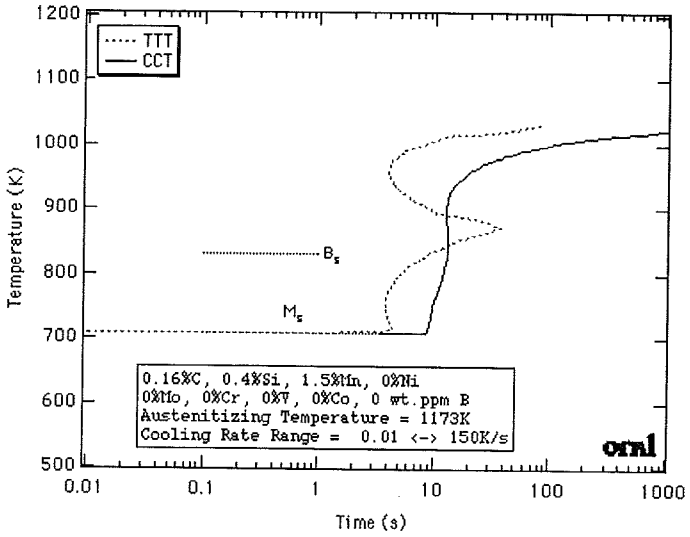

Figure 6: TTT and CCT diagrams calculated on Cambridge web site [14].

The chart on Figure 6 assumes that the material has been austenitised at 900°C.

Pictures 1 and 2 show SEM micrographs of the material as it was received from Hoogovens. At a low magnification, picture 1 shows the strongly banded structure oriented in the rolling direction. This is due to the microsegregation that takes place during the solidification of the liquid metal. Dendrites of ferrite δ form in an oriented way and the manganese remains preferably in the liquid phase. The banded structure is created by the mechanical deformation at high temperature of those dendrites. The presence of pearlite (seen on picture 2) is strongly dependent on the local concentration of manganese since this element has the effect to move the eutectoïd point to the left. Moreover, as the manganese lessens the eutectoïd level [15](i.e. the A1 temperature), its distribution has an effect on the microstructures that form upon cooling or heating through the (α,γ) phase transformation. When cooling, the first ferritic grains will appear in the regions poor in manganese. When heating, the first austenitic grains

will appear in the regions rich in manganese. The pictures 1 and 2 allow to think that the average grain size is around 5 μm.

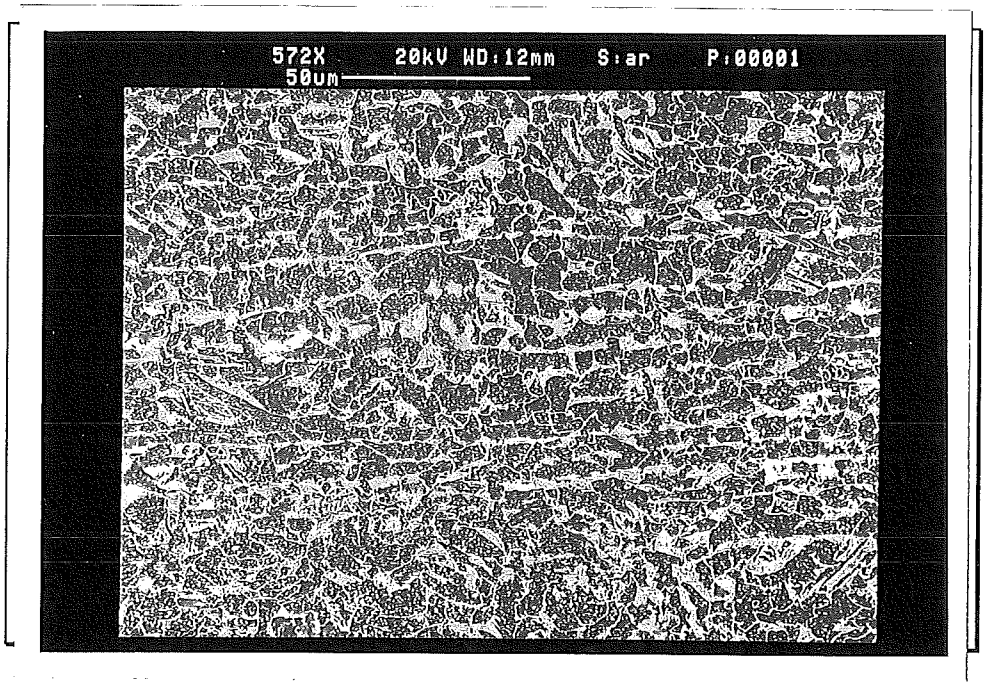

Picture 1 (AR) : SEM micrograph showing the hot-rolled microstructure of the material received from Hoogovens. A strongly banded structure is visible.

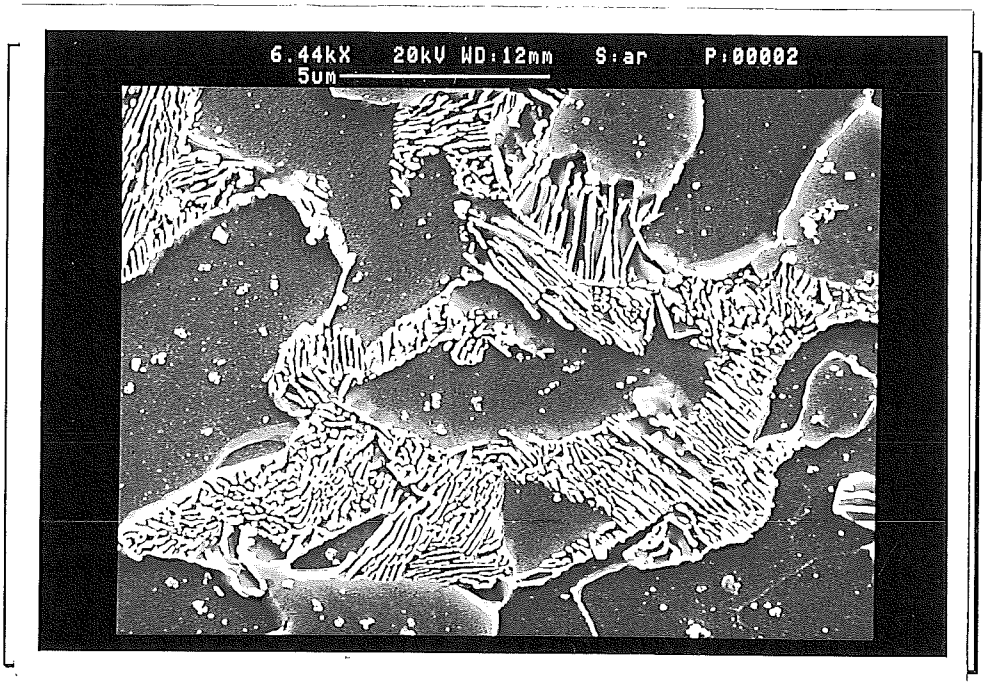

Picture 2 (AR) : SEM micrograph showing the ferritic-pearlitic microstructure of the material received from Hoogovens. The grain size is 5-10 μm.

2.2 Characterisation

2.2.1 Dilatometry

The main technique used in this investigation is dilatometry. All the experiments have been carried out in the Materiaalkunde at the Technische Universiteid Delft on a BAHR805. This apparatus belongs to the new generation of the technical instruments. Figure 7 might help to understand how the dilatometer works.

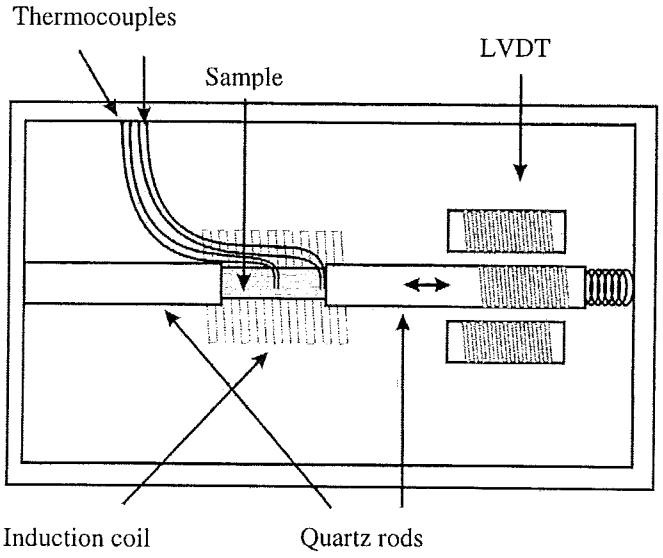

Figure 7: Schematic illustration of a dilatometer.

The sample, a solid cylinder 10 mm long and 4 mm in diameter is wedged between two quartz rod tensed by a spring. Two coils surround the sample : one is for the heating by high frequency induction and the other one projects a cooling gas during the possible quenches. Two cooling gases are available : nitrogen and helium. Nitrogen was used during the first experiments that required a quench, but it appeared clearly that it was not efficient enough. Thus helium was chosen, because of its higher calorific capacity, although it is more expensive.

Two thermocouples are welded on the surface of the sample. Only the temperature measured by the first one (welded in the middle of the sample) will be taken into account for the application of the temperature program, however the data measured by the second thermocouple can be used for the calculation of the temperature gradient that exists between the middle and the tips of the sample. The dilatation measurement employs a device called "Linear Variable Displacement Transducer". The value of $\Delta l(T)$ is set to zero at the beginning of the program, and this is always at the room temperature.

Experiment	Quenching mode	Bainitic holding	Temperature range
Gauging experiment	No	No	20-900 °C
For image analysis	Yes	No	20-800 °C
Isothermal trans.	Yes	Yes	20-900 °C
Test : 750 °C	Yes	Yes	20-950 °C

Table 4: Set of dilatometric experiments performed in this thesis work.

In order to have an idea of the range of temperatures covered by the experiments, one may look at the Table 4. About 55 experiments have been carried out. The two first ones were "gauging experiments", i.e. the aim was to measure the characteristic temperatures of the steel as well as its expansion coefficients. It is just a slow heating to the austenite region, followed by a slow cooling. A few experiments called here "For image analysis" consisted in an annealing, intercritical or not, followed by a quench to room temperature.

Most of the work was actually spent on the "Isothermal transformations" group; about twenty five experiments have been carried out according to the following process :

The sample is heated at the rate of 100 K/minute to one among three annealing temperatures : 750°C, 800°C or 900°C. It is annealed for 10 minutes, then quenched with helium gas to a level between 100°C and 500°C by steps of 50°C. This level is maintained for 15 minutes and is followed by a free cooling to the room temperature at the rate of 100 K/min. Those treatments are illustrated on Figure 8.

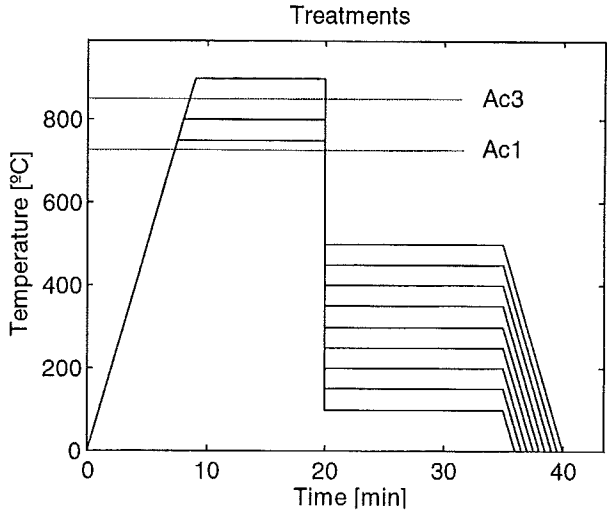

Figure 8: Representation of the dilatometric experiments performed for the analyse of isothermal transformations.

The horizontal dotted lines define Ac1 (= 725°C) and Ac3 (= 850°C). Finally, a few more "exotic" experiments, which were called "Test at 750°C", were performed. A maximum temperature of 950°C is reached on the whole set.

One must be aware that the BAHR805 is not just a conventional dilatometer. Indeed, a conventional device is just able to measure a change in length while the temperature is evolving. It is thus adapted for gauging measurements : slow heating, slow cooling. On the other hand, the apparatus used in this work is a "quench" dilatometer. It means that one can include quenching modes in the program, and the big interest is to measure the dilatation that takes place during an isothermal holding that follows the quench. This option is essential for someone who wants to draw TTT diagrams.

It is very important to check that the sample did not move between the rods during the experiment because it would introduce a jump in the change in length data. Unfortunately, it often happens that the gas blown destabilises the sample during the quench, ant it renders the experiment decayed.

When performing dilatometry experiments, one should always be aware of the decarburisation problems. At high temperatures, some carbon close to the surface may leave the sample because of the strong diffusion. If so, the following measurements and calculations would be falsified since the composition would have been locally changed. This is why it is important to look at the surface of a slice cut in the sample in order to see if there is, or not, a segregation between the edge and the centre. Concerning this work, a checking was done on some samples austenitised during 10 minutes at 950°C and no decarburisation was observed. Indeed, this phenomenon can appear only from higher temperatures (at least 1100 °C).

2.2.2 Microstructural characterisation

Some of the samples analysed by dilatometry were chosen for microstructural examination. Two slices about 1 mm thick were cut in each of them : one was taken in Louvain-la-Neuve for microscopical observation, and the other one was kept by Dr. Lie Zhao, from the Materiaalkunde, TUDelft, for X-ray analysis. Those samples were cut very carefully with a diamond saw so as to avoid the mechanically induced transformation of retained austenite. (TRIP effect).

Microstructures were studied by scanning electron microscopy (SEM) and by optical microscopy. The polishing has been done to a fineness in the diamond powder of 0.25 μm. In order to make possible the distinction between retained austenite and martensite by SEM observation, specimens were first annealed for 2 hours at 200°C and then etched with 2 %

nital (Norvanol + 2 % HNO_3). Because of the carbide precipitation during the annealing, the martensite appears as finely cracked grains, while austenite grains remain perfectly smooth [16].

The image analysis was performed on pictures scanned from the SEM with a semi-automatic routine working with Visilog. The application was the measurement of the fraction of phase in quenched samples. It required fifty pictures magnified around 1400 times and taken all around the facet of the sample. For each picture, a brightness threshold has to be defined in order to distinguish the ferrite from the martensite. It is important to take pictures properly scattered on the entire available surface because there may be some variation of the phase's fraction depending on the situation with respect to the edge of the sample.

2.3 Calculations

2.3.1 Dilatation-Phase fraction

As for the majority of the materials, steel undergoes a dilatation when it is submitted to a rise in temperature. If there is no phase transformation during the heating, the dilatation can be described by mean of an expansion coefficient. If there is a transformation, one must take into account the different crystallographic phases that coexist at a given temperature.

Two conventional techniques for the calculation of the phase fractions, for instance during a cooling from the austenitic region to the ferritic region, are presented here. The first one bears the name of "lever rule", whereas the second method involves the lattice parameters. (This lever rule should not be mistaken with the lever rule relevant for the phase diagrams.) The second method constitutes the basis of all further calculations in this work.

2.3.1.1 Lever rule

The volume fraction of austenite can be calculated as follows:

$$f_\gamma = \frac{\mathrm{fer} - \mathrm{cil}}{\mathrm{fer} - \mathrm{aust}} \qquad (1)$$

The lever rule method is illustrated on Figure 9 and by equation (1). The application of this method requires the assumption of proportionality between the phase fraction and the length change. By virtue of extrapolation of the linear expansion and contraction curves of the ferrite phase and the austenite phase, we can define these values :

- fer = Length change of a heated sample that would remain 100 % ferritic.
- aust = Length change of a cooled sample that would remain 100 % austenitic.
- cil (change in length) = Actual change in length of a sample cooled from 900 °C at 3K/min.

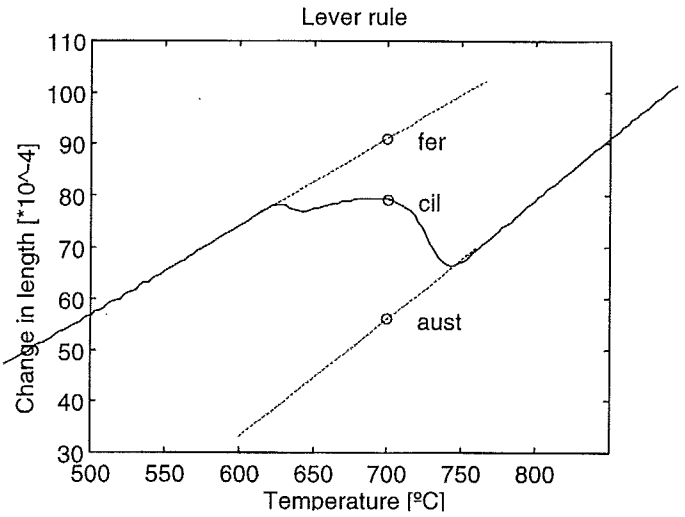

Figure 9: Illustration of the 'lever rule' on a dilatometric cooling curve.

Those values are temperature dependent, and, in this example, it is at 700°C. The lever rule is very easy to apply, but the assumption of proportionality is too strong. Furthermore, using this technique could not help to measure the amount of a new phase growing during the isothermal level of an intercritical annealing, or of a bainitic holding. As a matter of fact, precisely that kind of calculation was to be performed in this thesis work. Another kind of calculation has thus to be used.

2.3.1.2 Calculation based on the lattice parameters

The following developments mainly come from an article of Lie Zhao [17]. As explained in the previous pages, the dilatometer allows to measure the dilatation of a sample, which follows a temperature program, previously defined by the user. But it is technically easier to measure a length change ($\Delta l = l - l_0$) than a volume change ($\Delta V = V - V_0$), and those values can be linked thanks to the following formula.

$$1+\frac{\Delta V}{V_0} = (1+\frac{\Delta l}{l_0})^3 = 1+3*(\frac{\Delta l}{l_0})+3*(\frac{\Delta l}{l_0})^2+(\frac{\Delta l}{l_0})^3 \qquad (2)$$

Since the value of $\Delta l / l_0$ is very small, the square term $(\Delta l / l_0)^2$ and the cubic term $(\Delta l / l_0)^3$ can be neglected. The following relation is thus obtained:

$$\frac{\Delta l}{l_0} \approx \frac{1}{3}\frac{\Delta V}{V_0} \qquad (3)$$

Another way to write the equation (3) is:

$$\frac{\Delta l}{l_0} = \frac{V'(T) - V_0}{3 * V_0} \qquad (4)$$

Where $\Delta l = l(T) - l_0$. The values l_0 and V_0 characterise the initial dimensions of the sample. These values are going to be the reference in comparison with which the variation is calculated. The initial dimensions are defined as the dimensions of the sample at the beginning of the experiment, or at the beginning of the isothermal transformation. $V'(T)$ is the instantaneous volume and it is a function of the temperature.

Let us consider now the case of a phase transformation taking place upon cooling. We suppose that there is only one product phase and one parent phase involved, for instance, the ferrite (α) phase and the austenite (γ) phase. We have to consider now the volume fractions f_α and f_γ. The instantaneous volume $V'(T)$ of the equation (4) can be expressed as follows :

$$V = \sum (f_i V_i) = f_\alpha V_\alpha + f_\gamma V_\gamma \qquad (5)$$

The sum of the volume fractions of the phases remains very logically equal to 1. Equations (4) and (5) establish the relation between the volume fraction and the length change. The next step will be to decompose the terms V_α and V_γ by means of the lattice parameters and the expansion coefficients multiplied by the temperature. This will introduce the link between the change in length and the temperature.

Here is the application of this type of calculation to a transformation that occurs during an isothermal bainitic holding. Some values like the lattice parameters and the expansion coefficients are still unknown but the calculations that will be made on the heating curve of the gauging experiments will give them. Anyway, those values will be used in a formula that figures out the fraction of retained austenite all along the isothermal holding. Two different formulas must be written : one relevant for the completely austenitised samples, and the other one for the cases when the quench is carried out from an intercritical region.

Austenitised samples :

$$\frac{\Delta l}{l_0} = \frac{(2 * f_{\alpha-B} * a_{\alpha-B}^3 + f_{\gamma-B} * a_{\gamma-B}^3) - a_{\gamma-A}^3}{3 * a_{\gamma-A}^3} \qquad (6)$$

The sign '-*A* ' means "in the austenitising region" and '-*B* ' stands for "bainitic". As a matter of fact, it is considered in the following calculations that the transformation that occurs during the isothermal holding produces bainite, although we are aware that it is not pertinent in the

case of a martensitic transformation for instance. As bainite is mainly composed of ferrite, its contribution in the volume is measured via the ferrite lattice parameter '$a_{\alpha-B}$'.

In this equation, just as in the following one related to the intercritically annealed samples, what is looked for is the value of '$f_{\alpha-B}$' (which is equal to $1-f_{\gamma-B}$). It represents the fraction of bainitic ferrite, while the interlamellar cementite will be included in the '$f_{\gamma-B}$' term. The part of cementite in a steel of such a composition is quite low.

The change in length 'Δl' is the data measured by the dilatometer, while 'l' is the length of the sample : 10 mm. The different lattice parameters must be written as is :

$$\begin{aligned} a_\alpha &= a_{\alpha 0} * \alpha_{ferrite} * T \\ a_\gamma &= (a_{\gamma 0} + c_1 * x_1 + c_2 * x_2) * \alpha_{austenite} * T \end{aligned} \qquad (7)$$

One should remember that x_1 and x_2 are the weight concentration of carbon and manganese in the austenite, and c_1 and c_2 are appropriate coefficients for the effect of the carbon and the manganese. These elements have an influence on the size of the lattice parameter of the austenite, in which the alloying elements have a higher solubility than in the ferrite lattice.

As the manganese stands in the iron lattice as a substitutional element, we may assume that it diffuses slowly, and thus x_2 is constant. On the contrary, the carbon is much more mobile, and it obliges us to apply the following assumption : the carbon concentrates in the austenite. This is why x_1 must be written :

$$x_1 = \frac{0.16}{f_\gamma} = \frac{0.16}{1-f_\alpha} \qquad (8)$$

On a mathematical point of view, it is interesting to note that a nice form of the solution of the complete equation cannot be found easily. This is why the Newton-Raphson method is a good choice for solving this equation.

Intercritically annealed samples :

$$\frac{\Delta l}{l_0} = \frac{(2*f_{\alpha-I}*a_{\alpha-I}^3 + 2*f_{\alpha-B}*a_{\alpha-B}^3 + f_{\gamma-B}*a_{\gamma-B}^3) - (2*f_{\alpha-I}*a_{\alpha-I}^3 + f_{\gamma-I}*a_{\gamma-I}^3)}{3*(2*f_{\alpha-I}*a_{\alpha-I}^3 + f_{\gamma-I}*a_{\gamma-I}^3)} \qquad (9)$$

'$-I$' indicates the "intercritical region". In this case it must be taken into account that there is already some ferrite inside the sample before the isothermal transformation of the austenite

begins. This is why the term '$2 * f_{\alpha-I} * a_{\alpha-I}^3$', which represents the intercritical ferrite, is present in V' and V_0 at the same time. Note that '$f_{\alpha-I}$' is a constant, either 0.1 or 0.55, depending on the temperature of the intercritical annealing, 800°C or 750°C.

What is going to be calculated is '$f_{\gamma-B}$', which represents the fraction of (retained) austenite and also the fraction of interlamellar cementite that is produced by the bainitic transformation. Then it will be easy to find '$f_{\alpha-B}$', the fraction of bainitic ferrite, by using this formula :

$$f_{\alpha-B} = 1 - f_{\alpha-I} - f_{\gamma-B} \qquad (10)$$

The details for the expressions of the lattice parameters are the same than in the case of the completely austenitised samples.

2.3.2 Newton-Raphson

Newton-Raphson is the name of an iterated calculation technique that allows to find easily a root of any equation, and it is especially interesting for equations that cannot be solved in an analytic way. The equation that must be solved should be written in the following way : $F(x) = 0$. The origin of the formula can be explained by the development of $F(x)$ in a Taylor series starting from a point x_0.

$$F(x) = F(x_0) + (x - x_0)F'(x_0) + \frac{(x - x_0)^2}{2!}F''(x_0) + \ldots \qquad (11)$$

If this Taylor series is truncated after the term of the first order, and if we are looking for a root, i.e. $F(x) = 0$, we get

$$0 = F(x) = F(x_0) + (x - x_0)F'(x_0) \qquad (12)$$

and thus

$$x = x_0 - \frac{F(x_0)}{F'(x_0)} \qquad (13)$$

As the Taylor series was truncated, the equation (13) is only an approximation of the solution. A better approximation can be found by repeating the operation as suggested by the following formula :

$$x_{i+1} = x_i - \frac{F(x_i)}{F'(x_i)} \qquad (14)$$

This method is extremely powerful but it needs the evaluation of the value of the derivative $F'(x_i)$. This can be done easily in the following way :

$$F'(x_i) = \frac{F(x_i + \varepsilon) - F(x_i - \varepsilon)}{2\varepsilon} \qquad (15)$$

where ε is a fixed small number. Once the difference between x_{i+1} and x_i has come under a defined threshold, the iteration is stopped. The user also has to define a starting value x_0 ; this one should be chosen close to the expected root in order to improve the convergence.
The Newton-Raphson method has been used in this work for the resolution of all the equations involving the phase fractions, function of the lattice parameters, who are themselves function of the phase fraction.

2.3.3 Matlab

Most of the calculations have been performed with the mathematical software MATLAB. Indeed, it is very convenient for the handling of big data files such as those produced by the dilatometer. A non-expert user can quickly manage with it as the programming language is simplified in comparison with a language like Pascal. It is obviously very adapted to the functional programming, i.e. one can define functions that will be used by different programs. Another advantage is that no compilation is necessary so the programs can be modified pretty easily. And a great interest of using Matlab is that one can present his results on very functional and readable charts. Unlike with Microsoft Excell, for instance, the user does not have to settle a lot of parameters in the picture, and, furthermore, the pictures do not need lots of memory on the hard drive of the computer, because the file format is postscript.

3. Results

This chapter contains three types of results : dilatometric observations, calculations based on the dilatometric data, and microstructural examinations. All of them are distributed throughout four sections. Section 3.1 is about information on the low silicon steel that were obtained thanks to gauging experiments. The second section (Section 3.2) develops a calculation based on the heating part of the gauging experiment. Section 3.3 , the biggest part, contains examinations of the bainitic holdings as well as calculations. The chapter ends with the section 3.4, which contains an analyse of a quite exotic dilatometric experiment.

3.1 First measurements

This part comprises results that could be obtained by the analyse of the data of the first gauging experiments. A slow heating to the austenitic region followed by a slow cooling allowed to measure the characteristic temperatures, the expansion coefficients and the transformation curves upon cooling and heating as well as at the equilibrium.

3.1.1 Characteristic temperatures

The first dilatometric experiment that was performed aimed to get basic information on the material such as the temperatures Ac1, Ac3, Ar1 and Ar3. For this, a sample was heated to 900°C at the rate of 3 K/min, which is the industrial practice, then it was kept at this level during 30 minutes, and finally cooled at 3 K/min. The whole experience lasted 10h30 ; this is sketched on Figure 10 hereunder.

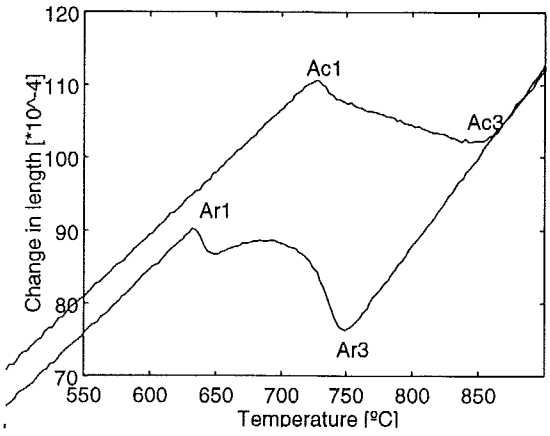

Figure 10: Dilatation of a sample heated to 900°C at 3 K/min, then cooled at 3 K/min.

One can properly see the phase transformation that takes place upon the heating as well as the one that takes place upon the cooling. We can notice that, at 900°C, the sample is completely austenitised. The second chart also represents the change in length, but this time as a function of the temperature. Therefore it is possible to measure the characteristic temperatures.

	Ac1	Ac3	Ar1	Ar3
°C	728	848	626	738

Table 5: Characteristic temperatures of the low-silicon steel.

'c' stands for *'chauffer'* ('to heat' in French), and *'r'* stands for *'refroidir'* ('to cool' in French). The temperature A2 is the one at which the iron becomes ferromagnetic when cooling down. It is possible to measure it by looking at the curve that shows the electric power spent in the coil as a function of the temperature (figure 11). As a matter of fact, there is a big step at 750°C that indicates the A2 temperature. The ferromagnetic transition demands a special amount of energy, just like a fusion would do.

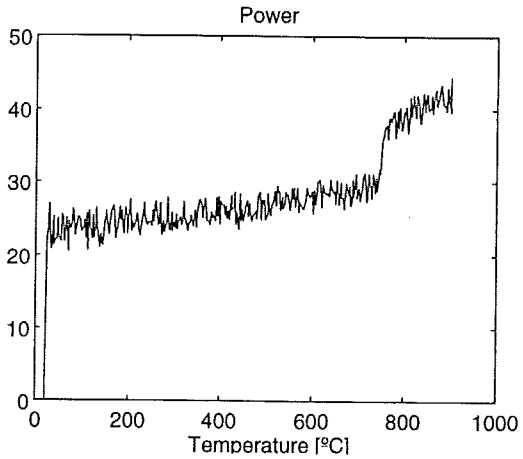

Figure 11: Electric power spent in the induction coil upon heating of a sample.

As we are dealing with the characteristic temperatures of a steel with a determined composition, we are able to calculate the temperatures corresponding to the 'bainite start' and the 'martensite start'. Here are Andrew's formulas [18] :

$$Bs = 830 - 270*[C] - 90*[Mn] - 37*[Ni] - 70*[Cr] - 83*[Mo] \qquad (16)$$

$$Ms = 539 - 423*[C] - 30.4*[Mn] - 17.7*[Ni] - 12.1*[Cr] - 7.5*[Mo] \qquad (17)$$

For our steel composition, we get

Bs =	652°C	Ms =	426°C

Those values agree with the TTT and CCT diagrams obtained from Bhadeshia's web site [14].

3.1.2 Expansion coefficients

Another important information that a dilatometer can bring is about the expansion coefficients. It is very important to have accurate values for them since they enter into account for all the calculations. Just by looking at the dilatation curve of this low silicon steel, one can set his ideas about those coefficients. A deeper research will follow in the section 3.2.

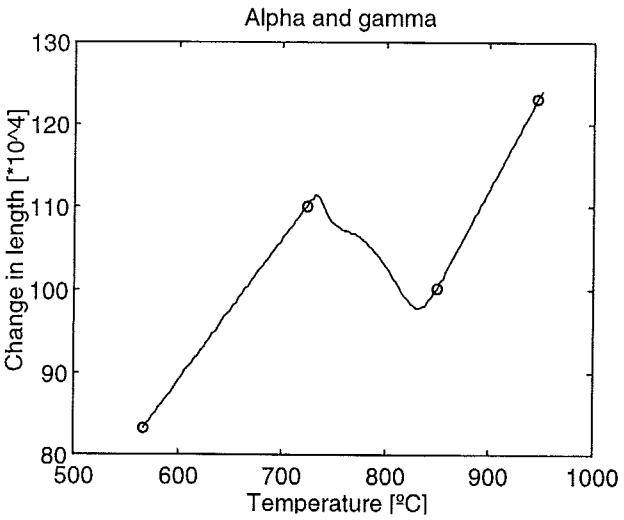

Figure 12: Dilatation curve upon heating of a sample at 3 K/min.

Figure 12 shows the change in length as a function of the temperature during the heating. The rings indicate the boundaries of the sections on which the expansion coefficient are calculated. The derivative of this curve is plotted on the Figure 13. The mean values of the expansion coefficients are calculated between the boundaries, and we get : $\alpha_\alpha = 17.14*10^{-6}\ K^{-1}$, for the ferrite, and $\alpha_\gamma = 23.62*10^{-6}\ K^{-1}$ for the austenite. Of course, these parameters do not depend on the temperature here although they should. α_α is just a mean value between 550°C and 725°C, and α_γ is between 850°C and 950°C. In the further development, a more accurate coefficient will be obtained for the ferrite, but we will keep $23.5*10^{-6}\ K^{-1}$ for the austenite.

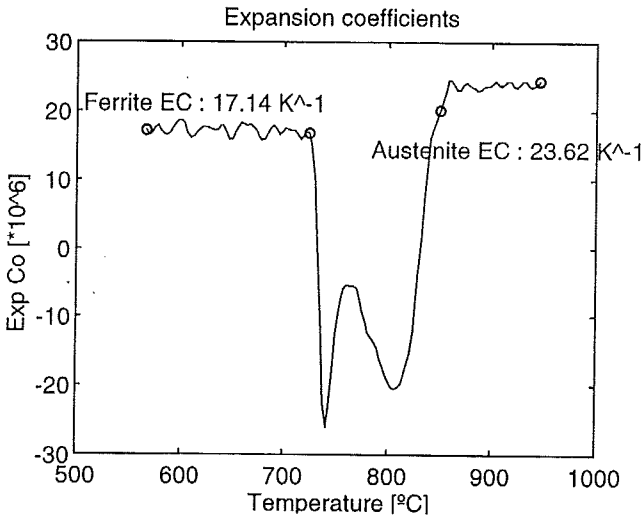

Figure 13: Measured expansion coefficient as a function of the temperature. The given values are for the averages on the regions defined by the rings.

3.1.3 Transformation curves

This comprises the cooling part and the heating part. What is meant by 'cooling part' is the transformation of the austenite into pearlitic ferrite during the experiment at 3 K/min. Figure 14 illustrates the phase transformation upon cooling. How can one measure the austenite fraction that disappears during the cooling ? As explained earlier, we can do it with the lever rule described in figure 9, or with a calculation based on the lattice parameters.

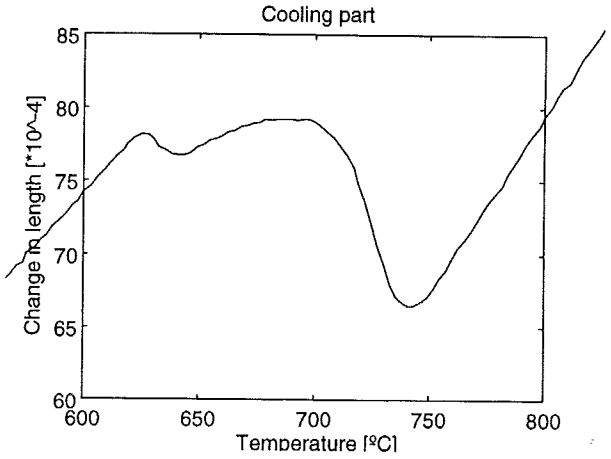

Figure 14: Dilatation curve measured upon cooling.

The result of the lever rule method is plotted on Figure 15. It is necessary to remember the previously established characteristic temperatures: Ar1 = 626°C and Ar3 = 738°C. The tips of the lever rule curve seem to be a little bit too much on the right.

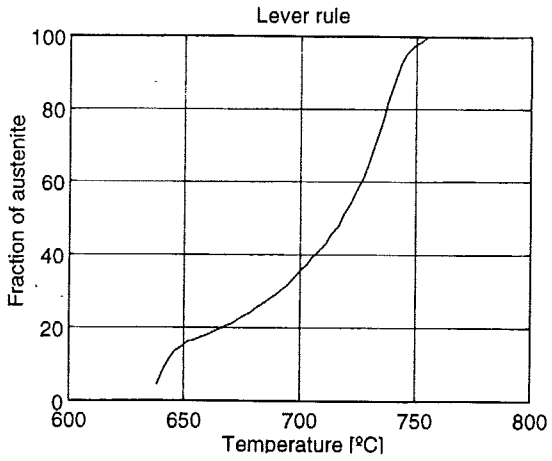

Figure 15: Calculated fraction of the austenite that disappears upon cooling. By the 'lever rule' method.

It is worth trying another kind of measurement for the phase fraction. The curve on Figure 16 is the result of a calculation that involves the lattice parameters : Theo Kop, from the Materiaalkunde in TUDelft, proposed a program applied to the pearlitic transformation during the cooling of a completely austenitised steel. The result seems in better agreement with the measured values of Ar1 and Ar3. Both lever rule and Theo Kop's program show an angle in the curve when the last 20 % of austenite finally transform into pearlite.

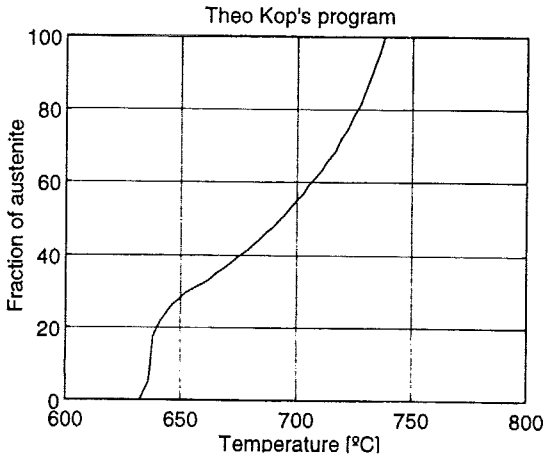

Figure 16: Calculated fraction of the austenite that disappears upon cooling. By a method based on the lattice parameters, and programmed by Theo Kop.

As a matter of fact, a quick calculation gives about 20 % of austenite when the eutectoïd level is reached : $\frac{0.16-0.02}{0.78-0.02}=18.5\%$.

After this quick look at the cooling part, the investigation continues with the heating part. The ring in the inflexion on the curve of the Figure 17 indicates the end of the decomposition of the cementite contained in the pearlite. The fraction of coming austenite can be calculated by the lever rule method. It requires to draw linear extensions for both ferrite and austenite (Figure 18), and then the equation (1) is applied. The result is displayed on Figure 19.

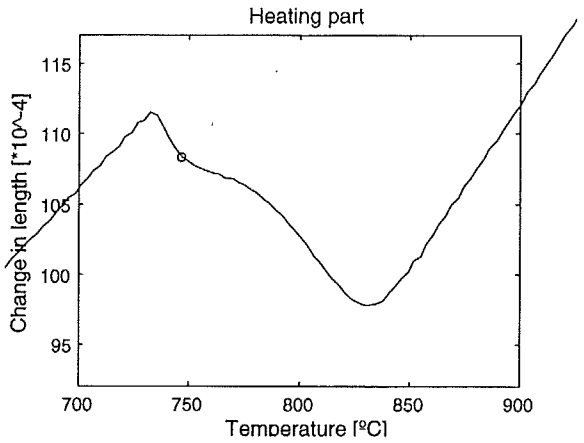

Figure 17: Dilatation curve upon heating at 3 K/min.

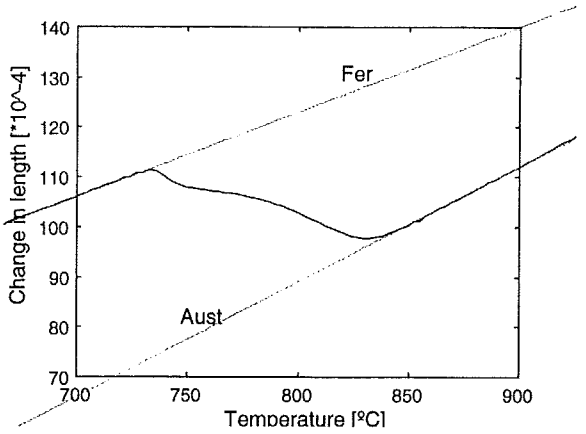

Figure 18: Application of the 'lever rule' method upon heating. Extensions for the ferrite and for the austenite have been drawn.

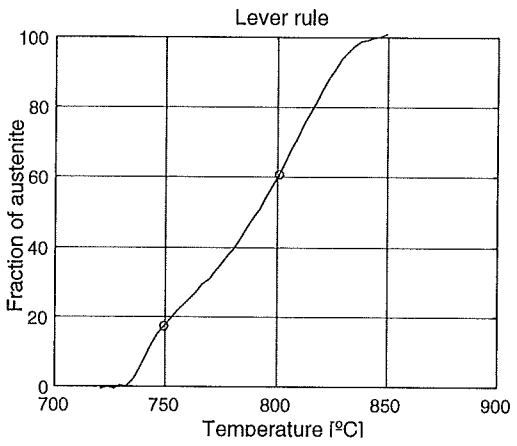

Figure 19: Fraction of austenite calculated by 'lever rule' upon heating.

One should remember that Ac1 = 728°C and Ac3 = 848°C. These values are fitting quite well with the chart that yields the fraction of austenite during the heating. One can still observe a slight inflexion around 20 % of austenite. It corresponds to the end of the decomposition of the pearlite.

The introduction of this thesis talks about an intercritical annealing, i.e. a thermal treatment in which a steel is maintained for several minutes at a temperature comprised between Ac1 and Ac3. The idea is to get, at the end of this intercritical annealing, a microstructure that contains both ferrite and austenite.

It is worth remembering that most of the experiences performed in this research includes a bainitic or a martensitic holding preceded by either a complete austenitising or an intercritical annealing. It is therefore time to choose the parameters of these treatments.

The phase fraction depends on the chosen temperature, as can be seen on Figure 19. As this curve corresponds to the heating, it is a good starting point for the choice of two intercritical temperatures. If the first one must give around 20 % of austenite, 750°C seems to be a good choice. And if we want more than 50 % of austenite, we can take 800°C as a second intercritical temperature. Finally, the choice of an austenitising temperature must be done according to the conventional rule : = Ac3 + 50 K. This is why 900°C was chosen.

When the distribution of the phases during cooling and heating at low rates is known, one must check it with an MTData calculation. The relative positions of the curves with respect to the equilibrium curve should fit.

3.1.4 MTData calculation of the equilibrium

The MTData software allows to calculate the distribution of the phases at the equilibrium, just on basis of the composition of the alloy [19]. The assumption intended by 'equilibrium' is that every alloying element would have enough time and kinetic energy to diffuse from one phase to another. For instance, all the carbon and the manganese would go in the austenite, while the silicon would go in the ferrite.

Applied to our case, the crystallographic phases that must appear in the current calculation are

- ferrite : Body Centred Cubic.
- cementite.
- austenite : Face Centred Cubic.

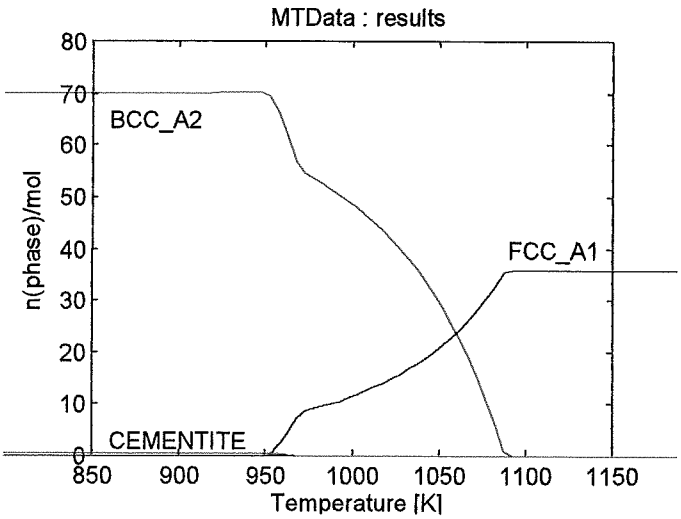

Figure 20: Output data of an MTData calculation of the equilibrium. Three phases are taken into account: ferrite, austenite and cementite.

Figure 20 gives the concentration of unit cells of those phases as a function of the temperature. The number of cementite unit cells is very low, even under 950 K, because this steel has a low carbon content (0.16 wt. %), and because the cementite unit cell is quite big compared to the ferrite and the austenite cells. Beside this, it is obvious that the ferrite (at low temperatures) has approximately two times more unit cells than the austenite (at high temperatures). This result can be drawn in such a way that we get the percentage of austenite as a function of the temperature. Indeed, this is the third curve of Figure 21.

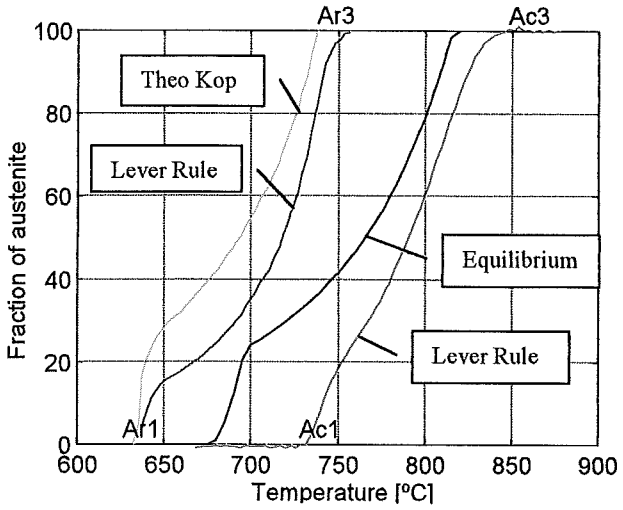

Figure 21: Synthesis of the previously calculated curves for the austenite fraction.

The first curve in figure 21 is the fraction of austenite during the cooling calculated by Theo Kop's program, the second one corresponds to the cooling as well but calculated by the lever rule, while the last curve corresponds to the heating, by lever rule. The approximate positions of Ac1, Ac3, Ar1 and Ar3 help to understand that the equilibrium curve is properly situated in the middle with respect to the heating and the cooling curves.

A good thing would have been to calculate the para-equilibrium curve. In this case, the assumptions are that the carbon can still diffuse perfectly, but the bigger atoms like manganese and silicon, which are in a subtitutionnal solution position, cannot move, i.e. they remain well distributed among each phase. The para-equilibrium is a situation that can be reached in a few minutes, to the opposite of the complete equilibrium that requires several hours, maybe several days. An intermediate assumption is closer to the reality of an intercritical annealing of 10 minutes.

3.2 Calculation upon the heating data

This part deals with different calculations based on the dilatometric data coming from the slow heating of the gauging experiment. The calculation method that is employed here is the one developed in the section 2.3.1.2. First results are about the ferrite (3.2.1 and 3.2.2); while others allow to produce a profile curve for the transformation of the ferrite into austenite (3.2.3). An interest of these calculations is the fitting of several parameters, which are summarised in the last part (3.2.4).

3.2.1 Calculation of the expansion coefficient of the ferrite

Here follows the results of a program that calculates the expansion coefficient of the ferrite. By using the least square method, it fits a parabolic curve with the experimental heating curve of the change in length as a function of the temperature. Figure 22 presents the experimental curve as well as the fitting curve.

The second degree equation obtained for the parabola is :

$$-2.939 + 0.131 * T + 0.00003747 * T^2 = 0 \qquad (18)$$

where the temperature is expressed in Celsius degrees. Let us remark that the second root of this equation should give the temperature of the room where and when the experiment was performed. As a matter of fact, the change in length is set to zero at room temperature. In this case it was 22.4°C.

A correct result for the expansion coefficient can be found by dividing the 2 last terms by T.

$$\alpha_{fer} = (0.131 + 0.00003747 * T) * 10^{-4} \quad [K^{-1}]$$
$$\alpha_{fer} = (13.1 + 0.003747 * T) * 10^{-6} \quad [K^{-1}] \qquad (19)$$

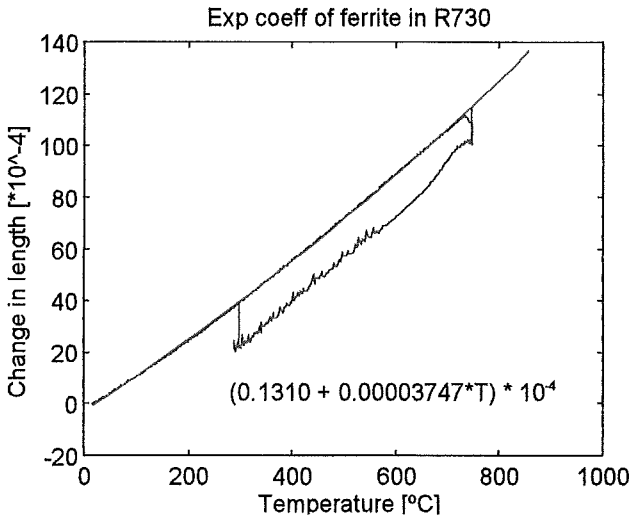

Figure 22: Fit of a parabolic curve (red) to the heating part of a experimental curve (blue).

3.2.2 Lattice parameter of the ferrite and the cementite

In the previous paragraph, a value for the expansion coefficient of the ferrite was calculated. Actually, our material is composed of ferrite with some cementite and the expansion coefficient used in the calculation should take into account the presence of cementite. The object of this part is the calculation of values for the initial (read at T = 20°C) lattice parameters for the ferrite phase and the cementite phase. One way to do that is to plot an

experimental curve of a heating from 20°C to Ac1, beside a second plot of a simulated change in length using given coefficients.

The simulation can be done by using the formula (4) described earlier.

$$\frac{\Delta l}{l_0} = \frac{V'(T) - V_0}{3 * V_0}$$

As in this range of temperature the alloy is composed of ferrite and cementite, one needs to know the proportion of the phases. For a steel containing 0.16 wt. C, if we consider that all the carbon resides in the cementite, a quick calculation shows that there is 2.1 % of Fe_3C.

V_0 is the initial relative volume, i.e. it is equal to V' when $T = T_0 = 20°C$.

Here is an expression for $V'(T)$, the current relative volume of the sample (it depends on the current temperature) :

$$V'(T) = 2 * 0.979 * a_\alpha^3(T) + \frac{1}{3} * 0.021 * a_\theta^3(T) \qquad (20)$$

where a_α is the lattice parameter of the ferrite and a_θ is the lattice parameter of the cementite.

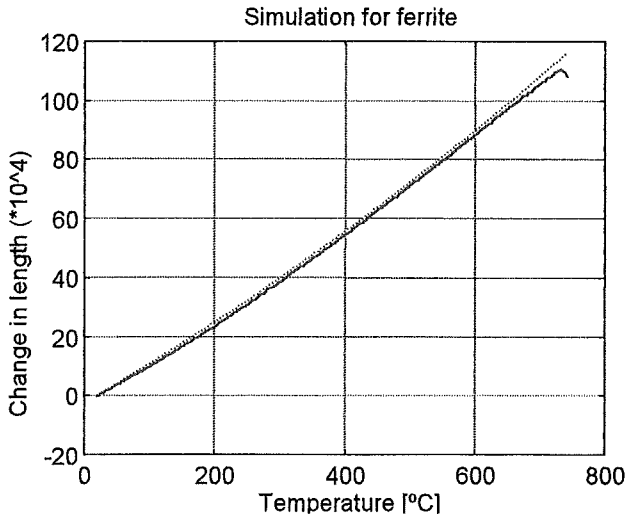

Figure 23: Fit of a calculated dilatation curve (red) to an experimental dilatation curve (blue).

Figure 23 holds the experimental dilatation curve (blue) and the calculated dilatation curve (red and dotted). The deviation between them has been drawn on the Figure 24. Using the parameters $a_{\alpha 0} = 2.8830$ Å, $a_{\theta 0} = 4.5234$ Å, $b_{\theta 0} = 5.0883$ Å, $c_{\theta 0} = 6.7426$ Å, we have a correct estimation of the dilatation, since the difference remains small under Ac1. This calculation takes into account only two phases, so it is not correct anymore once cementite starts to dissolve as austenite appears, i.e. once Ac1 has been reached.

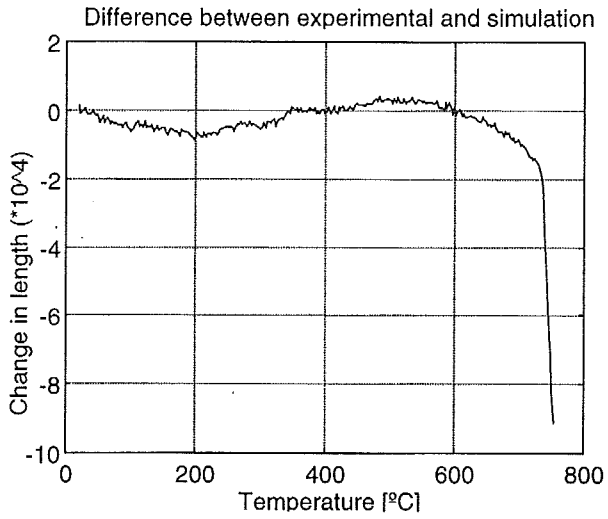

Figure 24: Difference between the curves showed on the figure 23.

3.2.3 Transformation curve

Here comes an important result of this work. Using a calculation that implies the lattice parameter and the change in length as a function of the temperature, it was possible to determine the amount of austenite that appears during the heating of this low silicon steel.

3.2.3.1 Calculation

Only two phases can be taken into account in the calculation : ferrite and austenite. That is why the temperature range on which it is acceptable starts at the end of the decomposition of the pearlite, i.e. when the only phases that remain are ferrite and austenite.

Here is the expression for the change in length, adapted from equation (6) [17] :

$$\frac{\Delta l}{l_0} = \frac{2 * f_{\alpha-I} * a_{\alpha}^3 + f_{\gamma-I} * a_{\gamma-I}^3 - V_0}{3 * V_0} \qquad (21)$$

The *-I* stands for *intercritical.* The idea is to calculate $f_{\gamma-I}$ (= 1 - $f_{\alpha-I}$) as the temperature and the change in length are known. The lattice parameter of the ferrite is given by the following equation :

$$a_{\alpha} = a_{\alpha 0} * (1 + 13.04 * 10^{-6} * T + 0.003702 * 10^{-6} * T^2) \qquad (22)$$

and the lattice parameter of the austenite is

$$a_{\gamma-I} = (a_{\gamma 0} + c_1 * x_1 + c_2 * x_2) * (1 + 23.5 * 10^{-6} * T) \qquad (23)$$

Equations (22) and (23) are identical to the equations (7) except for the values of the expansion coefficients, which have been modified according to the above calculation. As the

solubility of alloying elements is much higher in the austenite, their concentrations have an important effect on its overall lattice parameter. One way to take this effect into account is to add a term including the weight concentration (x) multiplied by a coefficient (c). In the case of this alloy, the important elements in solution are the carbon and the manganese. The weight concentration of the carbon in the austenite is written x_1 while x_2 stands for the manganese. Usual values for c_1 and c_2 are 0.033 and 0.00095 [20-21]. Let us notice that the effect of the carbon is much stronger than the effect of the manganese. The silicon prefers to go in the lattice of the ferrite, so it does not exert a big influence on the lattice of austenite [15]. An important assumption that must be done was previously presented as the equation (8).

$$x_1 = \frac{0.16}{f_{\gamma-I}} \qquad (8)$$

In the intercritical region, all the carbon concentrates in the austenite. Indeed, carbon is gammagene, and diffusion is high enough at temperatures where austenite can appear, i.e. above Ac1, since the carbon atom is small and diffuses easily.

The solution of the complete equation can be found by using the Newton-Raphson method.

Let us look at the result for heating up to 900°C.

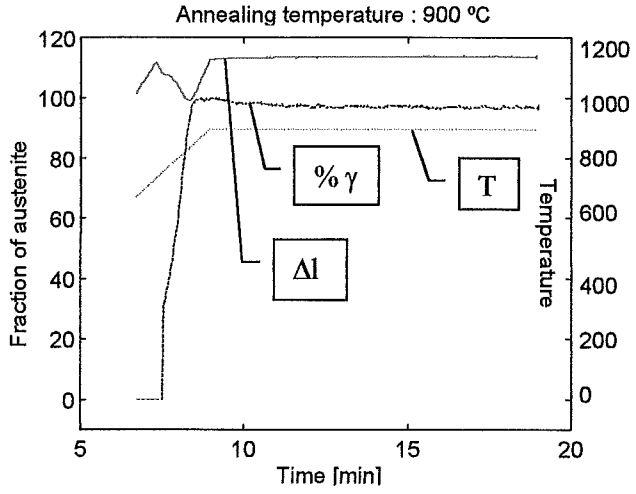

Figure 25: Representation of the end of a heating to 900°C followed by an intercritical annealing of 10 minutes.

The chart of Figure 25 describes the heating to 900°C of a sample in the dilatometer. The X-axis represents the time of the experience. As the heating rate is 100 K/min, 900°C is reached after 9 minutes. The dotted blue line is the temperature. The continuous line is the

change in length of the sample. And the third line represents the fraction of austenite, calculated with the equation (21).

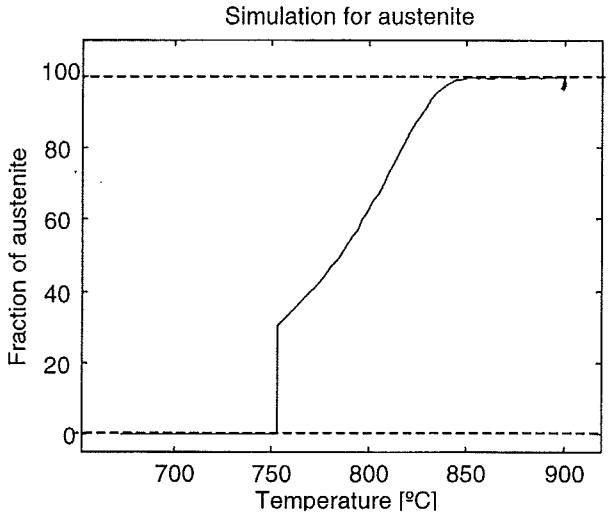

Figure 26: Calculated fraction of austenite that appears upon heating to 900°C.

This first result (showed again on Figure 26) was used in order to set parameters such as the expansion coefficient of the austenite and the coefficients for the carbon and the manganese. Let us look at the fraction of austenite as a function of the temperature. The upper part should remain at 100 % and it should be flat. The first thing is to define an expansion coefficient for which the slope of the upper part was equal to zero, and then define the coefficients c_1 and c_2 for carbon and manganese for which the plateau was set at 100 %. As a matter of fact, c_1 and c_2 are fitting parameters. The finally chosen values are $c_1 = 0.046$, $c_2 = 0.00103$ and $\alpha_\gamma = 23.5*10^{-6}\ K^{-1}$.

Let us see now where goes this new "heating curve" with respect to the lever rule curves that were talked about in the part 2.2.2.4. On Figure 27, the green curve is the one calculated presently and that is plotted on Figure 26. Remember that the blue curves correspond to the cooling part, the black one is the equilibrium and the red one is the fraction of austenite during the heating calculated by the lever rule.

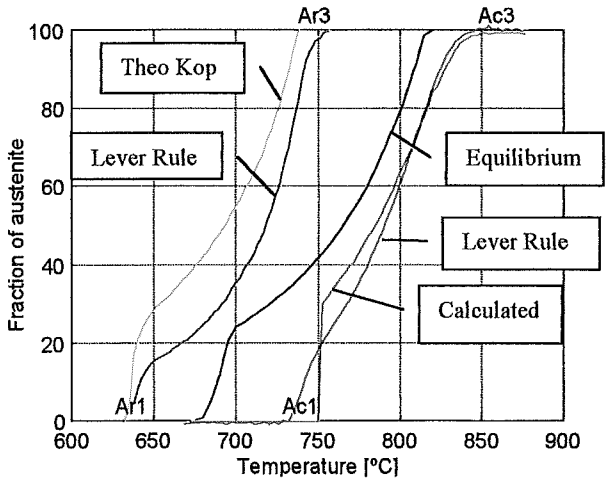

Figure 27: Synthesis of the calculated curves for the austenite fraction as a function of the temperature. (Same chart than this of the figure 21, but with the curve of the figure 26.)

Now that we have values for the fitting parameters, the calculation can be applied to a heating up to 750°C followed by an intercritical annealing of 10 minutes.

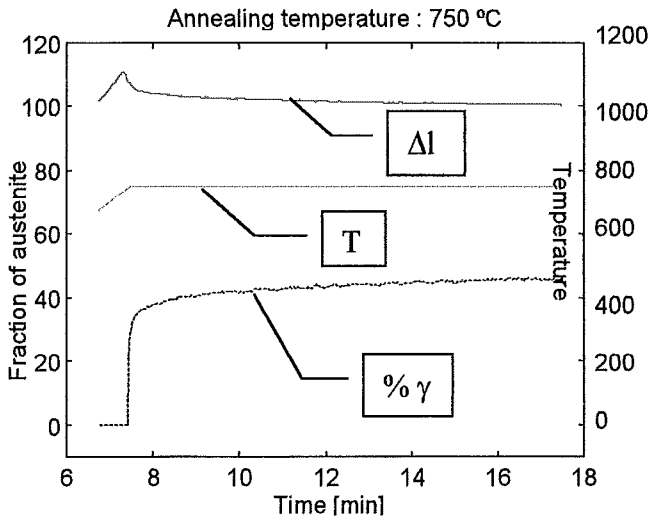

Figure 28: Representation of the end of a heating to 750°C followed by an intercritical annealing of 10 minutes.

On Figure 28, the dotted line still represents the temperature just like on Figure 25, the continuous line is the change in length and the interrupted one is the fraction of austenite. One can notice that once 750°C has been reached, there is still some transformation all along the annealing of 10 minutes. At the end, the calculation of the equation (21) gives an austenite amount of about 46 %. Remembering the assumption that all the carbon concentrates in the

austenite, the carbon concentration can be calculated with the equation (8). The result is showed on Figure 29 and it stabilises at 0.35 wt. % C at the end of the annealing. This number will have an important influence on the future transformation(s) of this austenite, since carbon slows down the formation of ferrite upon cooling [15].

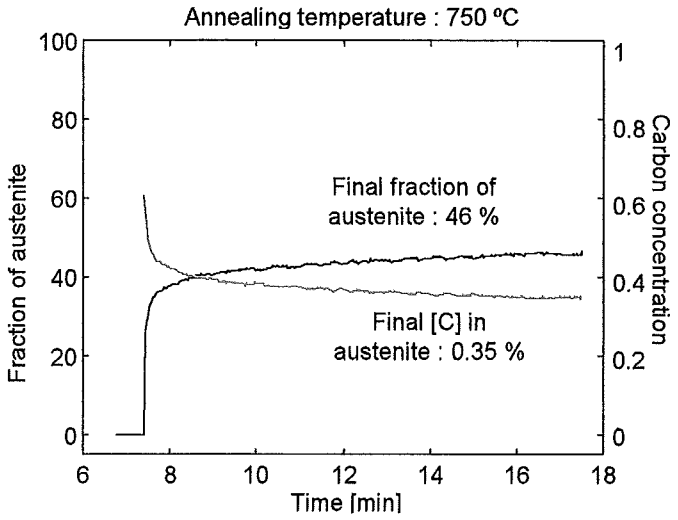

Figure 29: Representation of the calculated fraction of austenite, as well as the carbon concentration in the austenite during an intercritical annealing at 750°C.

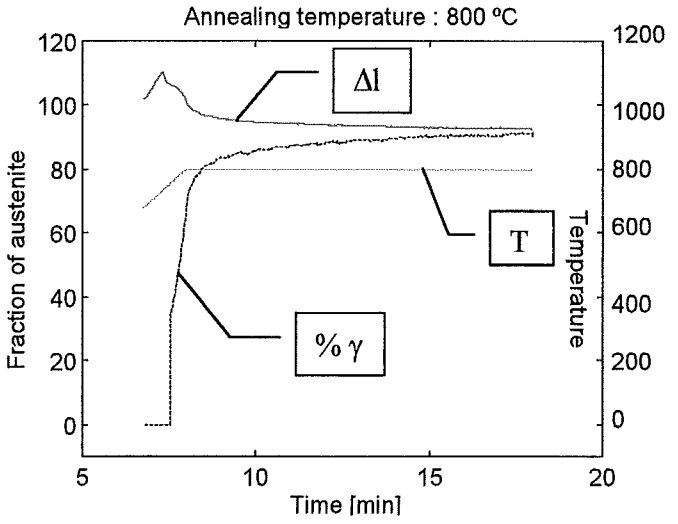

Figure 30: Representation of the end of a heating to 800°C followed by an intercritical annealing of 10 minutes.

The third heat treatment in the heating part is an intercritical annealing at 800°C. Results of the calculation based on the equation (21) is showed on Figure 30. We can expect that there will be more austenite formed by the end of the annealing than in the case of the annealing at

750°C. The curves of Figure 30 show obviously that more than 10 % of the final austenite has been formed after the 800°C level was reached. According to the calculation, the fraction of austenite should be 91 % at the end of the 10 minutes annealing. That would mean an austenite charged with 0.18 wt. % C, which is not very different from the overall concentration (figure31).

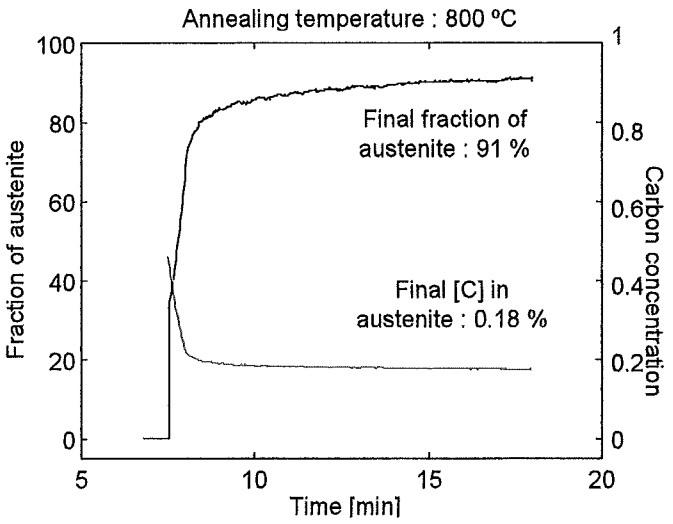

Figure 31: Representation of the calculated fraction of austenite, as well as the carbon concentration in the austenite on an intercritical annealing at 800°C.

In order to set the ideas concerning the effects of the different annealing treatments, one can look at the pictures showed in the Figure 32 to 34. Remember that those results are yielded by the calculation based on the equation (21). Only the phase fractions presented hereafter will be taken into account in the further calculations.

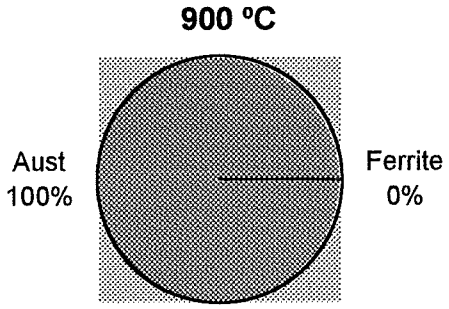

Austenitised at 900°C during 10 minutes.

Carbon concentration in the austenite : 0.16 %.

Figure 32

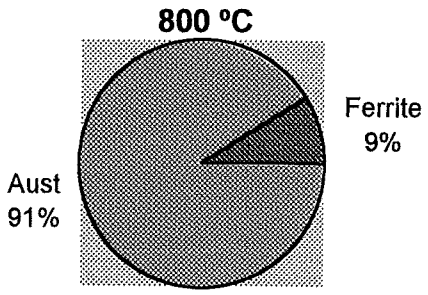

Annealed at 800°C during 10 minutes.

Carbon concentration in the austenite : 0.18 %.

Figure 33

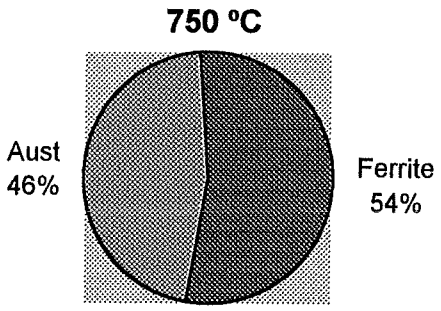

Annealed at 750°C during 10 minutes.

Carbon concentration in the austenite : 0.35 %.

Figure 34

During the ulterior cooling, the ferrite will remain the same. What is going to interest us is what will happen to the austenite in the continuation of the thermal treatment.

3.2.3.2 Microstructure analysis

The usual way to measure the fraction of phase in an intercritically annealed sample is to quench it to the room temperature and practice image analysis on the metallographic specimen. A sample was heated according to the temperature program described on Figure 35 and then quenched so that the austenite was completely transformed into martensite.

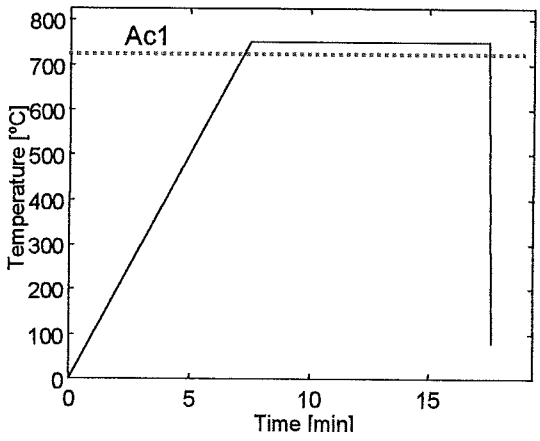

Figure 35: Heat treatment for the image analysis of a sample annealed at 750°C.

After having followed the procedure described in the section 2.2.2, the final result for the sample annealed at 750°C (picture 3) is a fraction of 44.2 % for the bright phase, which is the martensite. The standard deviation for the whole data is 2.77 %. The fraction of austenite is therefore around 44 % as well.

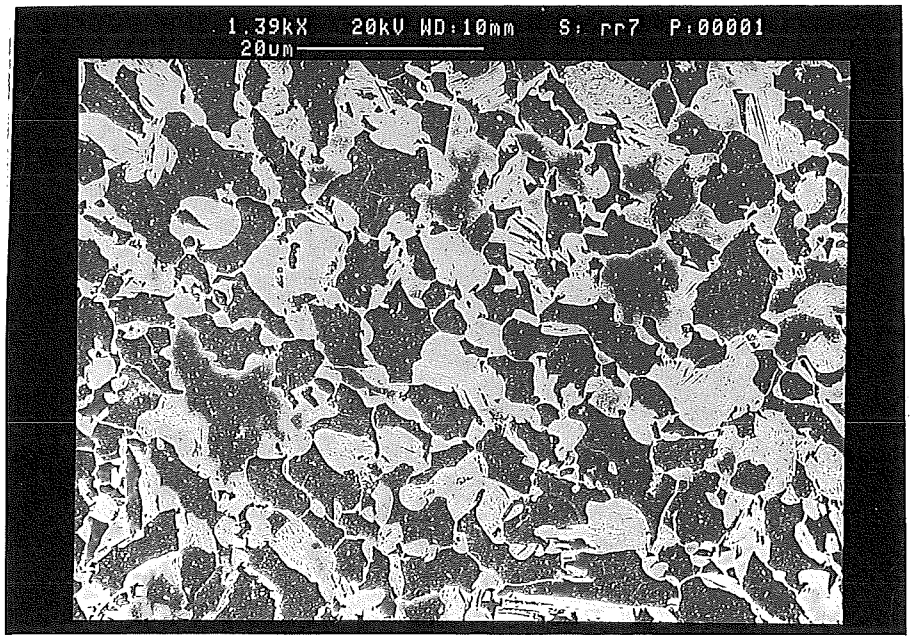

Picture 3 (RR7) : SEM micrograph of a sample intercritically annealed at 750°C for 10 minutes, then quenched to room temperature. Magnification : 1400 X.

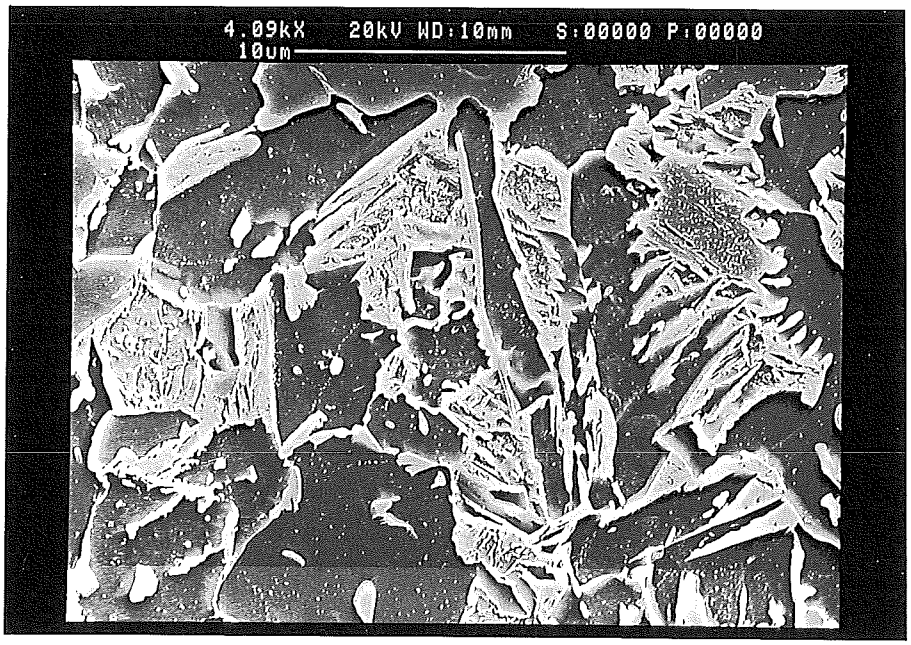

Picture 4 (RR8) : SEM micrograph of a sample intercritically annealed at 800°C for 10 minutes, then quenched to room temperature.

The SEM micrographs of the sample annealed at 800°C were also analysed with Visilog. The result obtained yields 58.1 ± 5.2 % of martensite, i.e. austenite before the quench.

3.2.4 Fitting parameters

Here is a table that summarises the whole set of coefficients that have just been defined. It includes the expansion coefficients, the lattice parameters, and the coefficients c_1 and c_2 of the equation (23). These numbers are mostly inspired from a paper of Dyson and Holmes [20], and have been refined to fit the calculation. In a first time, the assumption is that the composition of the alloy is the one given by Hoogovens, i.e. from the table 1.

	Mn	Si	C
Wt. %	1.5	0.4	0.16

Table 1: Composition given by Hoogovens.

For this composition, the parameters are presented in the Table 6 :

Ferrite :	$a_{\alpha 0}$	= 2.883 [Å]	at 0 °C
	α	= (13.1 + 0.003747*T)*10^{-6}	T expressed in °C
Cementite :	$a_{\theta 0}$	= 4.5234 [Å]	at 20 °C
	$b_{\theta 0}$	= 5.0883 [Å]	at 20 °C
	$c_{\theta 0}$	= 6.7426 [Å]	at 20 °C
	α	= 5.311*10^{-6} − 1.942*10^{-9}*(T+273) + 9.655*10^{-12}*$(T+273)^2$	T expressed in °C
Austenite :	$a_{\gamma 0}$	= 3.5972 [Å]	at 25 °C
	α	= 23.5*10^{-6}	
	c_1	= 0.046	
	c_2	= 0.00103	

Table 6: Chosen parameters when the composition is defined by the table 1.

The parameters have also been calculated assuming the composition that has been measured in Delft, i.e. from the table 2.

	Mn	Si	C
Wt. %	1.47	0.28	0.14

Table 2: Composition measured at the TUDelft.

In this case, the only parameters that are different from those of the Table 6 are c_1 and c_2, from the equation (23). As a matter of fact, these are the only parameters who depend on the concentration of the alloying elements. In this case, they must be set at :

c_1	0.052
c_2	0.0011

Table 7: Parameters for the influence of the carbon and the manganese according to the composition defined in table 2.

Nevertheless, it seems more appropriate to work with the composition of the table 1 because of the complexion problems that may have appeared during the chemical analysis with the ICP.

3.3 Bainitic transformation

Firstly, the dilatometric curves will be observed and compared according to the thermal treatment applied to the samples. In the second part, there will be a short analysis of the microstructures obtained for the different annealings. And finally, we will see the results obtained by the calculations presented in the section 2.3.1 and applied to the data measured in 3.3.1.

3.3.1 Isothermal holdings

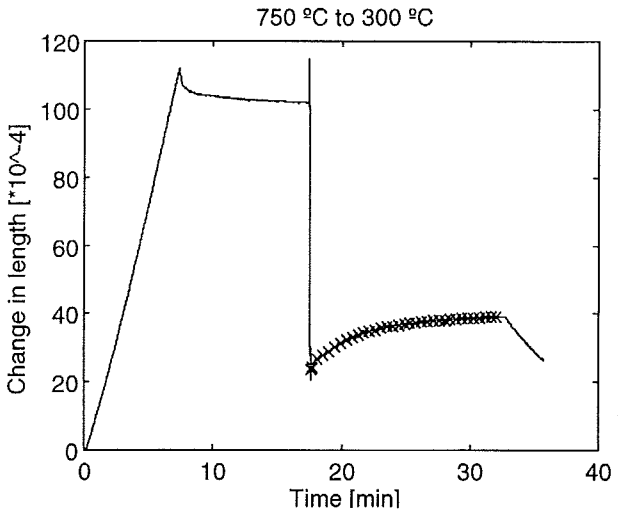

Figure 36: Typical dilatation curve of an experiment that comprises a bainitic holding.

As explained in the introduction of this text, the usual way to stabilise austenite down to room temperature is to impose a bainitic transformation. The mechanism is favourable to the survival of this phase out of its equilibrium. This is why I have been inquiring on the bainitic transformation for the composition previously described.

In a first approach we will consider that nothing happens during the quench and that the transformation occurs only during the 15 minutes holding. The figure 36 shows which part of the measurement is interesting for us. The part where the curve is thicker corresponds to the isothermal holding, in this case, at 300°C. What defines the beginning of the holding is the moment when the temperature has been stabilised at the very end of the quench. This point is indicated on the figure 37.

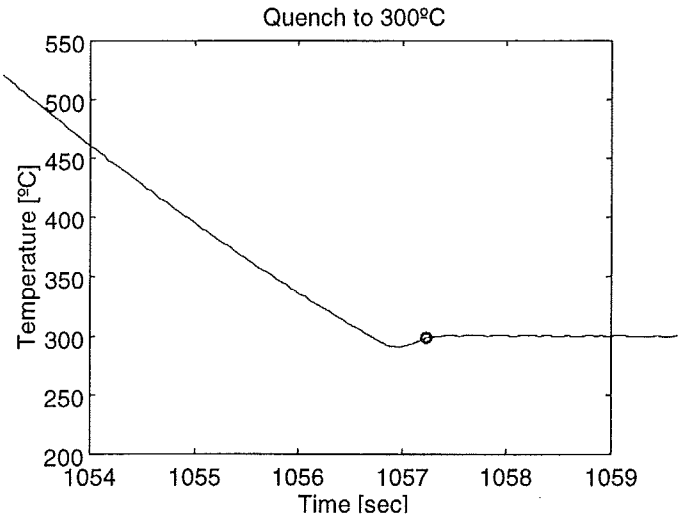

Figure 37: Shape of the end of a quench. The ring defines the moment when the isothermal transformation starts to be measured.

For each of the three different annealing temperature, the curves corresponding to every isothermal holding have been reported on one chart with a logarithmic time scale on the X-axis. The figure 38 contains the curves of the change in length during 15 minutes corresponding to the completely austenitised samples, i.e. austenitised at 900°C. The absolute vertical position of a single curve should not be taken into account as there may have been moves due to vibrations during the experiment. What is important is the absolute increase between the beginning and the end of the isothermal holding, and this is illustrated on the figure 39.

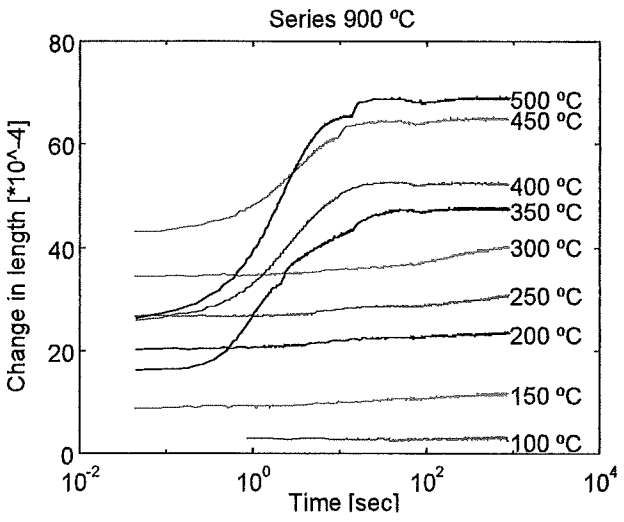

Figure 38: Set of dilatation curves corresponding to the isothermal transformations that takes place at different holding temperatures in the case of completely austenitised samples.

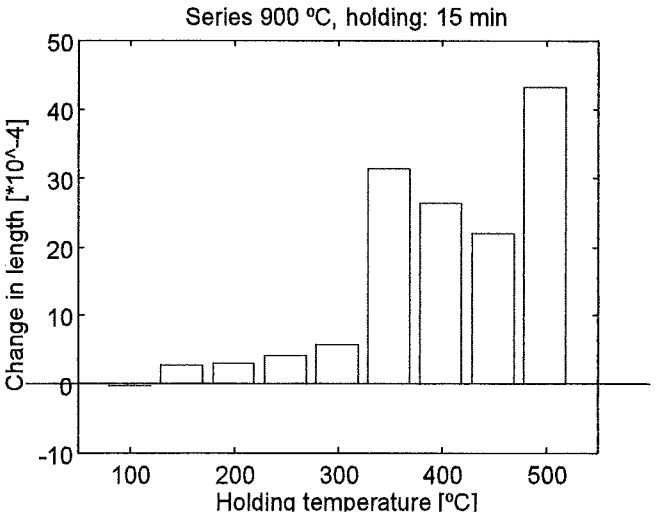

Figure 39: Total variation of the length upon the 15 minutes holdings showed on figure 38.

The results showed on the figures 38 and 39 are not like one could expect. Indeed, the absolute change in length should increase with lower holding temperatures, because the thermodynamical driving force for the transformation is increased as well. This behaviour is observed here only for the holding temperatures of 450°C, 400°C and 350°C.

On the other hand, one can notice that the transformations appearing for the holding temperatures of 300°C and under are very light in comparison to the upper levels. The fact is that, in those cases, a martensitic transformation has occurred during the quench, and the light increase of the change in length during the 15 minutes is due to a precipitation of carbides in

the martensite [22-23]. Generally, the incoherence is explained by the existence of phase transformations during the quench. This problem will be discussed in the fourth chapter.

Here comes the measurements on the isothermal transformations of the intercritically annealed at 800°C (figures 40 and 41).

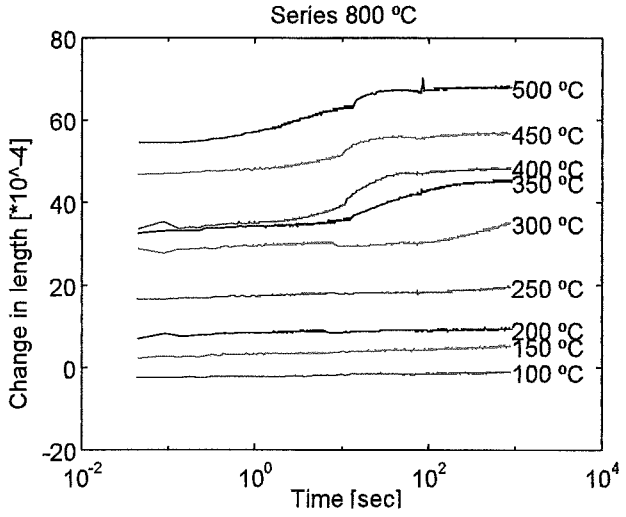

Figure 40: Set of dilatation curves corresponding to the isothermal transformations that takes place at different holding temperatures for samples intercritically annealed at 800°C.

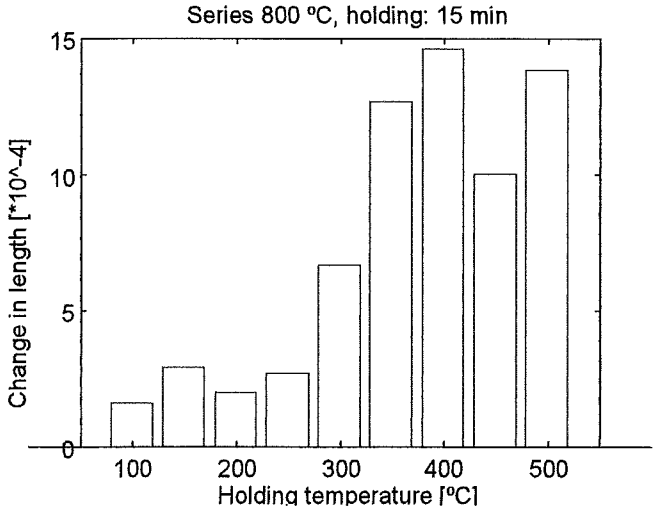

Figure 41: Total variation of the length upon the 15 minutes holdings showed on figure 40.

On a first look, the result seems to be quite equivalent to the case of the samples completely austenitised (Figure 38 and Figure 39). But actually, for the highest holding temperatures, the relative variation is about 2.5 times less (look at the scale of the charts) : for the 15 minutes isothermal transformation at 350°C, the variation is here of $13*10^{-4}$ and it was of $30*10^{-4}$

previously. This is surprising when one thinks that the starting amounts of austenite were of ±91 % (according to the calculation) and 100 %, i.e. not very different. The explanation for such a difference in relative variation of the change in length must be given in the fourth chapter of this paper (section 4.2.1).

What about the other intercritical annealing : 750°C ?

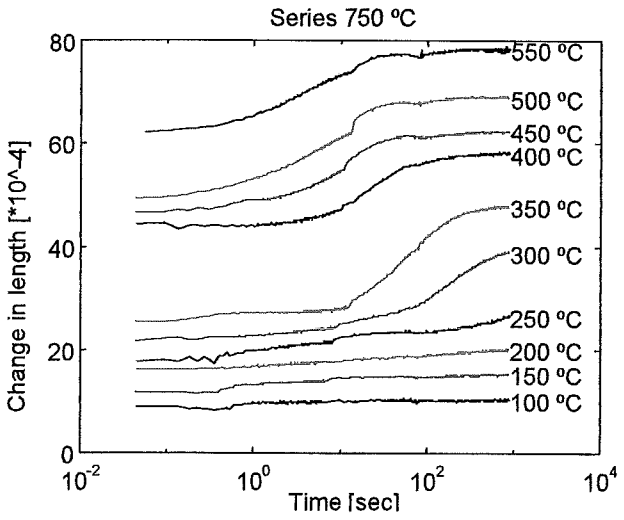

Figure 42: Set of dilatation curves corresponding to the isothermal transformations that takes place at different holding temperatures for samples intercritically annealed at 750°C.

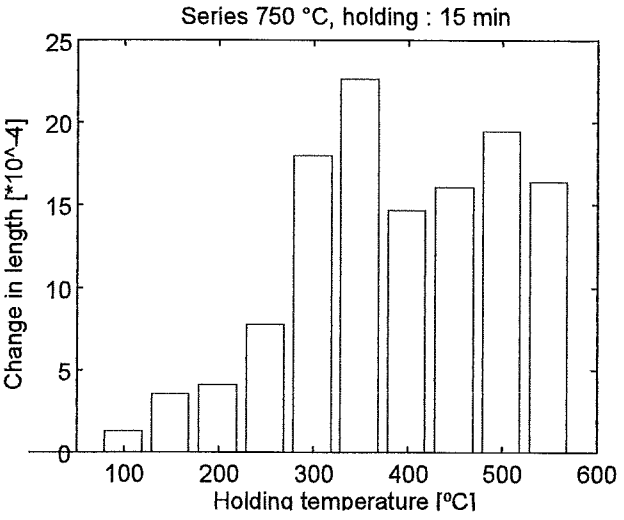

Figure 43: Total variation of the length upon the 15 minutes holdings showed on figure 42.

One can still observe the gap between the high and the low holding temperatures, but this time, 300°C belongs to the group that allows an important transformation. It means that the

temperature for the martensitic transformation (Ms) has decreased. Indeed, if we repeat the calculation of Ms with Andrew's equation (17), but this time for an austenite that contains 0.35 wt. % C, we get 290°C. This value is more than 100 K under the Ms of the completely austenitised steel. Another interesting remark is that the mean variation of the change in length all along the 15 minutes is slightly higher in this case than for the annealing at 800°C although there was less austenite to be transformed (45 % instead of 90 %).

The charts of the figures 44 to 46 indicate the variation of the change in length for the first minute of the isothermal holding. When compared to the charts for 15 minutes, it becomes obvious that most of the transformation happens during that first minute, as there is almost no difference between the results presented in these charts and those previously showed.

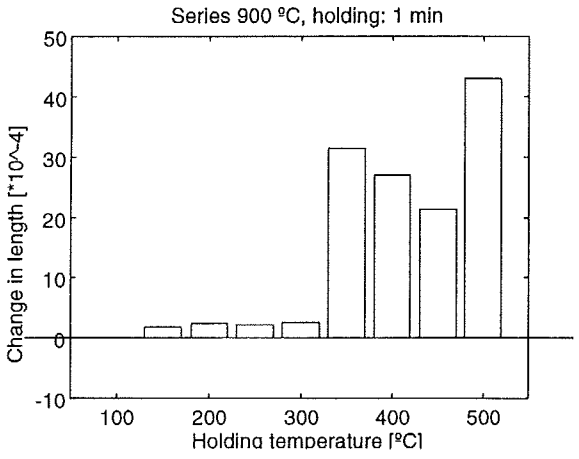

Figure 44

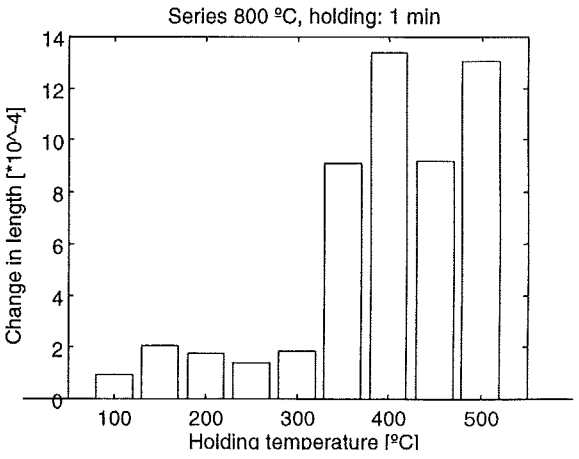

Figure 45

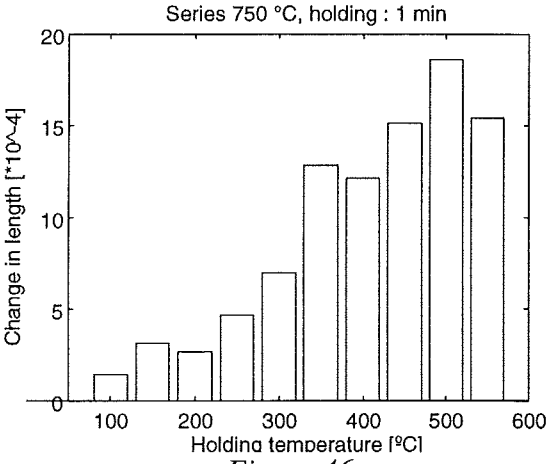

Figure 46

Change in length after 1 minute of isothermal holding for :

Austenitised samples (figure 44).

Samples annealed at 800°C (figure 45).

Samples annealed at 750°C (figure 46).

What is worth to be noticed is the value of the "750°C" series corresponding to the holding temperature of 300°C (Figure 46). It is quite lower for a holding of 1 minute ($7.5*10^{-4}$) than

for the 15 minutes ($18*10^{-4}$). It means that that treatment causes an isothermal transformation more widely spread in the time. Indeed, 300°C is still a little bit higher than Ms, and it is cold enough to slow down a diffusive transformation.

3.3.2 Microstructure analysis

What is the effect of the annealing temperature on the bainitic transformation ? It is visible by the shape of the dilatation curve during the isothermal holding. A comparison between three experiments might help. Three bainitic holdings at 350°C have been plotted on the Figure 47:

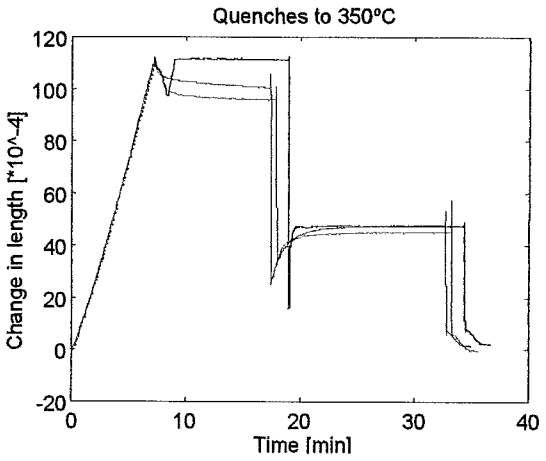

Figure 47: Dilatation curves for experiments with different intercritical annealing temperatures (750°C, 800°C and 900°C), followed by an isothermal holding at 350°C.

The three experiments showed on the figure 47 and, separately, on the figures 48 to 50 differ by their austenitisation conditions and have the same temperature of isothermal holding: 350°C. The annealing temperatures were 900°C, 800°C and 750°C. What is interesting for us is the shape of the curve after the quench; the three charts of the figures 48 to 50 have the same scale, so that the curves can be properly compared.

Independently of the amplitude of the variation (that has been partly explained earlier), let us look at the slope of the curves, which gives an idea of the transformation rate. It is very fast in the case of the completely austenitised sample, whereas the higher carbon content of the third sample tends to slow down the isothermal transformation.

Firstly, the rate of the transformation of austenite into ferrite is very dependent on the carbon concentration. Furthermore, it is not necessarily the same phase that forms since Ms depends on the carbon concentration in the austenite. After a full austenitisation at 900°C, Ms is around 400°C, and this means that the phase formed at 350°C is martensite. On the contrary, after an intercritical annealing at 750°C, Ms is around 300°C.

Microstructures corresponding to the three different treatments are visible on the pictures 5 to 7. One can see on the picture 5 that the austenitising treatment has increased the grain size from 5 μm to about 10 μm (It can be seen even better on the picture 11). On the other hand, the microstructures showed on the pictures 6 and 7 look quite like those of the pictures 4 and 3 respectively, in what concerns the phase proportions. But the microstructure visible on the picture 7 is decomposed bainite, since the bainitic holding was performed at 350°C and Ms is around 300°C.

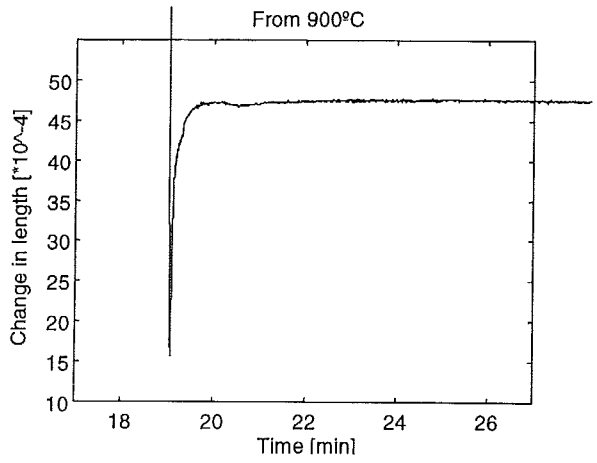

Figure 48

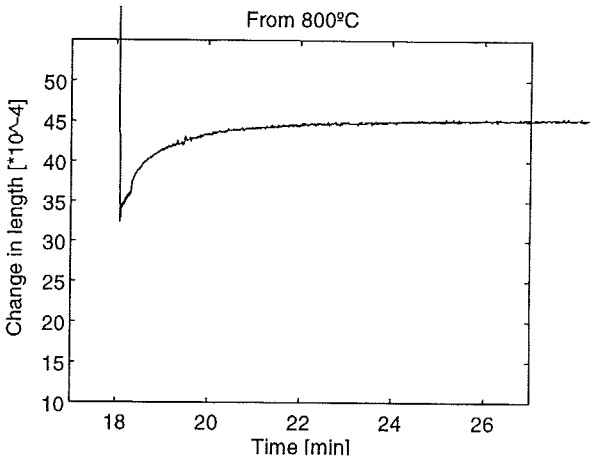

Figure 49

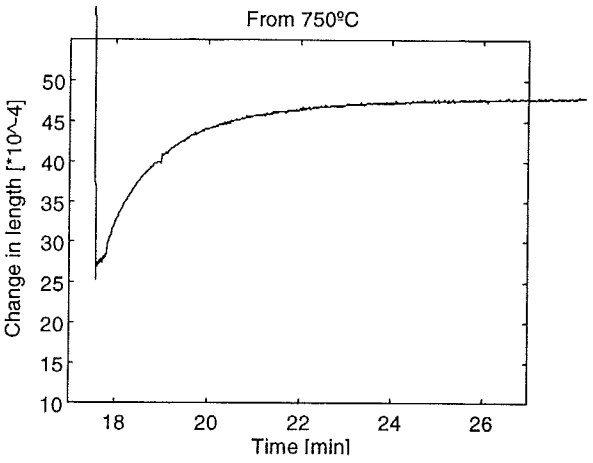

Figure 50

Dilatation curves of experiments with an isothermal holding at 350°C, following a quench from:

900°C (figure 48)

800°C (figure 49)

750°C (figure 50)

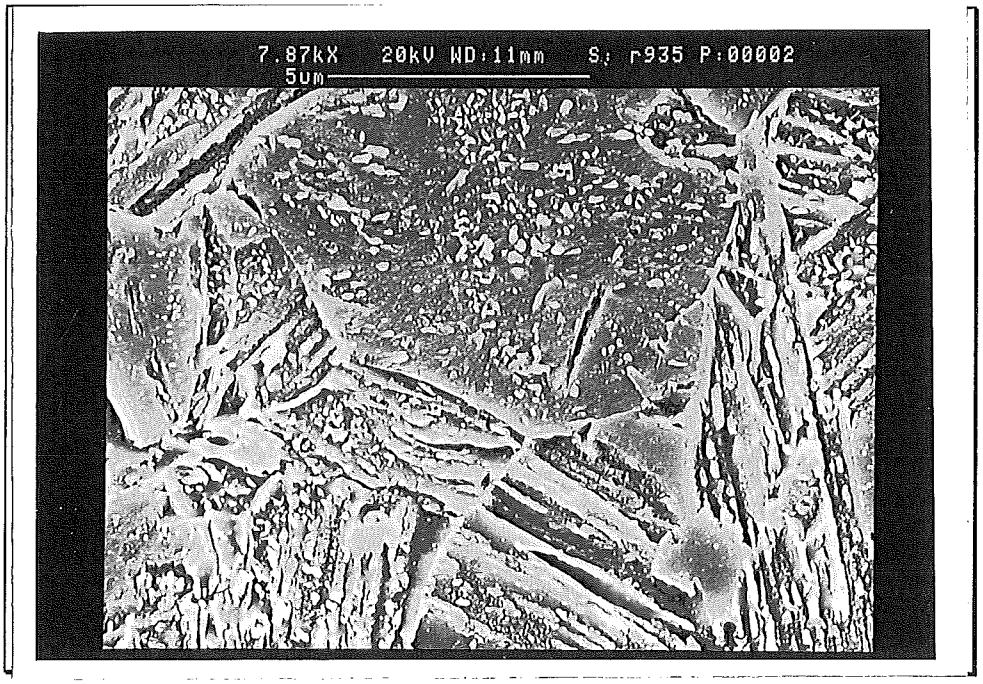

Picture 5 (R935): SEM micrograph of a sample austenitised at 900°C for 10 min, then quenched to 35 °C and held at that temperature for 15 min.

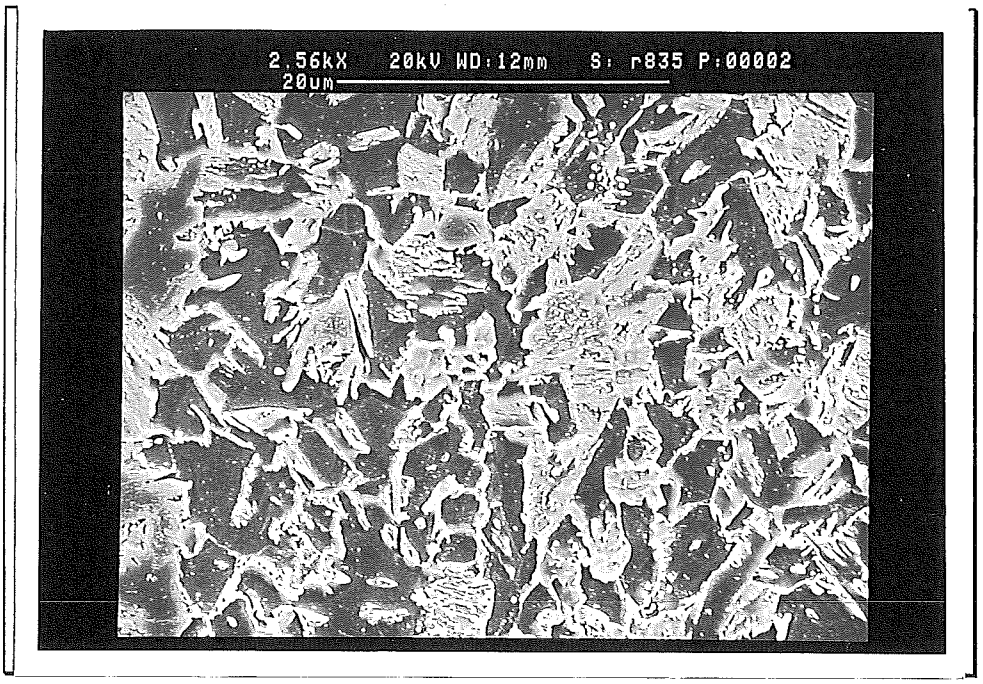

Picture 6 (R835): SEM micrograph of a sample austenitised at 800°C for 10 min, then quenched at 350°C and held at that temperature for 15 min.

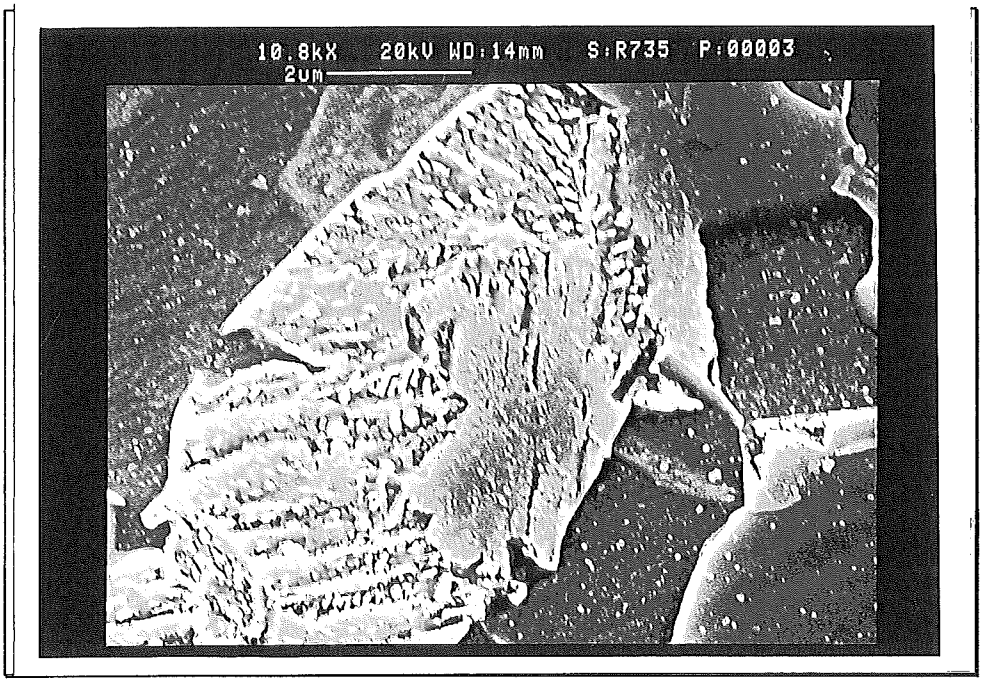

Picture 7 (R735): SEM micrograph of a sample austenitised at 750°C for 10 min, then quenched at 350°C and held at that temperature for 15 min.

3.3.3 Calculation on the bainitic holding

The section 2.2.1 has already described the equations that will be used in this part. Equation (6) will be applied to the completely austenitised samples, while the equation (9) stands for the intercritically annealed samples. The calculation is now possible because the dilatometric data is available since the section 3.3.1, and also because parameters have been summarised in the section 3.2.4.

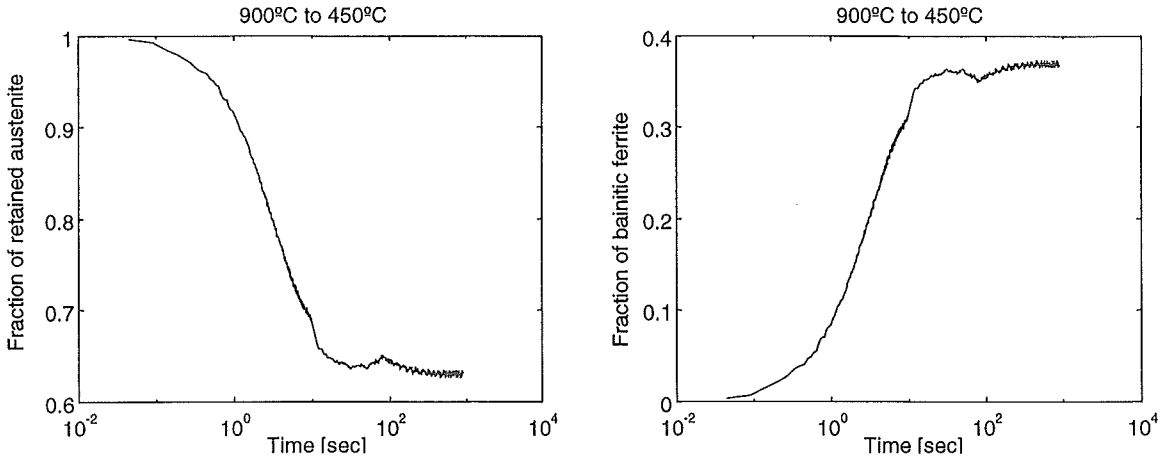

Figure 51: (a) Calculated fraction of austenite that disappears during the isothermal holding at 450°C, following a quench from 900°C. (b) Calculated fraction of bainitic ferrite that appears during the isothermal holding.

Figure 51 shows the result for the isothermal transformation at 450°C, coming from 900°C. One should be aware that the scale on the Y-axis of the two charts are different. Unfortunately, this result is obviously wrong. It is simply impossible to keep more than 60 % of untransformed austenite at 450°C with this kind of steel. The reality is that there are not anymore 100 % of austenite at the beginning of the isothermal holding. We will try to solve that problem in the fourth chapter.

What about the result for a sample intercritically annealed at 800°C ? (Figure 52)

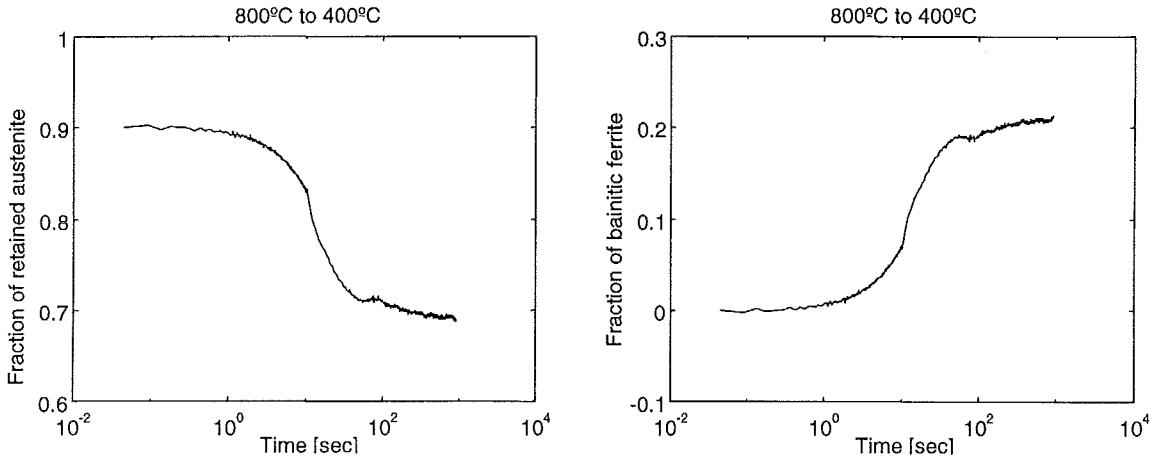

Figure 52: (a) Calculated fraction of austenite that disappears during the isothermal holding at 400°C, following a quench from 800°C. (b) Calculated fraction of bainitic ferrite that appears during the isothermal holding.

Although 400°C is very far from the austenitic region, the fraction goes from 90 % to hardly 68 %. The problem is the same as in the case of the austenitised samples : there was not 90 % of austenite at the end of the quench. It seems that it is worse in this case : the calculation foresees the formation of 23 % of bainitic ferrite versus 37 % for the previous experience.

At last, there is the isothermal transformation of a sample annealed at 750°C (Figure 53). The left picture suggests that there is a little bit more than 10 % of austenite remaining. But do not forget that it includes the cementite that is produced by the bainitic transformation. It is very acceptable in comparison to the two previous results; it seems that these data do not meet the same problem, i.e. some transformation of the austenite during the quench.

Therefore, the experiments of the series "750°C" are chosen in order to draw a TTT diagram.

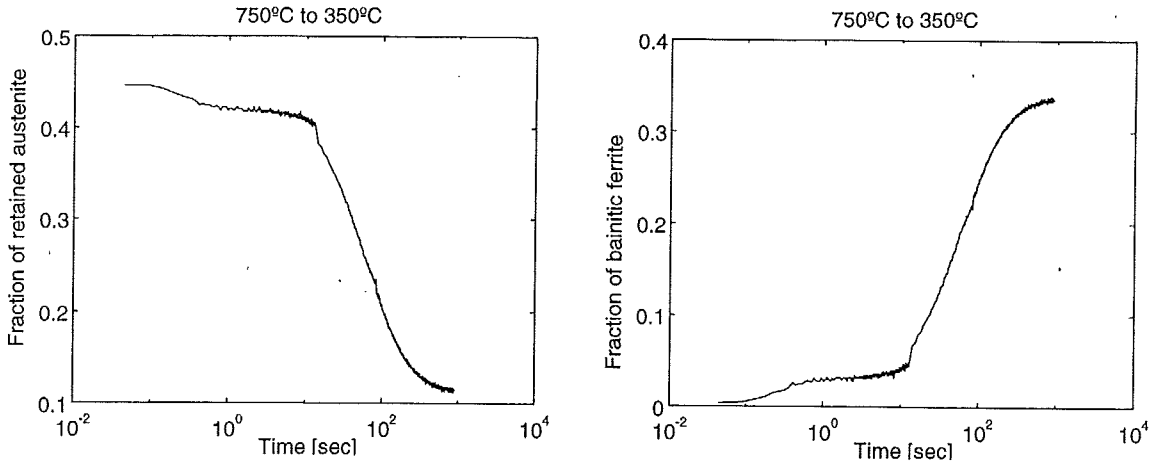

Figure 53: (a) Calculated fraction of austenite that disappears during the isothermal holding at 350°C, following a quench from 750°C. (b) Calculated fraction of bainitic ferrite that appears during the isothermal holding.

3.4 Intercritical annealing at 750ºC : test

This section is based on the study of a very particular experiment : the idea is to carry out an intercritical annealing at 750°C, but this time, coming from high temperatures. In a first time, the experiment is described, then the dilatometric results are presented, and the microstructure photographs come at the end.

3.4.1 Introduction

Sybrand van der Zwaag has suggested a strange experiment : why not compare an intercritical annealing that would follow a heating from room temperature as usual (figure 54), with an intercritical annealing that would be preceded by a full austenitisation at 950 °C (figure 55) ?

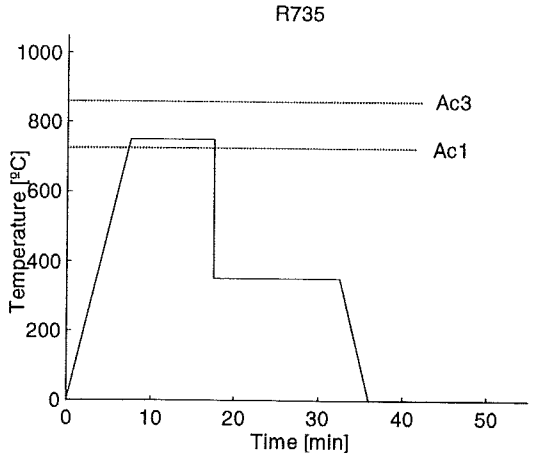

Figure 54: Classical heat treatment for the production of TRIP-aided multiphase steel. The intercritical annealing at 750°C is performed coming from low temperatures.

There are several ideas hidden behind this experiment :

- To compare the amounts of austenite contained in the samples at the end of the intercritical annealing.
- To compare the growth of the austenite grains inside a ferritic matrix with the growth of the ferrite grains inside an austenitic matrix.
- To observe the influence of the starting microstructure on the kinetics of the bainitic transformation.
- To look at the grain size of the austenitised samples.

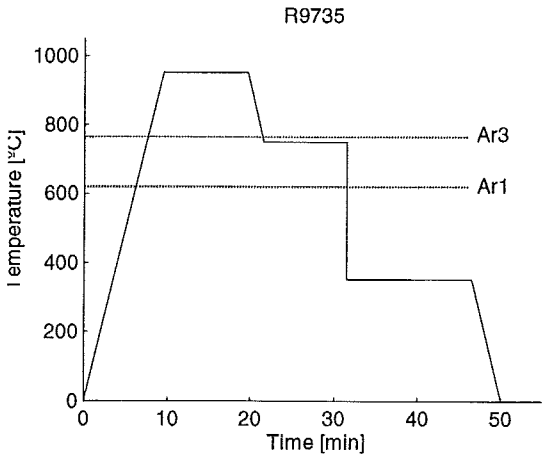

Figure 55: Heat treatment with an intercritical annealing at 750°C performed coming from a higher temperature.

Another way to understand this experiment is to look at the figures 56 and 57. During heating, when the dilatation curve crosses the dotted line at 750°C, the transformation has already begun. Whereas when cooling, the formation of ferrite hardly begins at 750°C. Now, what happens during the 10 minutes of annealing ? One may think that the volume fraction of austenite is going to evolve towards the equilibrium described by the MTData curve in the section 3.1.4.

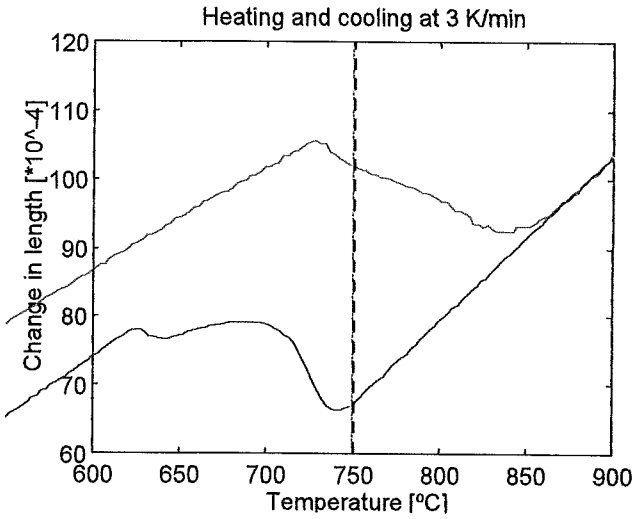

Figure 56: Dilatation heating curve (red) and cooling curve (blue). The vertical dark dotted line shows the temperature of the intercritical annealing.

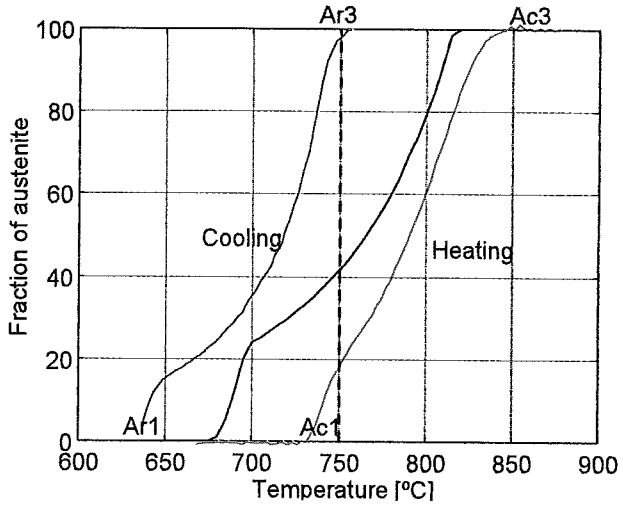

Figure 57: Distribution of the phases during cooling (blue) and heating (red). The dark dotted curve shows the temperature of the intercritical annealing.

3.4.2 Dilatometry

Before we observe the bainitic transformations, let us look at the annealings. The charts of the figure 58 and figure 59 show that although the annealings are performed at the same temperature (750°C) and for 10 minutes, the difference between the dilatations of the samples is quite important. A first explanation for this deviation is that the phase distributions at 750°C is very different in the two cases. A quick look at figure 57 teaches that the sample that is cooled to 750°C contains a lot more austenite than the one that is heated to 750°C. Indeed, the

10 minutes holding cannot re-establish the equilibrium. And since the austenite lattice is more compact than the ferrite's, the sample with a lot of γ phase presents a lower dilatation.

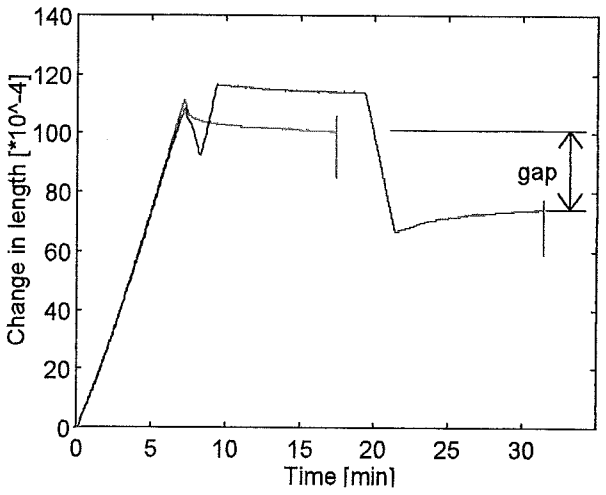

Figure 58: Dilatation curves of the experiments described by the figures 54 (red) and 55 (blue), but it is stopped at the end of the intercritical annealings.

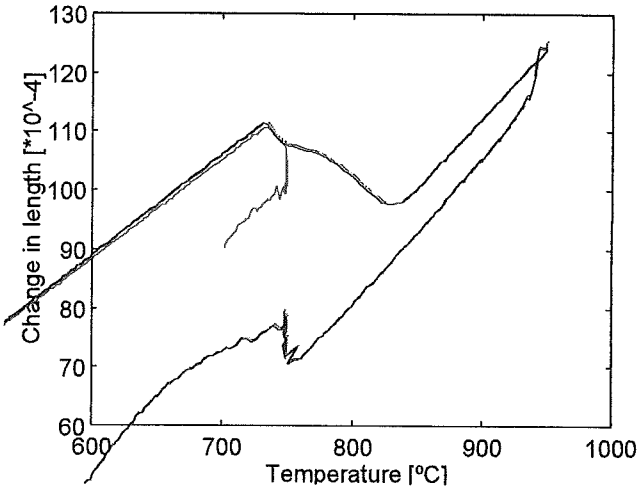

Figure 59: Dilatation curves of the experiments described by the figures 54 (red curve) and 55 (blue curve), but it is stopped at the end of the intercritical annealings.

Let us look now at the bainitic transformation that follows these intercritical annealings. The figure 60 contains the complete curves of the experiments presented on the figure 54 and figure 55. The transformations that occur at 350°C after the quench have really different profiles. While the usual treatment, i.e. without austenitisation, yields a quite slow transformation, the other one produces a very fast reaction. The reason for this resides in the mutual austenite concentrations. Indeed, since the γ phase of the austenitized sample is larger,

it has a lower carbon concentration than the γ phase of the other sample. And it is well known that the the higher the carbon content in the austenite, the more the phase transformations are slowed down [15].

3.4.3 Microstructure

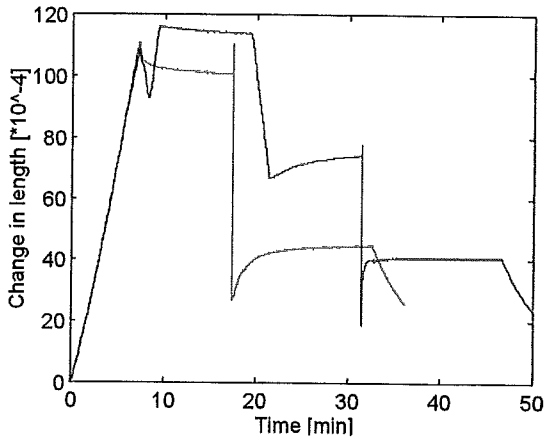

Figure 60: Complete dilatation curves of the experiments described by figures 54 and 55.

Looking at the micrographs will help to compare the microstructures : in the first case, the austenite has grown in the ferrite, and in the second case, the ferrite has grown in the austenite. The microstructure of a sample intercritically annealed at 750°C has already been showed on the picture 3 in the section 3.2.3.2 devoted to the calculation during the heating. The austenite has nucleated on the grain boundaries of the pearlitic microstructure. The measurements showed that the sample contained around 44 % of austenite at the end of the annealing. It was investigated by both calculation and image analysis.

Picture 8 that follows represents the sample that has undergone the treatment described by the figure 55. This picture is magnified only 65 times so that one can see the huge spots measuring nearly 1 millimetre. The microstructure between the spots is banded, just like the one of the original samples received from Hoogovens.

The big spots, visible on picture 8, measure more than 500 µm. They are fully martensitic with very large grains measuring sometimes more than 50 µm long (picture 10). On the other hand, the banded structure, which can be seen besides the martensitic spots on the picture 8, contains a mix of ferrite and martensite in similar proportions. Its grain size remains around 10 µm, according to the picture 9. This is more or less the same grain size than that of the samples completely austenitised and quenched under Ms (picture 5). It is obvious that everything that is martensite on the pictures was austenite before the quench to 350°C.

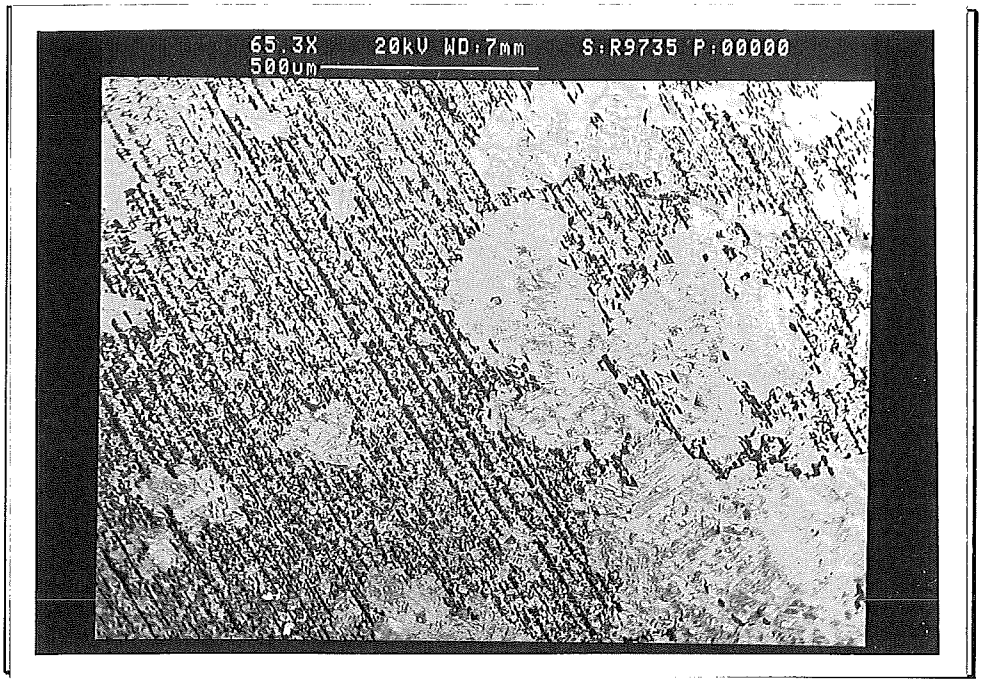

Picture 8 (R9735) : SEM micrograph at low magnificence of the sample that has undergone the treatment defined on the Figure 55.

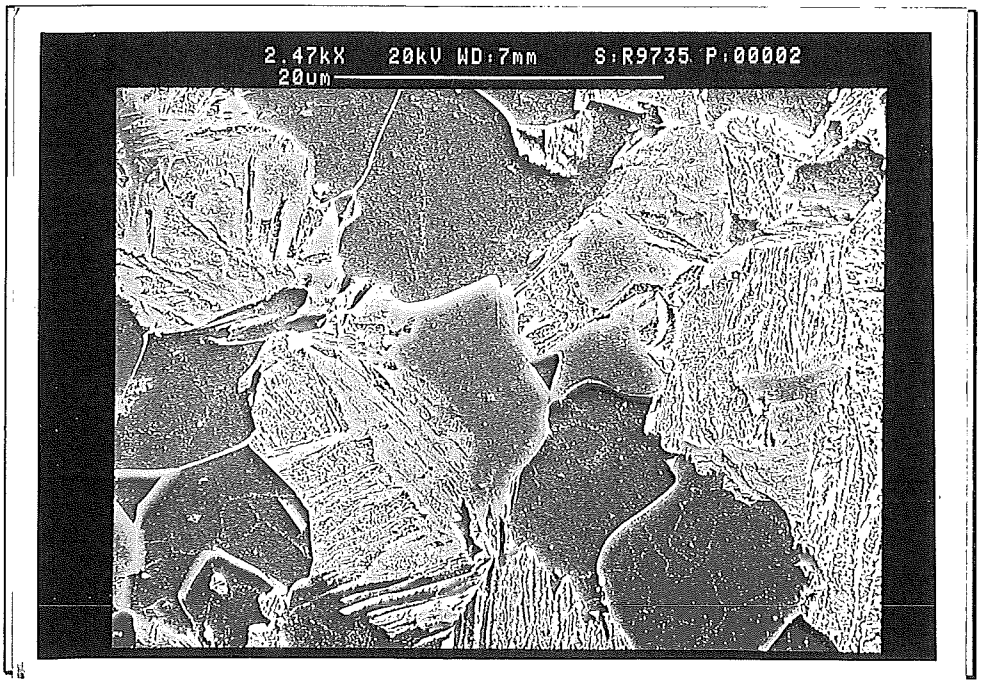

Picture 9 (R9735): SEM micrograph at high magnificence of the banded structure visible on the picture 8.

Picture 10 (R9735): SEM micrograph at high magnificence of a martensitic spot seen on the picture 8.

4. Discussion

The first section of this chapter (4.1) contains an interpretation of the calculation applied on the heating curve, which was developed in the section 3.2. It is followed by a short explanation of the results of the isothermal holding, and an investigation on the encountered experimental problems (4.2). The third point presents one of the most important outcome of this work : a TTT diagram (4.3), while the fourth part tries to retire information from the failed experiments (4.4). Another calculation method is presented in 4.5. The results of the exotic experiments on the intercritical annealing are discussed in 4.6. Finally, the appropriate ways for stabilising the austenite are presented in 4.7.

4.1 Heating calculation

The results obtained in section 3.2 are summarised in Table 8.

	Calculation	Image analysis
Annealing at 750°C	46 %	44.2 ± 2.8 %
Annealing at 800°C	91 %	58.1 ± 5.2 %

Table 8: Fraction of austenite calculated or measured at the end of the intercritical annealings.

For the sample annealed at 750°C, the results of the calculation and the image analysis seem to agree quite well. Since the image analysis technique is accurate with a standard deviation of 2.77 % on 50 pictures, this is a good result.

For the sample annealed at 800°C, the result of the image analysis yields 58.1 ± 5.2 % against 91 % for the calculation. A possible explanation for that great difference is that a part of the austenite has transformed into ferrite before Ms was reached. Looking at the curve that describes the quench (Figure 61), one can observe a slight hump in the slope, which could correspond to a partial transformation of austenite into ferrite [17].

This theory is confirmed by microstructural observations of the picture 4. Indeed, there are hints of ferritic laths perpendicular to the grain boundaries. This is the typical aspect of the Widmanstätten ferrite, which is nothing else than ferrite formed during a fast cooling. This

would explain the fact that the measured fraction of austenite is smaller than the calculated fraction since a part of it would have transform into Widmanstätten ferrite during the quench.

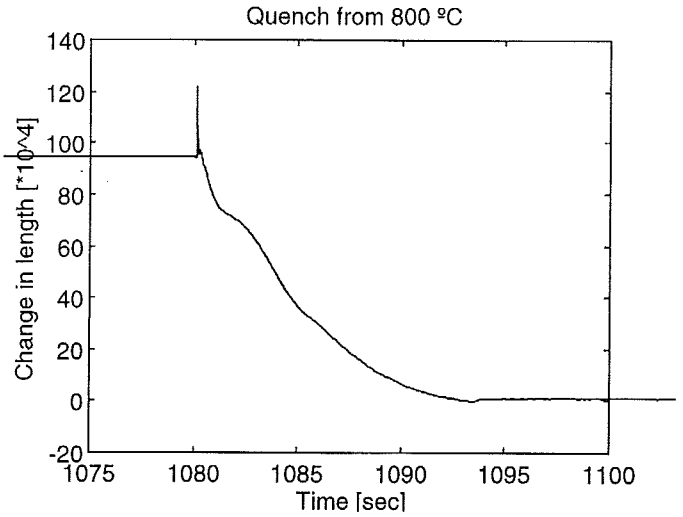

Figure 61: Dilatation curve showing the phase transformation that has occurred during a quench from 800 °C to room temperature.

A question that might be asked now is : "Why would there be a transformation during the quench in the case of the annealing at 800°C and not for 750°C ?". The explanation is that, in the first case, the carbon concentration in the austenite is high enough to prevent a transformation before Ms has been reached. In the second case, the cooling rate is not high enough to get rid of the formation of ferrite. According to the equation (8), the austenite of the samples annealed at 750°C contain about 0.35 wt. % C, against 0.18 wt. % C for the samples annealed at 800°C.

4.2 Bainitic transformation

This section presents an interpretation of the results that were obtained in the section 3.3. Once the main problem is localised, it will be deeper investigated, with eventually the help of a CCT diagram. The last point of this section deals with the inaccuracies encountered with the stability of the calculation presented in the section 2.3.1.2.

4.2.1 Synthesis of the results on the isothermal holdings

In the section 3.3.1, a big difference was measured between the change in length of the series 900°C (figure 39) and the series 800°C (figure 41) during isothermal holding, although the amounts of austenite that had to be transformed were close (100 % and 90 %). The average of the relative change in length was measured to be about 2.5 times less in the second case. This

problem can be explained by the fact that the quenches were not perfect, i.e. there were transformations during the quenches. In the case of the annealing at 800 °C, there was more transformation during the quench than in the case of the complete austenitising (900°C). Indeed, if there is a big fraction transformed during the quench, the variation measured on the isothermal holding, which corresponds to the continuation of the transformation, is small.

Another question evoked in the section 3.3.1 was : why is the change in length measured for the 750°C series (during isothermal holding (figure 43)) bigger than the change in length measured for the 800°C series (figure 41) although in this second case there is twice as much austenite to be transformed ? The answer is that a big part of the austenite was transformed during the quench in the 800°C series, and nothing was transformed upon quenching in the 750°C series. The present section aims thus to investigate on what happens during the quench.

The strange measurements of the section 3.3.1 have induced strange results in the calculations of the section 3.3.3. The results of the calculation applied to the dilatometric data of the isothermal holding are presented in the charts of the figures 51 to 53. It is deceiving for the series 900°C and 800°C, but it is acceptable for the series 750°C. Indeed, the proportions of stabilised austenite for the two first series are exaggerated. The problem resides in the fact that the program assumes that there is respectively 100 % and 91 % of austenite at the beginning of the isothermal holding. There was actually much less austenite left in those samples at that moment. Only the last series (annealing at 750°C) seems to present more acceptable results for the calculation. The following part attempts to give an explanation for this phenomenon.

4.2.2 Quenches

Most of the experiments that were performed on the dilatometer BAHR805 presented a quench in their temperature program. One important advantage of that machine is that the sampling rate can be chosen up to 1000 Hz. When applying such a high sampling rate to the quench, it finally allows to draw a very accurate curve that describes the quench.

In the set of the experiments performed, there are three different types of quenches, depending on the starting temperature : 900°C, 800°C or 750°C.

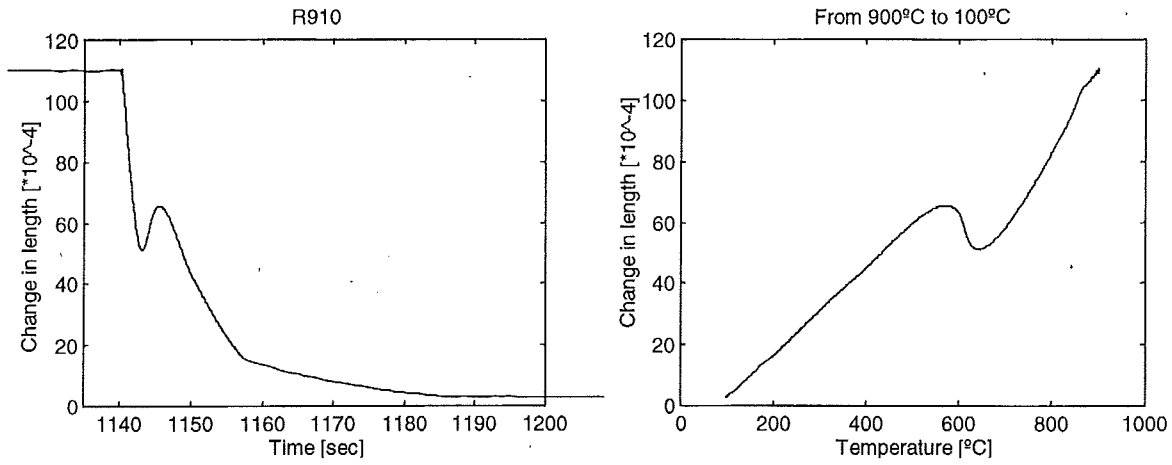

Figure 62: Dilatation curve of a quench from 900 °C showed (a) with the time as X-axis, (b) with temperature as X-axis.

The charts of figure 62 represent the same quench from 900°C to 100°C : the first one with the time on the X axis and the second one with the temperature. An important transformation occurred around 600°C during the cooling. This is of course a problem for someone who wants to use that experiment to draw a TTT diagram. Actually, the cooling rate was not high enough. This is to be compared with quenches performed from intercritical temperatures.

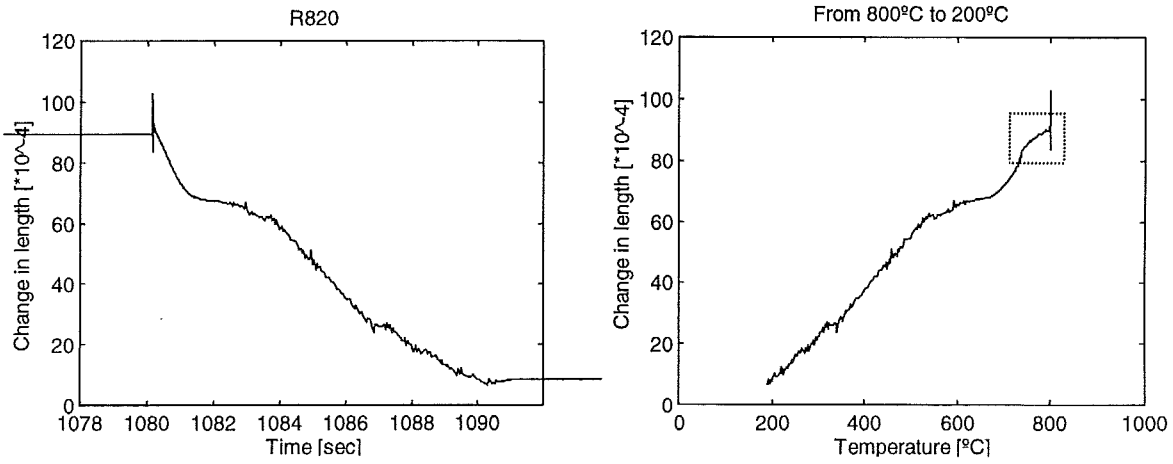

Figure 63: Dilatation curve of a quench from 800°C showed (a) with time in abscise axis, (b) with temperature in abscise axis.

Figure 63 show a quench performed from 800°C to 200°C, where there should be about 90 % of austenite at the beginning. An important transformation is visible around 700°C, which is sooner than in the case of the completely austenitised sample (figure 62). We will see later that those transformations at 600°C and 700°C are not exceptional phenomenons. Another

characteristic of that quench is the existence of a plateau at the very beginning of the quench, and it is visible on the second chart.

Finally, an analyse of the quench described by the figure 64, going from 750°C to 100°C, shows that it does not present any transformation before Ms (290°C) is reached. (Therefore that series could be used for the drawing of a TTT diagram.)

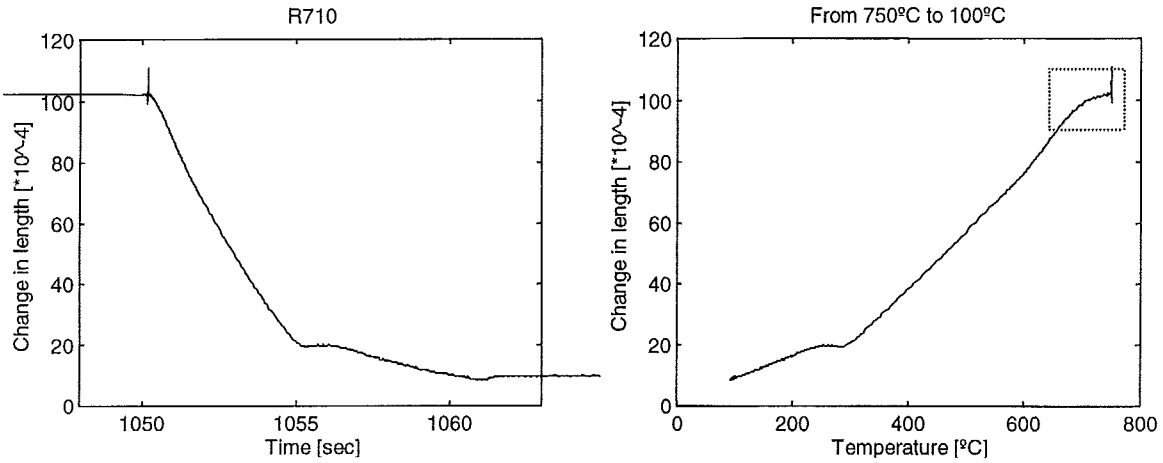

Figure 64: Dilatation curve of a quench from 750°C showed (a) with time in abscise axis, (b) with temperature in abscise axis.

One should remark that, alike the previous experiment, there is a plateau at the top of the slope on the second chart. Those plateaux are due to the effect of a temperature gradient from the core of the sample to its surface. When the helium blow begins, the surface is cooled earlier than the whole sample. And, as the thermocouple is welded on the surface, it indicates a lower temperature than the real overall temperature, which is naturally related to the exact change in length. Anyway, this artefact has no awkward consequences for the use of the data. All the considerations established here are based on the analyse of several experiments for each one of the three cases.

4.2.3 CCT Diagram

It has been stated that, for two series, the main problem in the quenching was the too low cooling rate. CCT diagrams are the appropriate tools to measure the critical cooling rate of a specific steel composition. The following diagram has been released by a program written by Pieter van der Volk, from the Materiaalkunde, TUDelft. The program is not finished yet, so the output (Figure 65) may look a little bit rough, nevertheless, the aim is achieved.

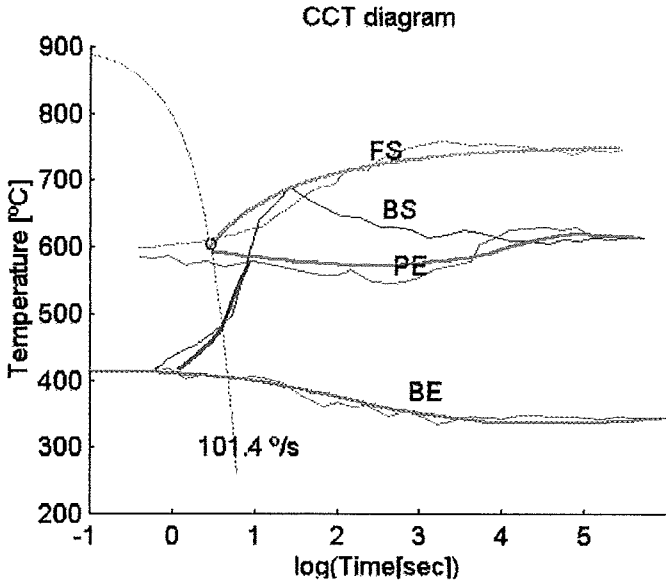

Figure 65: CCT diagram for the composition described in table 1 and assuming that the material has been austenitised at 900°C.

As usual, CCT diagrams are made for completely austenitised steels; in this case : at 900°C. Unfortunately, it does not produce CCT diagrams for steels that were intercritically annealed. The diagram is composed of four lines: FS (ferrite start), BS (bainite start), PE (pearlite end), (BE : bainite end). The user has to find his way through it by redrawing the curves with thicker plots. The program also calculates the position of a nose before which the ferrite cannot form. For this composition, the nose is at 601°C and after 2.9 seconds.

The critical cooling rate values then: $CCR = \frac{900-601}{2..951} = 101.4\,\text{K/sec}$. There is no information about the critical cooling rate required to get rid of the formation of bainite.

4.2.4 Stability of the calculations

The results presented in the section 3.3.3. were yielded by a matlab program. It is important to know how the result can be influenced by a slight change in the input data. The figures 66 to 68 show the calculated fraction of bainite for three different input parameters. The three charts contain the so-called fractions of bainitic ferrite that appear during the isothermal transformations at 350°C of samples quenched from 750°C, 800°C and 900°C respectively.
The curve in the middle is the one corresponding to the parameters of the table 6, while the upper curve corresponds to an increase of 0.1 % of the austenite lattice parameter, and the lower curve corresponds to an increase of 0.1 % of the ferrite lattice parameter.

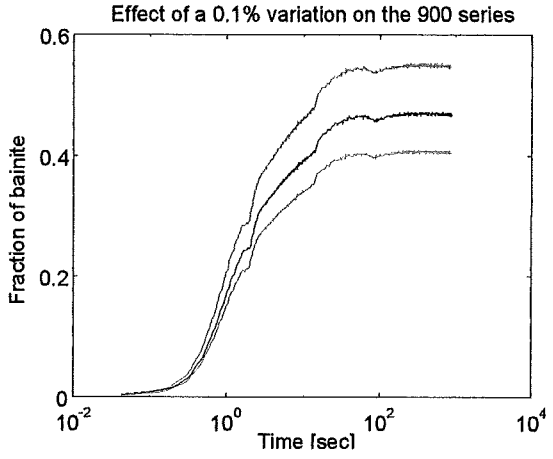

Figure 66

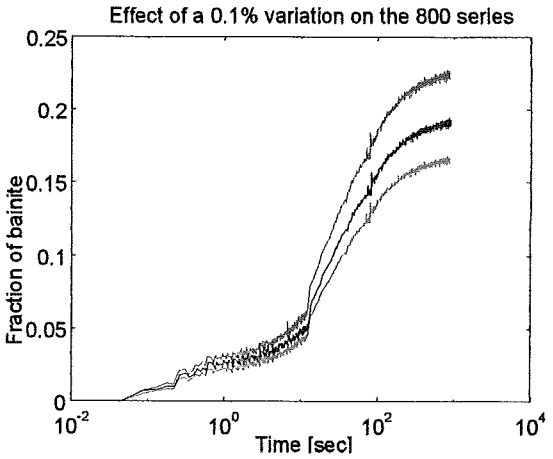

Figure 67

Calculated fraction of bainitic ferrite formed during an isothermal holding following an annealing at 900°C (figure 66), 800°C (figure 67), 750°C (figure 68). The dark curve is the original, while the blue one corresponds to an increase of 0.1% of the austenite lattice parameter, and the red curve corresponds to an increase of 0.1% of the ferrite lattice parameter.

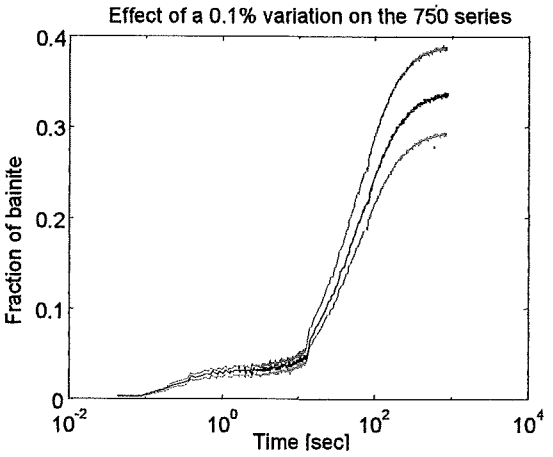

Figure 68

As one could expect, an artificial increase of the lattice austenite parameter induces an under-estimation of the amount of this phase in comparison to the ferrite, which is therefore over estimated. And, logically, an increase of the ferrite lattice parameter has the opposite effect. What is very important to note here is that a slight change (0.1 %) in the input data can create, for a holding of 15 minutes, a variation of more than 5 % in the result. As a matter of fact, this calculation technique based on the lattice parameters is unstable, i.e. the error is quickly amplified. It means that it is dangerous to rely on the results without checking it by a different characterisation technique. This is a strong limitation to this type of calculation, and it is essential to be aware of it.

4.3 TTT diagram for the annealing at 750°C

It was demonstrated in section 4.2 that the data corresponding to an intercritical annealing at 750°C were relevant to draw a TTT diagram since no transformation occurred during the quench.

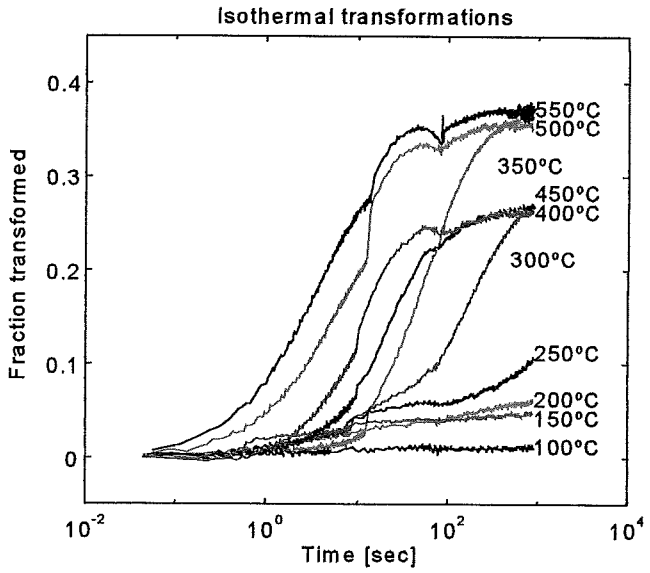

Figure 69: Calculated fractions of transformed phase during isothermal holdings at 10 different temperatures. The material was intercritically annealed at 750°C.

Figure 69 shows the curves of the fraction transformed for the different holding temperatures, from 100°C to 550°C. This chart is available in the appendix of this paper for a better view. As the fraction of the so-called bainitic ferrite goes up to nearly 40 %, the Y-axis can be cut in seven pieces of 5 % in order to plot the TTT diagram. It is worth noticing that the 0 % transformation line cannot be defined this way, so it will be omitted.

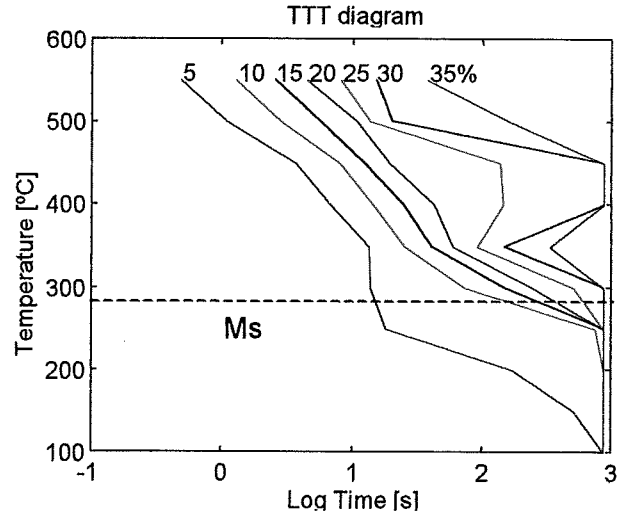

Figure 70: TTT diagram drawn on the basis of the calculated fractions of phase transformed described in the figure 69.

The diagram of the figure 70 is relatively regular except for the holding temperature of 350°C where there is a peak. There is no clear boundary between the bainite region and the ferrite

region, but this is normal for low alloyed steel [15]. On the other hand, we can see quite well that Ms is between 250°C and 300°C. The value of 290°C was calculated earlier with the equation (17). As a matter of fact, the martensitic transformation is extremely fast so that it occurs during the quench and the only thing that one can observe later is carbide precipitation, which does not produce an important change in length [22-23]. Because of kinetics reasons, the precipitation is more important at higher holding temperature, and it explains the slight levelling from 100°C to 250°C.

Figure 71 and figure 72 show two camemberts as illustrations of the phase's distribution inside the sample at the end of the isothermal holding at 500°C and 200°C, according to the calculation.

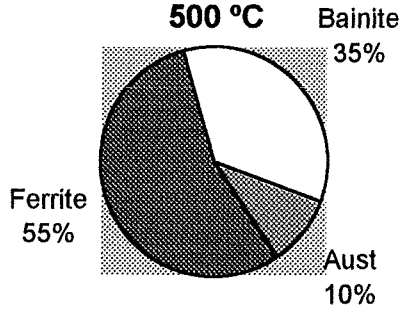

Figure 71: Distribution of the phases after the following treatment: 750°C/ 10min/ 500°C/ 15min, according to the calculation.

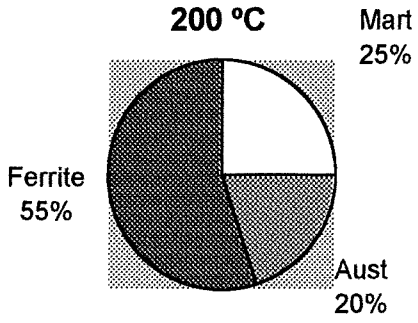

Figure 72: Distribution of the phases after the following treatment: 750°C/ 10min/ 200°C/ 15min, according to the calculation.

Figure 71 : at 500°C, the phase that forms is bainite. According to the calculation, its amount goes up to around 35 %, so that there remains 10 % of untransformed austenite, which is quite a high volume fraction. The section 4.7 will come back to this part of the discussion. Figure 72 : at 200°C, we are between Ms and Mf. A linear relation between the fraction of martensite and the temperature leads to think that there must be something like 25 % of martensite versus 20 % of austenite remaining. This austenite will finally transform to martensite during the later cooling to the room temperature. Figure 73 shows a 3-dimensions TTT diagram based on this data. The surface contains the iso-transformation curves. This chart was drawn with the software Matlab. A bigger picture is available in the appendix.

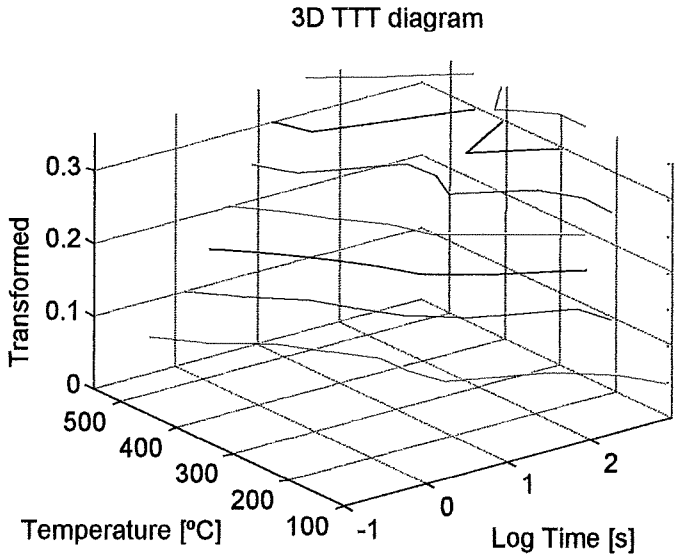

Figure 73: Three-dimensions TTT diagram (the same as the one of figure 70).

4.4 Decayed series

As described in the section 4.2, the data corresponding to the intercritical annealings at 800°C and 900°C were not relevant to plot TTT diagrams because of the parasite transformations taking place during the quenches. On the other hand, these dilatometric data contain many interesting information about the steel in a metallurgical point of view. The experiments were not pointless.

4.4.1 Quenches from 900°C

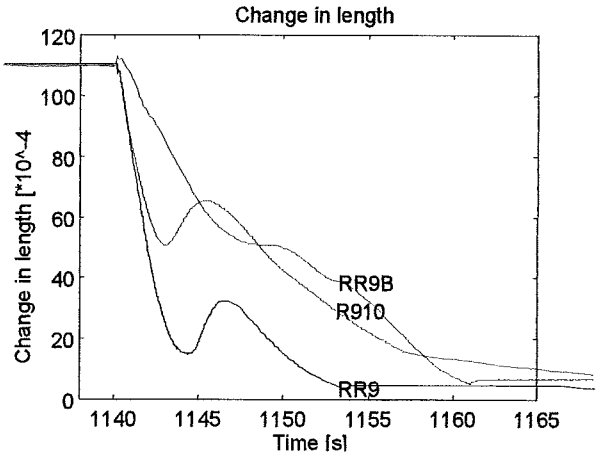

Figure 74: Dilatation curves of three quenches carried out from 900°C and called R910, RR9 and RR9B.

The quenches performed with the dilatometer present important inaccuracies. The user can be victim either of a lack of gas pressure during the blowing or of a lack of heat transfer by

convection from the gas to the sample. Nevertheless, the use of helium is an amelioration compared to the nitrogen. In order to describe the difficulties that one meets when performing quenches, the charts of the figure 74 represent three quenches from 900°C under different aspects.

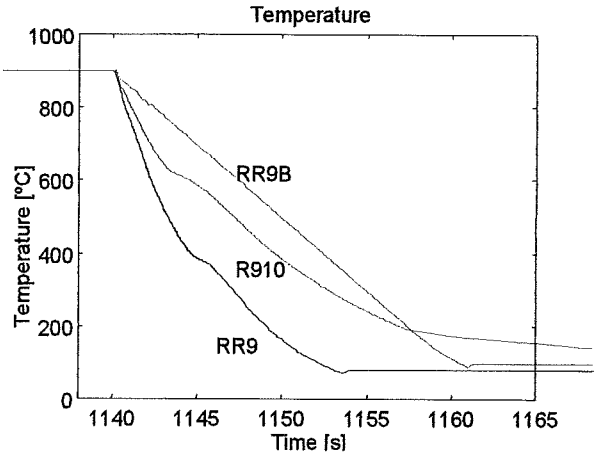

Figure 75: Curves showing the temperature of the sample for 3 quenches from 900°C.

The first quench, called R910, was programmed at the cooling rate of 300 K/sec. Of course, one should be aware that the real cooling rate could never be so high, this is why the program put the quenching gas still available for 20 seconds more, which should be long enough for the sample to join the programmed isothermal holding temperature.

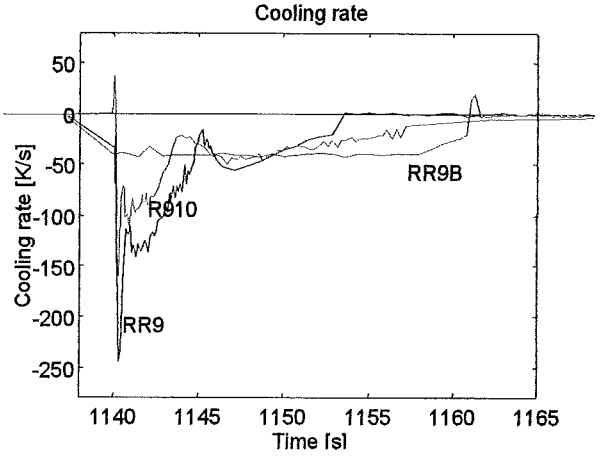

Figure 76: Instantly measured cooling rate for 3 quenches from 900 °C.

RR9 was programmed to quench at the rate of 150 K/sec, and it managed quite well, in comparison with R910. Both transformations in R910 and RR9 are visible on figure 74 of course, but also on figure 75. The heat released by the transformation induces a slight hump in

the slope at the temperatures of 600°C and 400°C respectively. RR9B has been quenched at 40 K/s, and the figure 75 shows that it is quite smooth beside R910 and RR9.

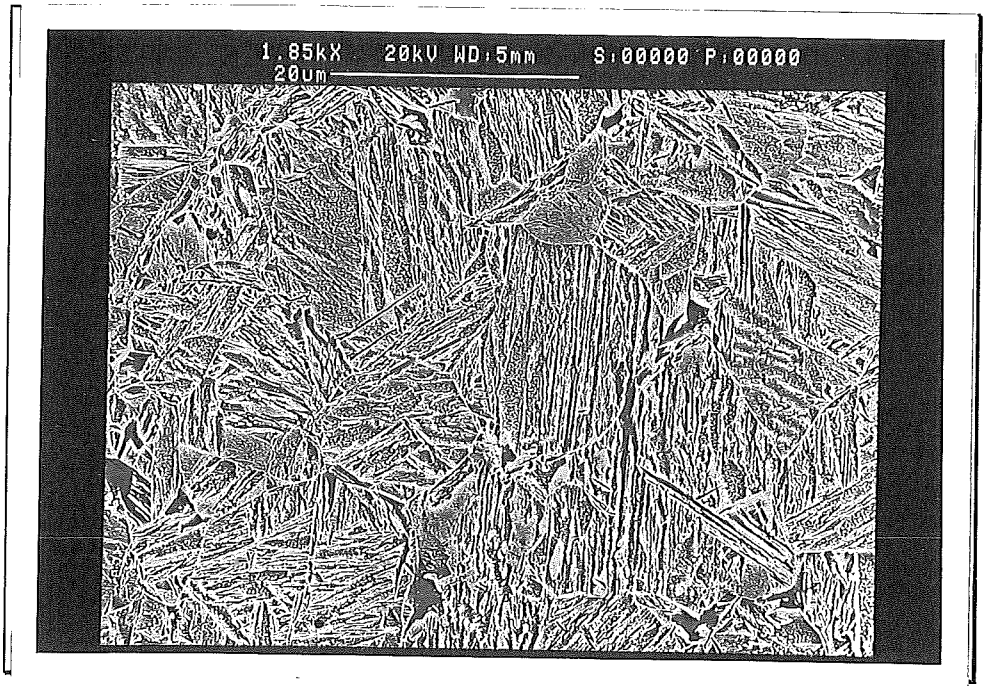

Picture 11 (RR9): SEM micrograph of a sample austenitised at 900°C for 10 minutes, then quenched to room temperature. It is fully martensitic. Grain size : ± 15 μm.

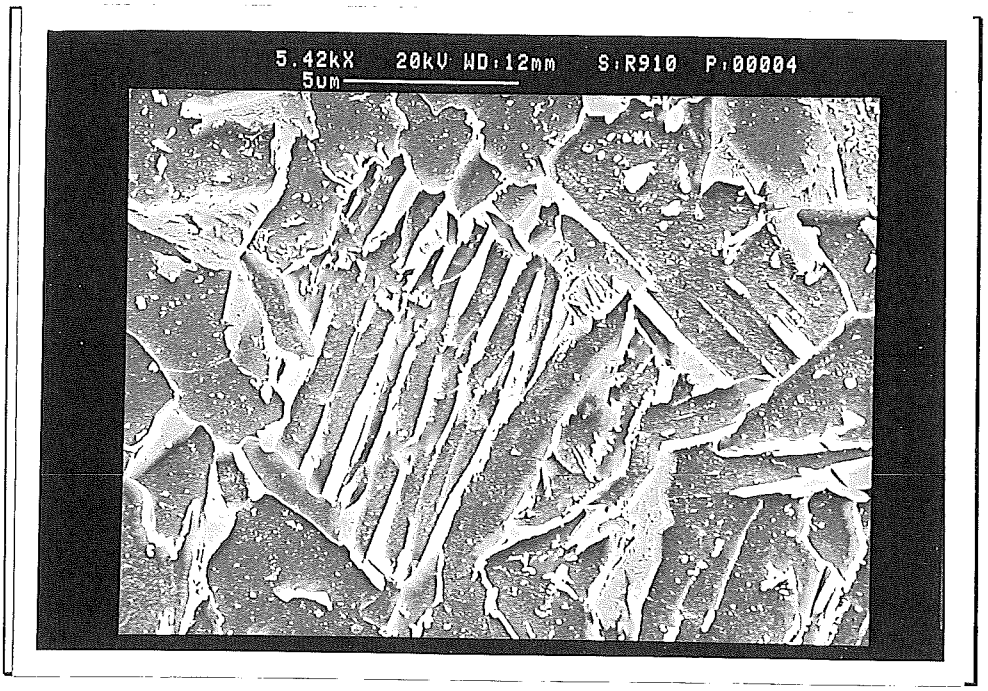

Picture 12 (R910): SEM micrograph of a sample austenitised at 900°C for 10 minutes then quenched to 100°C. Bainite or Widmanstätten ferrite.

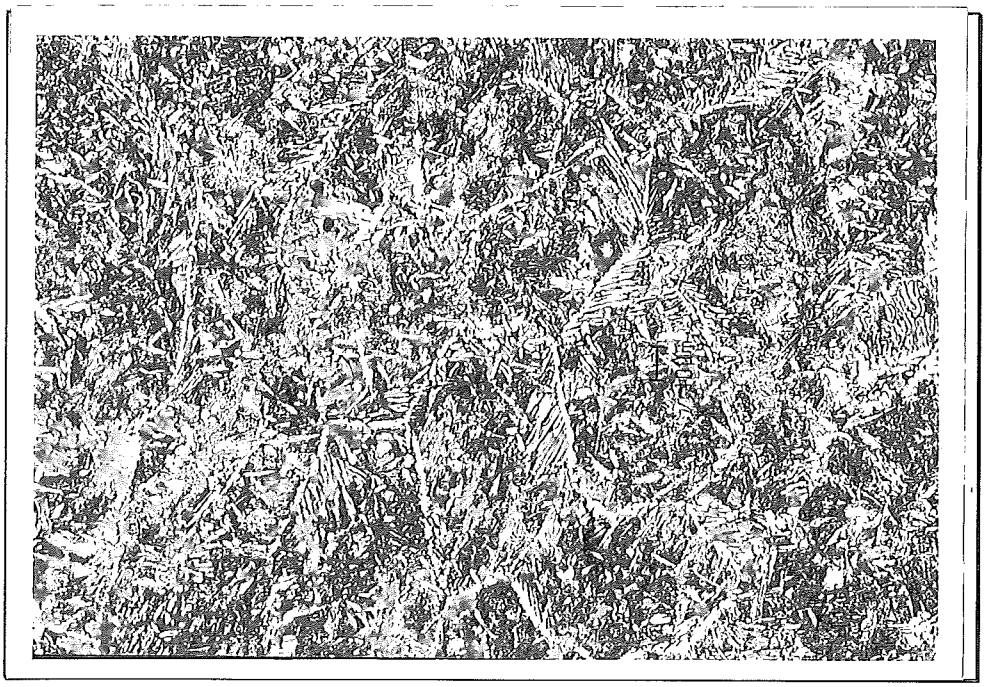

Picture 13 (R910): Optical micrograph of a sample austenitised at 900°C for 10 minutes then quenched to 100°C. Acicular ferrite of Widmanstätten.

Figure 76 shows the derivative of the curves showed in figure 75. It also gives an idea of the maximum cooling rates that have been reached (more than 200 K/s).

The conclusion is that only the experiment "RR9" reaches Ms without having undergone any other transformation. A better control during the quenches for the whole set of experiments would have been possible if hollow samples had been used. Indeed, hollow samples are lighter, which means a smaller weight of material that must be cooled with the same gas blow. Furthermore, it is possible to add a pipe in order to blow gas inside the sample. On the other hand, only solid samples allow to perform microscopy afterwards, since hollow samples are too thins.

Picture 11 presents the microstructure of sample RR9, while picture 12 and 13 present the microstructure of sample R910. As expected, the first one contains 100 % of martensite, while the microstructure of the second one is more complex. The sample R910 has been firstly analysed with a scanning electron microscope (SEM) on the picture 12, and one could not say if the microstructure was constituted of bainite or Widmanstätten ferrite. According to H.K.D.H Bhadeshia, an optical microscope is more appropriate for the distinction between

acicular ferrite and bainite. With an optical microscope, the bainite appears dark and the acicular ferrite appears clear, as can be seen on picture 13 [24]. R910 is acicular ferrite.

4.4.2 Elements for CCT diagrams

If, for the intercritical annealing at 800°C and 900°C, the quenches are too slow for the construction of TTT diagrams, the experiments can still be useful to collect data for CCT diagrams. Indeed, the cooling rates were measured for each quench, as well as the temperatures where some transformation begin. The following figures might help to understand how measurements were done.

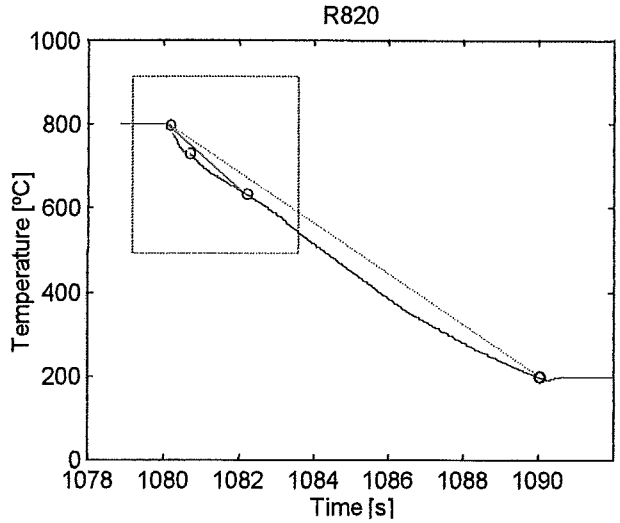

Figure 77: Measurement of the cooling rates after 0.5 and 2 seconds, and the average cooling rate.

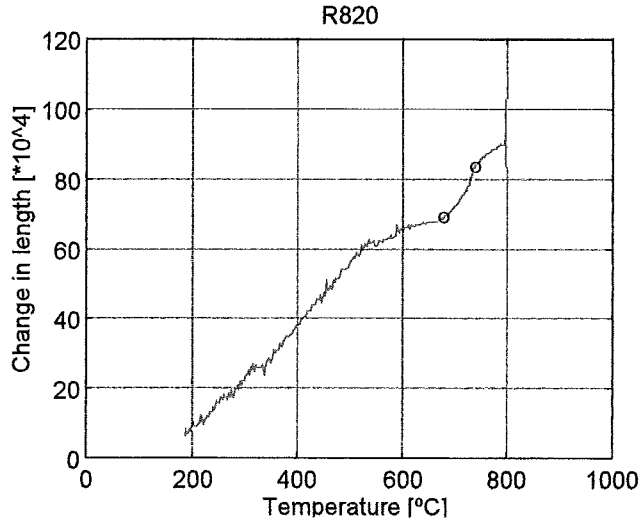

Figure 78: Identification of the temperature of the transformation that occurs during the quench.

The example showed on figures 77 and 78 is a quench from 800°C down to 200°C. On the first chart, one can see that the top and the end of the slope must be defined. Three values are calculated on figure 77:

- the average cooling rate during the first half second. (135 K/s in this case).
- the average cooling rate during the two first seconds. (81 K/s).
- the overall average cooling rate. (61 K/s).

The second chart (figure 78) presents the change in length as a function of the temperature, which allows to identify the temperatures at which a transformation begins or ends. On this example, there is the end of a "temperature gradient effect" around 740°C (as related in the section 4.2.2), and the beginning of a transformation around 680°C. These measurements have been applied to all the quenches that have been performed in this work.

The interest is, firstly, to see if there are important variation for measurements that should be identical, and secondly, to get the transformations temperatures, for instance for the transformation that occurs during the quench from 800°C. The results for the quenches from 900°C are summarised in the table 9.

From – To	CR at 0.5 s	CR at 2 s	Average CR	First Transf.	Sec. Transf.
900-80	196	145	63	440	
900-100	107	95	17	660	
900-100 bis	41	41	38	600	400
900-150	132	107	54	560	"410"
900-200	137	111	57	560	"400"
900-250	140	106	61	600	"380"
900-300	135	103	51	600	
900-350	134	137	85	"450"	400
900-400	130	119	86	"500"	400
900-450	126	111	77	580	
900-500	149	140	120	"740"	

Table 9: Synthesis of the parameters measured on samples quenched from 900°C.

Except for the "900-100 bis", where the program was set at 40 K/s, and "900-80", which is an exception, the average cooling rates after 0.5 and 2 seconds do not vary too much, whereas the overall cooling rate is higher for shorter quenches, i.e. for quenches to higher holding temperatures. As one may notice that the instantaneous cooling rate does not stop to decrease

all along the quench, it is normal that the average cooling rate of a longer quench will be slower.

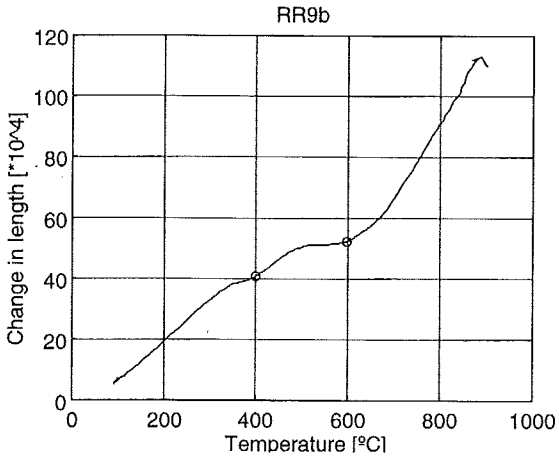

Figure 79: Dilatation curve of a quench carried out from 900°C at 40 K/s.

Concerning the temperatures of the main transformations, we can roughly identify 600°C and 400°C. In the table 9, the figures surrounded by quotation marks identify a less pronounced transformation. According to Andrew's formula, 600°C corresponds to the bainite start, while 400°C corresponds to the martensite start. The quench at 40 K/s allows to see the formation of both bainite and martensite. One can also notice that the slope of the curve is more important before the first transformation than after the second one. ($\alpha_{austenite} > \alpha_{martensite}$)

From – To	CR at 0.5 s	CR at 2 s	Average CR	First Transf.	Sec. Transf.
800-80	132	93	58	"740"	700
800-100	99	72	44	"740"	700
800-150	128	88	67	"740"	700
800-200	135	81	61	"740"	680
800-250	114	74	61	"740"	700
800-300	103	71	64	"740"	700
800-350	129	94	84	"740"	700
800-400	138	91	86	"740"	700
800-450	101	71	67	"740"	715
800-500	142	97	92	"740"	680

Table 10: : Synthesis of the parameters measured on samples quenched from 800°C.

The main characteristics of the quenches described by the table 10 are the end of the plateau around 740°C and the beginning of a transformation at already 700°C. At the beginning of the quench, the sample contains about 10 % of ferrite and the carbon enrichment of the austenite

is around 0.18 wt. %. This amount of carbon is still low and cannot hinder a diffusive phase transformation, furthermore, the small ferrite phase (10 %) constitutes excellent nucleation sites. This explains the fact that in the case of an annealing at 800°C, the austenite transforms faster than after a complete austenitisation at 900°C (transformation at 700°C instead of 600°C).

From – To	CR at 0.5 s	CR at 2 s	Average CR	First Transf.	Sec. Transf.
750-80	83	89	54	"725"	300
750-100	152	110	61	"725"	290
750-150	130	94	64	"725"	295
750-200	101	103	79	"725"	300
750-250	81	72	61	"725"	290
750-300	96	79	69	"725"	
750-350	120	94	90	"725"	
750-400	107	78	71	"725"	
750-450	77	72	71	"725"	
750-500	113	102	102	"725"	
750-550	132	102	104	"725"	"680"

Table 11: Synthesis of the parameters measured on samples quenched from 750°C.

As for the 800°C series, the 750°C series, described on the Table 11, also show a pronounced "gradient effect" plateau whose end is around 725°C. For tempering at temperatures lower than 300°C, a fast phase transformation is observable near 290°C and it corresponds to the Ms temperature of the austenite charged with 0.35 wt.% C. No transformation was experienced above the martensite start, and this is why the data coming from the 750°C series was kept for the drawing of a TTT diagram.

Indeed, the reason why there was no parasite transformation is that the higher carbon content has stabilised the austenite enough to push the transformation noses to the right (on a TTT diagram) [15].

In a general way, one can see that, for comparable experiments, the values of the cooling rates differ quite much despite the fact that programmed cooling rate were identical. It is very difficult to get two times the same results, in what concerns the quenches. This illustrates the fact that even on a very good dilatometer, a quench is still something difficult to control, however it must be easier with hollow samples.

4.5 Remedy: Formula applied upon the quench

This part sketches out a technique for the calculation of the phase fraction transformed during a quench, in contrast to an isothermal tempering. In the equation (3) ($\frac{\Delta l}{l_0} = \frac{V - V_0}{3 * V_0}$), we can express $\Delta l = Y - Y_0$. In the case of the isothermal holding, the reference (Y_0) for the calculation of the growth of the new phase was simply the change in length measured at the end of the quench, i.e. at the holding temperature, and when no transformation had occurred yet. This value could be kept constant as the holding was carried on in isothermal conditions. The method can easily be adapted to a non-isothermal transformation, if the reference Y_0 is properly dependent on the temperature. Hence in the coming calculation, Y will be the measured data while Y_0 will be calculated making the assumption that the phase fraction remains constant. Let us firstly look at the reference curve beside the data curve in the case of a quench from 800°C to 350°C on figure 80.

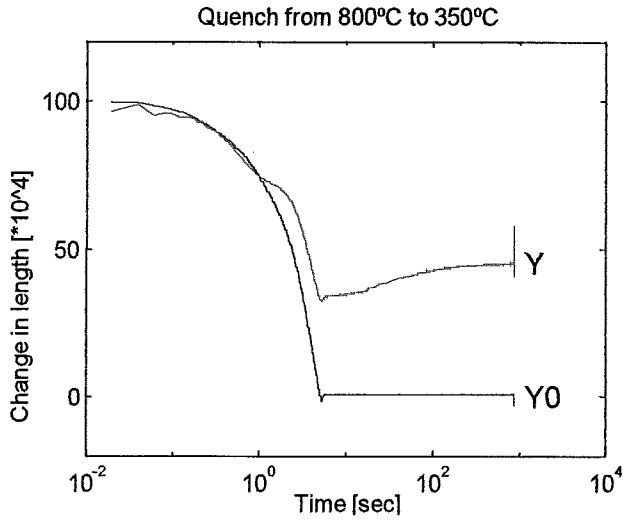

Figure 80: Dilatation curves from the beginning of the quench (800°C) to the end of the isothermal holding (350°C). Red: experiment, blue: calculated assuming that the austenite does not transform.

Thanks to the logarithmic X-axis, it is easy to distinguish the quench, that lasts about 10 seconds, and the isothermal holding that goes on for 15 minutes. In this case, the reference curve Y_0 shows the change in length of a sample that would contain 90 % of austenite and 10 % of ferrite and that would not undergo any transformation. Something happens in the microstructure when the Y curve moves away from Y_0 during the quench (around 1 second),

and we can see that there is still a transformation going on during the tempering because the change in length still increases.

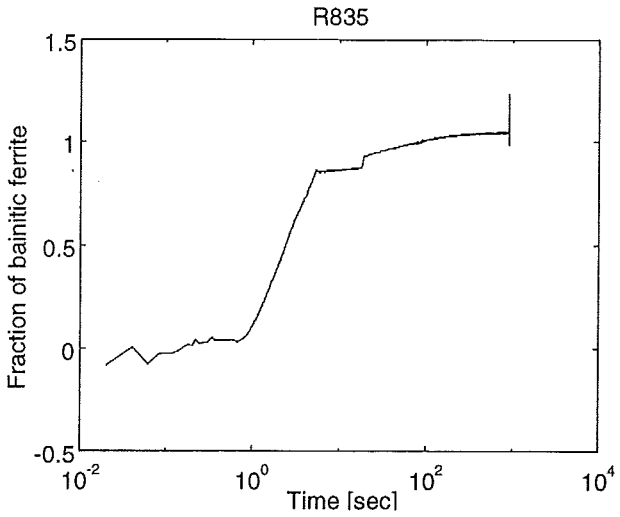

Figure 81: Fraction of bainitic ferrite calculated on the basis of the results showed on figure 80.

The values of $\Delta l = Y - Y_0$ can now be used by the equation (6) or (9) in order to calculate the amount of bainitic ferrite. The figure 81 presents the result obtained for the example mentioned above. It indicates that the transformation starts after about one second, then it grows very fast until the end of the quench and it finally goes on slowly. A problem is that the bainitic ferrite fraction goes up to more than 100 %, which is impossible. That inaccuracy is mainly due to a bad estimation of the expansion coefficient of the austenite. On the figure 80, one can see that the calculated change in length at the temperature of 350°C is close to 0, which seems to low with regard to the previously observed experiments.

From the beginning of this work, we have made the assumption that the expansion of the γ phase as a function of the temperature is linear, and so that α_γ values $23.5*10^{-6}$ K^{-1}. Actually, the expansion of the austenite is non-linear, and it is difficult to get good data for its expansion coefficient at lower temperatures. One way to refine this parameter is to choose a dilatometry experiment where we know that no transformation happened during the quench, and to make fit the calculated values of the change in length to the measured data. Indeed, the figure 82 shows the quench from 750°C to 350°C. The fit seems quite good in this case, as the curves remain close to each other, but looking at the figure 83, which is the calculated fraction of bainitic ferrite, we see that the growth of the ferrite phase is inverted when the Y_0 curve

happens to be above the *Y* curve. It may be due to the fact that the experimental data are falsified by the "plateau" effect. This imperfection adds to the difficulty of the calculation.

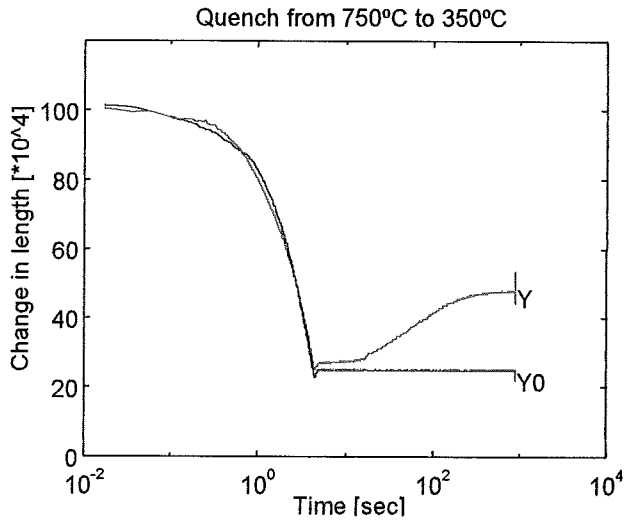

Figure 82: Dilatation curves from the beginning of the quench (750°C) to the end of the isothermal holding (350°C). Red: experiment, blue: calculated assuming that the austenite does not transform.

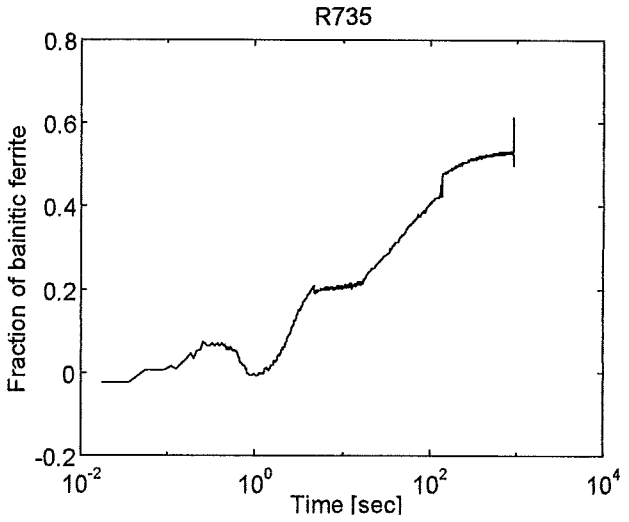

Figure 83: Calculated fraction of bainitic ferrite on basis of figure 82.

As a final example, we may look at the figures 84 and 85, which show the result of this calculation applied to the quench of a completely austenitised sample, i.e. from 900°C. Hence there is a real problem with the accuracy of the evaluation of the expansion coefficient of the austenite phase. Solving this problem is quite difficult since a good estimation of this parameter would require new experiments, and in order to get a higher precision, the value

should be given by a polynomial equation taking the temperature into account to the third degree.

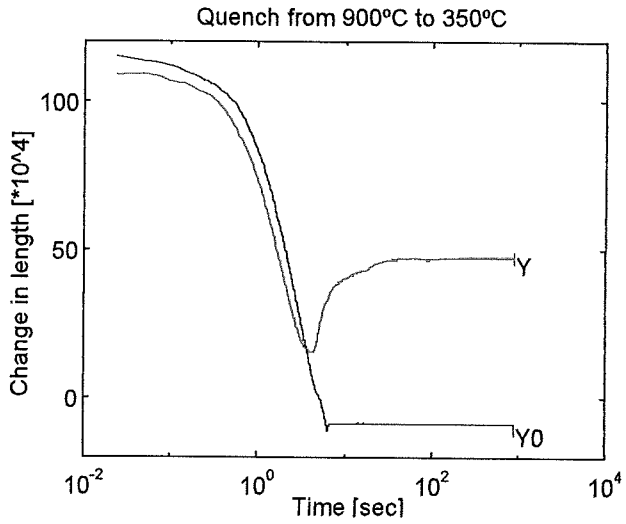

Figure 84: : Dilatation curves from the beginning of the quench (900°C) to the end of the isothermal holding (350°C). Red: experiment, blue: calculated assuming that the austenite does not transform.

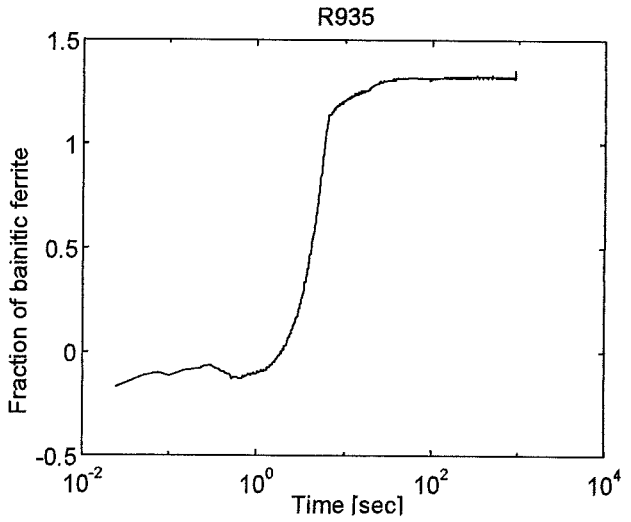

Figure 85: Calculated fraction of bainitic ferrite on basis of figure 84.

4.6 Intercritical annealing at 750ºC : test

4.6.1 Explanations for the gap between the annealings at 750°C

The gap is visible in figure 58. Three explanations are faced :

- The first explanation for the deviation between the two dilatation curves was linked to the difference in the phase fractions and to the fact that the austenite is more compact than the ferrite. It has been detailed previously.
- A second track is the possible experimental deviation. Indeed, the absolute measure for the change in length is not always reliable : the height of two different dilatation curves can sometimes differ, especially when the treatment contains a quench, which might move the sample between the quartz rods (figure 7). But as there was no such operation for these experiments before the end of the annealing, this second explanation can be ignored.
- Finally, a deviation can be seen in the fact that one of the two samples has undergone a holding at 950°C. As it has been austenitised, its pearlite has been decomposed and then it comes back in a different way. As a matter of fact, the pearlite formed after the hot rolling is not the same than the one that will be formed later, and thus the overall dilatation is changed. This theory was proposed by Theo Kop, from the Materiaalkunde in the TUDelft.

4.6.2 Microstructure

The microstructure showed on the picture 8 is very strange because of its strong heterogeneity. Nobody could explain the reasons of that strange phenomenon. All the more, it cannot be due to a mistake since the experiment was performed twice, and since the dilatation data files prove the accuracy of the treatment.

After a long time of thinking, the beginning of an explanation exists. The figures 56 and 57 show us that coming from 100 % of γ phase at high temperatures and stopping at 750°C, we are really on the Ar3 point, which means that some ferrite should begin to appear in the austenite matrix. Actually, at Ar3, the driving force for the formation of ferrite is very low, thus very few nuclei of α phase succeed to reach the critic size. And, as the temperature is quite high, the diffusion is such that the surviving nuclei are able to grow quite fast.

These words account for the partition of the microstructure in two : a fully austenitic region and a ferritic region. Now let us say that the austenitic region will become, during the quench,

the fully martensitic structure that one can see on the picture 10. The problem now is : why is there a banded structure instead of huge ferrite grains ?

As a matter of fact, the assumption of the growth of only a few ferritic grains does not hold since the picture 9 shows relatively small grains of ferrite beside grains of martensite (10µm). Nevertheless, the banded structure is related to the non-homogene repartition of the manganese, when the metal is hot-rolled. As this element is in a substitutional position, it does not move a lot during the next thermal treatments, and thus it confers a so-called memory to the microstructure. Since the manganese is gammagene, austenite will appear preferably near it, and as a consequence, ferrite will appear preferably away from it. Finally, the distribution of the carbon through the microstructure is influenced by the distribution of the manganese, and it explains the fact that the pearlite is aligned in the sample [15].

Furthermore, an important effect of this non-homogeneity is that the temperature Ar1 is different from one place to another depending on the local concentration in the alloying elements. This may have introduce different types of nucleation during the intercritical holding at 750°C.

Unfortunately, it still does not give the key to the current problem.

4.7 Amount of retained austenite

Since this research is partly an investigation on the possibilities of producing a low silicon TRIP-aided multiphase steel, it was interesting to observe the samples heat treated with the dilatometer and to look for possible retained austenite. Among the whole set of heat treatments, figure 86 recalls those that were applied for the study of multiphase steels.

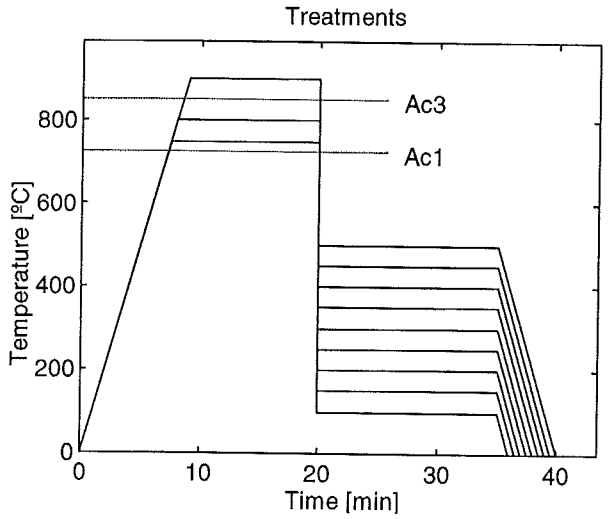

Figure 86: Thermal treatments for the drawing of three TTT diagrams.

Three annealing temperatures were faced (750°C, 800°C, 900°C), and the duration of the annealings was of 10 minutes. Concerning the holdings, they were spread from 100°C to 500°C by steps of 50°C, and were lasting 15 minutes. Which of these thermal treatments are the most susceptible to give stabilised austenite ? As already written in the introduction (1.2.2), the stabilisation of the austenite is the result of a two-steps carbon enrichments : the first one during an intercritical annealing, and the second one during the formation of bainite, ideally on the second isothermal holding. Ever since, between the two annealing temperatures, the one that provides the best carbon enrichment is 750°C, as observed in the section 3.2.3. Then, for this series, which one of the holding temperature was the best ? Since the Ms temperature was calculated around 290°C for an austenite enriched at 0.35 wt. % C, and Bs was calculated at 600°C (with Andrew's formulas (16) and (17)[18]), all the levels comprised between Ms and Bs are worth to be analysed more closely.

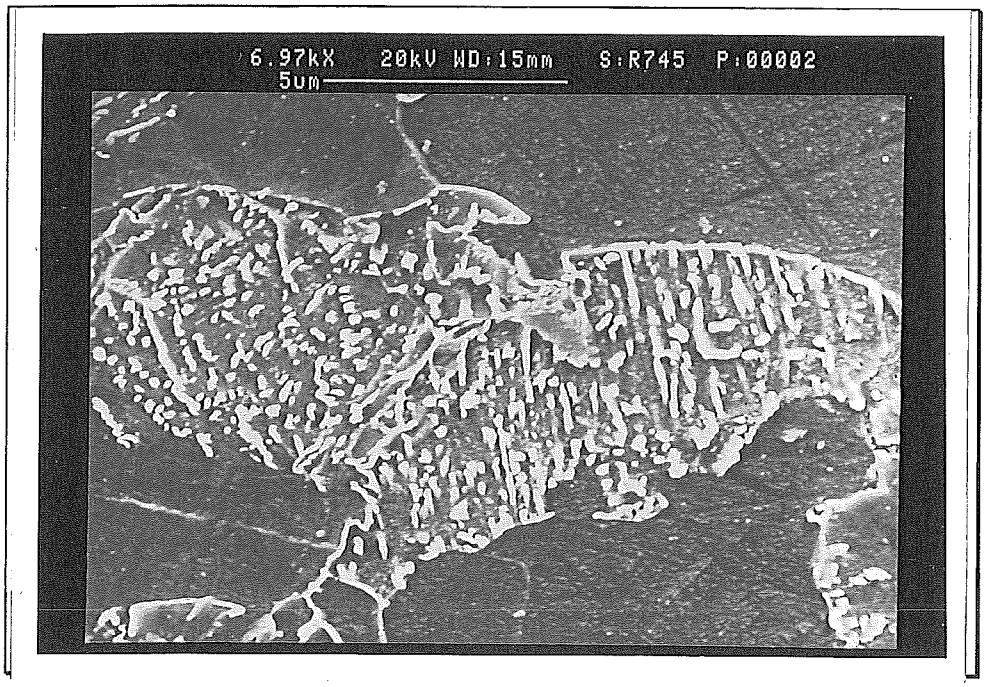

Picture 14 (R745) : SEM micrograph of a sample annealed at 750°C for 10 minutes, quenched to 450°C, then held for 15 minutes.

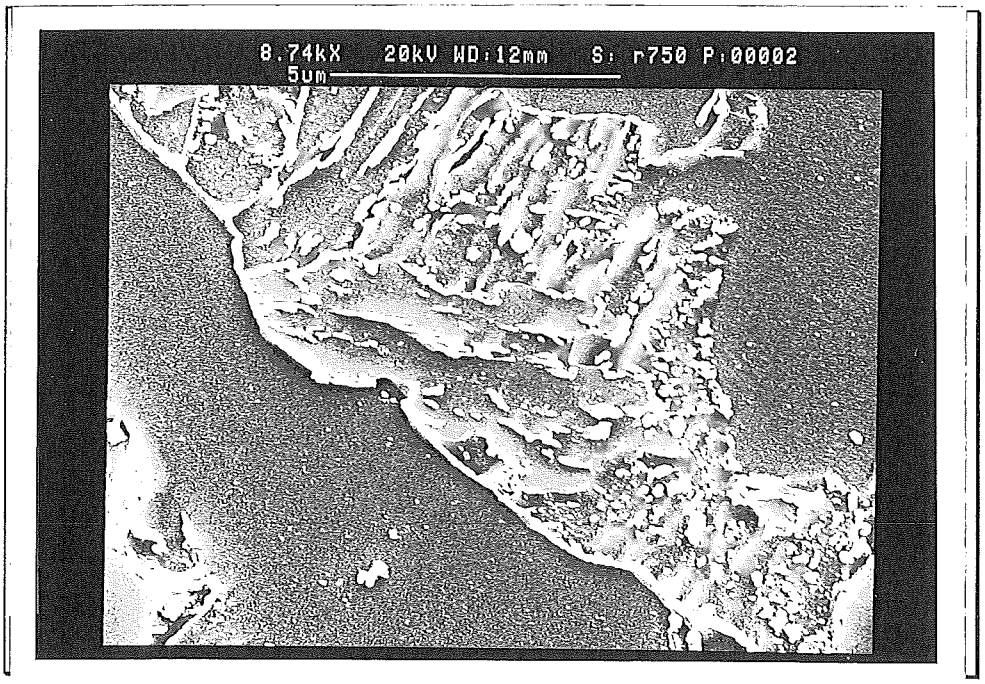

Picture 15 (R750) : SEM micrograph of a sample annealed at 750 °C for 10 minutes, quenched to 500°C, then held for 15 minutes.

The samples corresponding to those treatments were thus analysed by scanning electron microscopy and X-ray diffraction (performed by Lie Zhao, from the TUDelft). The result of the microscopy analysis is that no stabilised austenite could be observed with the SEM, and the results of the measurements performed by X-rays prove to be very low. As a matter of fact, there was not enough silicon to impeach carbides precipitation in the austenite. The pictures 14 and 15 show the microstructures of samples annealed at 750°C and quenched respectively to 450°C and 500°C.

One can see on both pictures 14 and 15 that the grain surrounded by ferrite is decomposed bainite. Indeed, the clear lines that are crossing the grain are carbides that were precipitated on the sides of the ferritic laths during the bainitic transformation [9]. Retained austenite cannot be observed in these microstructures, neither by the SEM, nor by X-ray diffraction. Maybe this austenite is too thin to be detected by XRD. For high-silicon steels, large amounts of austenite had been obtained for a similar heat treatment : intercritical annealing at 750°C followed by a bainitic holding at 400-450°C for several minutes [25-26].

One can think that an unavoidable condition for stabilising austenite is to add a graphitising element such as silicon or aluminium in order to prevent cementite precipitation. This is not true and Pascal Jacques, from the Université Catholique de Louvain, has proved it. He has shown that it was possible to stabilise austenite in a low-silicon steel and to obtain the TRIP effect [5]. For the composition : 0.18 wt.% C, 0.39 wt.% Si and 1.33 wt.% Mn, and by applying the following heat treatment : 730°C/5 min/370°C/1 min, he could get up to 8.5 % of retained austenite. Furthermore, what influences the properties of a TRIP-aided steel is not only the amount of austenite that it contains, but also the stability of this phase. And as a matter of fact, the mechanical properties of the low-silicon TRIP-aided multiphase steel that was produced avowed to be excellent [5].

What explains the very low concentrations of retained austenite measured in the samples produced in the present work is the length of the isothermal holding. A bainitic holding of 15 minutes is too long (for a low silicon steel) since it allows most of the austenite to transform by carbides precipitation [5]. (The Mössbauer spectroscopy measurements of Pascal Jacques give an amount of 2 % of retained austenite for a holding of 10 minutes [5].) The austenite retention in low-silicon steels is only possible if the kinetics of the bainitic transformation are taken into account. The bainitic holding must be long enough for the carbon to diffuse out of the supersaturated ferritic laths into the surrounding austenite, but it should be stopped before the transformation of this austenite.

But one should keep in mind that one of the aims of the present work was to produce TTT diagrams, which explains the need to apply sufficiently long holding times, finally : 15 minutes. The samples could not therefore have undergone the ideal heat treatment for the production of TRIP-aided steels.

5. Conclusions

This study investigated the heat treatments for the production of a low-silicon low-carbon TRIP-aided multiphase steel by means of dilatometry. Programs have been written for the interpretation of the dilatometric curves of, firstly the transformation $\alpha \rightarrow \gamma$ upon heating, and secondly, the isothermal transformation during bainitic holding. The output of this second program have been used to release a TTT diagram for the phase transformations following an intercritical annealing at 750°C. For samples annealed at 800°C and 900°C, information on the transformations that occurred during the quench have been reported. It may be useful to draw CCT diagrams, for instance.

Moreover, a method for the measurement of the phase transformation during the quenches has been developed (Section 4.5). Besides the research for the TTT diagram, an experiment about the intercritical annealing has been carried out (Section 3.4). The observed microstructure still constitutes a mystery.

One should be aware that the calculation method developed in this thesis work require very accurate data for the different parameters that describe the material. Moreover, the calculated phase fractions are very dependent on the input data such as the lattice parameters and the expansion coefficients (Section 4.2.4). Furthermore, perfect quenches are needed for the calculation of TTT diagrams: the use of hollow samples are therefore recommended for the dilatometry tests.

The perspectives for the possible continuation of this work could be :

- to get some new dilatometric data, but with hollow samples this time.
- to try and refine the parameters for the calculations.
- to integrate the programs in a more efficient programmatic language.

For what concerns the steel grade that has been studied in this work, mechanical tests of this material are being carried out currently at the university of Aachen, Germany. Furthermore, the possibilities of production of a TRIP-aided multiphase steel of this composition have been investigated by Hoogovens. Laboratory simulations of a hot-dip galvanizing line have proved to give a satisfying result [13].

References

[1] H. Shirasawa, *"High-Strength steels for automative, symposium proceedings"*; C.E. Slater, Baltimore, MD ,1994, pp 3-10.

[2] I. Tamura, Metal Sc., 1982, vol **16**, pp 245-252.

[3] Anil K. Sachdev, Acta Metall., 1983, vol **31**, n° 12, pp 2037-2042.

[4] P. Jacques, PhD Thesis, UCL, Belgium, 1999.

[5] P. Jacques, X. Cornet, Ph. Harlet, J. Ladrière, F. Delannay, *"Enhancement of the Mechanical Properties of a Low-Carbon, Low-Silicon Steel by Formation of a Multiphased Microstructure Containing Retained Austenite"*, Metall. Mater. Trans. A, 1998, vol **29A**, pp 2383-2393.

[6] H. Koh, S. Lee, S. Park, S. Choi, S. Kwon, N. Kim, Scripta Mater., 1998, vol **38**(5), pp 763-769.

[7] H. K. D. H. Bhadeshia, D.V. Edmonds, Metall. Trans. A, 1979, vol **10A**, pp 895-907

[8] M. Takahashi, H.K.D.H. Bhadeshia, Mater. Trans. JIM, 1991, vol **32**, pp 689-695.

[9] H.K.D.H. Bhadeshia, *"Bainite in steels"*, The institute of Materials, London, 1992, pp 72-74.

[10] O. Matsumara, Y. Sakuma, Y. Ishii, J. Zhao: Iron Steel Inst. Jpn. Int., 1992, vol. **32** (10), pp. 1110-16.

[11] Anne Mertens, Project for the FRIA, 1997.

[12] G.R. Speich: *"Fundamentals of Dual-Phase Steels"*, R.A. Kot and B.L. Bramfit, eds., Trans. Met. Soc. AIME, Warrendale, PA, 1981, pp 3-45.

[13] Jacobien Vrieze, Walter Vortrefflich, Laurens de Winter, Hoogovens Research report, 1999.

[14] Bhadeshia H.K.D.H, *"Thermodynamic analysis of isothermal transformation diagrams"*, Metal Science, 1982, vol. **16**, pp 159-165.
http://Engm01.ms..ornl.gov/TTTCCTPlots.html

[15] F. Delannay, *"Compléments de Metallurgie Physique"*, Cours MAPR 2420, UCL.

[16] E. Girault, P. Jacques, K. Mols, P. Harlet, J. Van Humbeeck, E. Aernoudt, F. Delannay: *"Material Characterisation"*, 1998, vol. **40**(2), pp 111-118.

[17] L. Zhao, T. Kop, J. Sietsma, S. van der Zwaag, *"Dilatometric analysis of bainitic transformation in TRIP steels"*, 1999, to be published in Euromat '99.

[18] K.W. Andrews, J. Iron Steel Inst., 1965, pp 721-727.

[19] Caian Qiu, Sybrand van der Zwaag, *"Dilatation measurements of plain carbon steels and their thermodynamic analysis"*, Steel Research, 1997, issue **1**, pp 32-38.

[20] D.J. Dyson and B. Holmes, J. Iron and Steel Institute, May 1970, pp 469-474.

[21] N. Ridley, H. Stuart, L. Zwell, *"Lattice Parameters of Fe-C Austenites at Room Temperature"*, Trans. Met. Soc. AIME, August 1969, vol **245**, pp 1834-1836.

[22] K. H. Jack, *"Structural Transformations in the Tempering of High-Carbon Martensitic Steels"*, Sept. 1951, pp 26-36.

[23] J. Gordine, I. Codd, *"The influence of silicon up to 1.5 wt. % on the tempering characteristics of a spring steel"*, J.of the Iron Steel Inst., April 1969, pp 461-467.

[24] R.W.K. Honeycombe, H.K.D.H. Bhadeshia, *"Steels"*, MMS, Edward Arnold, 1995 (Sec. Ed.), pp 145-146.

[25] A. Ali, M. Ahmed, F.H. Hashmi, A.Q. Khan, Metall. Trans. A, 1993, vol **24A**, pp 2145-2150.

[26] Y. Sakuma, D.K. Matlock, G. Krauss, Metall. Trans. A, 1992, vol **23A**, pp 1221-1232.

6. Appendix

6.1 Guidelines/Manual bainitic transformation analysis program

Introduction

This program calculates from a dilatometric data file the fraction of bainite that forms during the holding at the transformation temperature. It uses the lattice parameters of austenite, ferrite and cementite as well as their expansion coefficients. The calculation involves the solvation of an equation by the iteration method of Newton-Raphson. Two cases are taken into account : the quench is done from a complete austenisation temperature or from an intercritical temperature. The user is asked for the annealing temperature, and in the case it is intercritical, he must give the fraction of austenite that was in the sample before the quench. The user also has to introduce the holding temperature at which the isothermal transformation is meant to occur.

Matlab environment

To run this program, you need a Matlab software on your computer. In the main directory named "*matlab*", a sub-directory (for instance :"*bain*") should be created in order to host the program files and the data files. This is also the place where the output files will be saved. At the beginning, the directory "*bain*" should contain the following files which are the main program and its sub-routines : *bainite.m, fprim.m, grf.m.*

Pre-processing

Make the input file. This is a table in wri format with 4 columns : anything(number of the value), time(s), temperature(°C), dilatation change ($*10^4$). The table must start at the very first line of the document, otherwise Matlab would not recocknize it as a matrix. Don't forget to put this wri file in the directory "*bain*".

Processing

In the Matlab main command window, type : cd bain, then "enter", and bainite followed by "enter". After the program has started, you will be asked for the name of the input file. If it is for instance *data.wri*, you must type : 'data' with the quotation marks.

Then you have to enter the name of the output file according to the same typing rules, for instance : 'output' and the file *output.wri* will be created at the end of the calculation and the results will be stored inside.

Finally, you are asked for the annealing and the holding temperatures of the experiment. In the case it is intercritical, you have to type the fraction of austenite present in the sample at the end of the annealing.

Post-processing

The program has released two windows ; the first one contains a graph of the retained austenite as a function of the time, and the second one is the amount of bainite as a function of the time.

The output file is a table of three columns : time(s), fraction of retained austenite, fraction of bainite. It can be converted then to an excell file or used as is by an other Matlab program.

The interest of using Matlab is that the user can easily make modifications to the program, for instance: the lattice parameters. For details, see the Matlab Primer.

6.2 Programs

```
disp('       BAINITIC TRANSFORMATION');

% BAINITE figures out the fraction of retained austenite that appears
%       during the bainitic transformation of a low silicon steel
%       quenched from an intercritical temperature. The data needed
%       is a four columns text file that contains the time in the second
%       column, the temperature in the third and the change in length
%       in the fourth. BAINITE uses the Newton-Raphson method on the
%       function GRF, which has been written by Lie Zhao.
%       The output is a .wri file that contains three columns. The first
%       one is for the time, the second one is for the austenite fraction
%       and the third one is for the bainite fraction.

global T, global DL, global FGI, global DL0;
name = input('Name of the input file .wri ? ');
eval(['load ',name,'.wri']);
atemp = input('Annealing temperature ? ');

if atemp == 900,
  FGI = 1;
```

```
else
  FGI = input('Fraction of austenite at the end of the annealing : ');
end;
htemp = input('Holding temperature ? ');
[r c]=size(eval(name));
Time = eval([name,'(:,2)']);
Temp = eval([name,'(:,3)']);
deltal = eval([name,'(:,4)']);
fgamma = zeros(r,1);
bain = zeros(r,1);
Time2 = zeros(r,1);

count1 = debut(name);

%       The function "debut" finds the beginning of the
%       isothermal holding, which defines DL0.

DL0 = deltal(count1);
time0 = Time(count1);

for count2 = count1:r,
  T = Temp(count2);
  DL = deltal(count2);
  fgb=0.5; twin=0;
  while (abs(fgb-twin)>0.0001),
    twin = fgb;
    fgb = fgb - (grf(fgb))/(fprim('grf',fgb));
    if abs(fgb-twin)>1000, error('No convergence.'), end
  end;
  fgamma(count2) = fgb;
  Time2(count2) = Time(count2) - time0;
  if
((Time(count2)<Time(count1)+900)+((Time(count2)>=Time(count1)+900)*(Temp(cou
nt2)<htemp-5))==0), break, end
end;

%       The "for" loop is needed to go through the data. And the
%       "while" loop is for the refining of the convergence in
%       the Newton-Raphson method.

bain = - (fgamma - FGI);

figure(1);
clf;
semilogx(Time2(count1:count2),fgamma(count1:count2),'w');
title([num2str(atemp),'ºC to ',num2str(htemp),'ºC']);
xlabel('Time [sec]');
ylabel('Fraction of retained austenite');

figure(2);
```

```
clf;
semilogx(Time2(count1:count2),bain(count1:count2),'w');
title([num2str(atemp),'ºC to ',num2str(htemp),'ºC']);
xlabel('Time [sec]');
ylabel('Fraction of bainitic ferrite');

output = [Time2(count1:count2),fgamma(count1:count2),bain(count1:count2)];
out = output';
fid = fopen([name,'op.wri -ascii'],'w');
fprintf(fid,'%4.4f\t %4.4f\t %4.4f\n',out);
fclose(fid);
```

```
function deb=debut(name)

% DEBUT prend comme argument le nom d'un fichier
%      de donnees dilatometriques. Il renvoie
%      alors l'indice de la ligne qui marque le debut de
%      la transformation bainitique.

dat = [1090 1070 1025 1060 1030 910 1020 1025 870 858;1200 1065 1075 1065
1040 910 1002 1020 861 0;1250 1157 900 1085 1125 870 995 1020 840 0];
asde = abs(name);
ro = asde(2) - 54;
te = 10*(asde(3)-48)+(asde(4)-48);
co = (te-5)/5;
deb = dat(ro,co);
```

```
function xprim = deriv(x)

[r c]=size(x);
xprim = zeros(r,2);
for count = 4:1:r-3,
  xprim(count,1) = x(count,2);
  xprim(count,2) = (x(count+3,3)+4*x(count+2,3)+5*x(count+1,3)-5*x(count-1,3)-
4*x(count-2,3)-x(count-3,3))/(x(count+3,2)+4*x(count+2,2)+5*x(count+1,2)-5*x(count-
1,2)-4*x(count-2,2)-x(count-3,2));
end;
```

```
function fpr = grfint(fgb)

% GRFINT is a function used by the programme BAINITE.
%      The root of this function gives the value of the volume
%      fraction of retained austenite. This function is inspired
%      from the equation (13).

global T, global DL, global FGI, global DL0;
x1 = 0.16;
```

```
x2 = 1.5;
aalpha = 2.883*(1+13.1e-6*T+0.003747e-6*T^2);
agammab = (3.6008+x1/fgb*0.046+x2*.00103)*(1+23.5e-6*(T-25));
agammai = (3.6008+x1/FGI*0.046+x2*.00103)*(1+23.5e-6*(T-25));
fpr = (fgb*(agammab^3-2*aalpha^3)+FGI*(2*aalpha^3-
agammai^3))/(3*(FGI*agammai^3+2*(1-FGI)*aalpha^3))-((DL-DL0)/10000);
```

6.3 Three-dimensions TTT diagram